Design of a probabilistic decision support tool for the cable installation of an Offshore Wind Farm

G. Leontaris

Delft University of Technology

Design of a probabilistic decision support tool for the cable installation of an Offshore Wind Farm

By

Georgios Leontaris

in partial fulfilment of the requirements for the degree of

Master of Science

in Sustainable Energy Technology

at the Delft University of Technology

May 2015

Supervised by:

Prof. dr. A. V. Metrikine, TU Delft

Prof. dr. ir. A. R. M. Wolfert, TU Delft

Dr. ir. O. Morales - Napoles, TU Delft

Ir. B. J. van Burgel, IHC Merwede

TU Delft Delft University of Technology

"Essentially, all models are wrong, but some are useful."

George E. P. Box, 1987

Abstract

During the past years a lot of attention has been drawn towards the development of renewables, due to the expected depletion of fossil fuels and political decisions. Offshore wind energy is considered as one of the most promising renewable energy sources, however the cost of offshore wind farms have not yet reached competitive levels. Hence public-private partnership initiatives, such as FLOW, were developed, aiming the reduction of the high cost of offshore wind farms.

The current thesis is part of the FLOW project and its main goal concerns the development of a probabilistic decision support tool which will help professional concept engineers in comparing different cable installation scenarios by taking into account uncertainties. The tool estimates the time needed to complete the cable installation and by this estimation, an insight to the total cost of the cable installation is provided. Thus the user can exploit the results provided by the designed tool in order to decide the optimal installation scenario.

Within the scope of the project the dependence of wind speed and wave height, was investigated using Copulas functions and random weather time series were constructed based on the estimated dependence. Also an algorithm which takes into account the uncertainties regarding the performance of the installation operations as well as the risk of potential failures was developed. The algorithm provides as output the CDF curve of the duration of a cable installation scenario. Based on the produced curve the user is able to estimate the duration of a cable installation scenario within a confidence level.

Finally the designed tool was used to simulate a realistic cable installation test case, provided by Van Oord. The results from the simulations indicate that the designed tool provides a better estimation of the duration of a cable installation scenario, since it takes into account more realizations of weather conditions, compared to the common practice which simulates this scenario for a number of observed weather time series. Also it can be used to compare different cable installation scenarios by estimating the time needed for their completion and provide an insight on the expected cost, incorporating weather uncertainties and failure risks.

Acknowledgements

During the time I spent working on the MSc thesis project, I realized that its completion would not have been possible without the assistance of other people. Hence, I would like to give my acknowledgments to those who were involved and supported me in my thesis.

I would like to express my deepest gratitude to Prof. Andrei Metrikine for trusting me with this interesting and exciting subject and for giving me the chance to work with a group of passionate engineers and brilliant people.

I am deeply grateful to Prof. Rogier Wolfert for his important guidance on matters concerning probabilistic planning techniques and his useful advice concerning the architecture of the tool.

I would like to thank, from the bottom of my heart, Oswaldo Morales-Napoles for an excellent collaboration and for his valuable guidance on the interesting field of Copulas. The countless meetings we had and his important feedback were of paramount importance towards the completion of my thesis. I am very grateful that I had the opportunity to share with him the feelings of excitement and fulfilment after the achievement of each goal of the project.

I would also like to sincerely thank Bart - Jan van Burgel for his valuable comments and for always being there when I needed him in order to provide his professional opinion and share his experience.

I would also like to thank Rene van Kessel and Paul Vernimmen from Van Oord as well as Robert Hasselaar from Deltares for showing interest in my work and sharing with me the required data for testing the tool.

Lastly, I would like to thank my family for believing in me and for supporting me both financially and emotionally through all these years, and my friends for the great time we had together.

Contents

1. Introduction

1.1. About Offshore Wind Farms

Over the last years, a lot of attention has been focused to the exploitation of renewable energy sources. The main reasons are: the dramatic increase of energy demand which lead to an increase of CO_2 emissions by the combustion of fossil fuels used to generate power and the depletion of fossil fuels. Moreover, the European Union has set a target of 20% of electricity production should come from renewable sources by 2020 [1]. Also, wind energy as the majority of renewable energy sources, produce electricity without emitting CO_2, which enhances the greenhouse effect and leads to global warming. Wind energy is one of the most promising in the field of renewables, due to the maturity of wind energy technology and its high potential. Observing the increase of wind energy field during the last years, it is considered that the growth will continue at a yearly rate of 35% reaching an installed capacity of 19 GW in Europe by 2015 [2] and 40 GW by 2020 [3]. Moreover, recently due to political events, European countries investigate alternative energy solutions in order to reduce the dependence on natural gas imported from Russia [9].

In that direction, offshore wind farms (OWF) have received much attention as an alternative way of power production since they present several advantages. Although, currently the rated power of OWF is small, it is expected to emerge in the future reaching large generation capacities and OWF will be able to compete the existing conventional power plants. Moreover, in offshore wind energy applications there is no need of taking into consideration the fluctuations of costs of raw materials as it is needed for power plants which run on fossil fuels. Compared to onshore wind farms, offshore wind farms overcome the drawbacks of onshore installations concerning the lack of suitable land space, especially in Europe where the population density is high, leading to bigger installations providing more power. Also, the "not in my backyard" opposition by residents who consider that wind turbines destroy the beauty of a natural landscape and cause problems by noise emission, is not observed in OWF. Furthermore it is experimentally proven that wind quality in the sea, is better than onshore, as there are not obstacles that cause turbulence effects and lower the velocity of the wind. This fact leads to lower fatigue which explains why wind turbines placed in the sea, tend to have a longer lifetime [4].

However, the most important disadvantage of OWF is considered its significant larger cost compared to onshore wind or combined Cycle Gas Turbines [5]. This large difference in the cost could be explained as a consequence of the high installation and operation and maintenance costs. Several studies have shown that OWF could contribute in achieving the percentage of 20% power production from renewables set by the EU, the cost of the installation should be reduced significantly. Concerning the construction of an OWF, the cost of the electrical infrastructure, including the infield cable installation, the grid connection and the construction of the substation, is between 15% and 30% of the total investment [3]. Further research on different fields should be performed in order to minimize the cost and make OWF more attractive to investors.

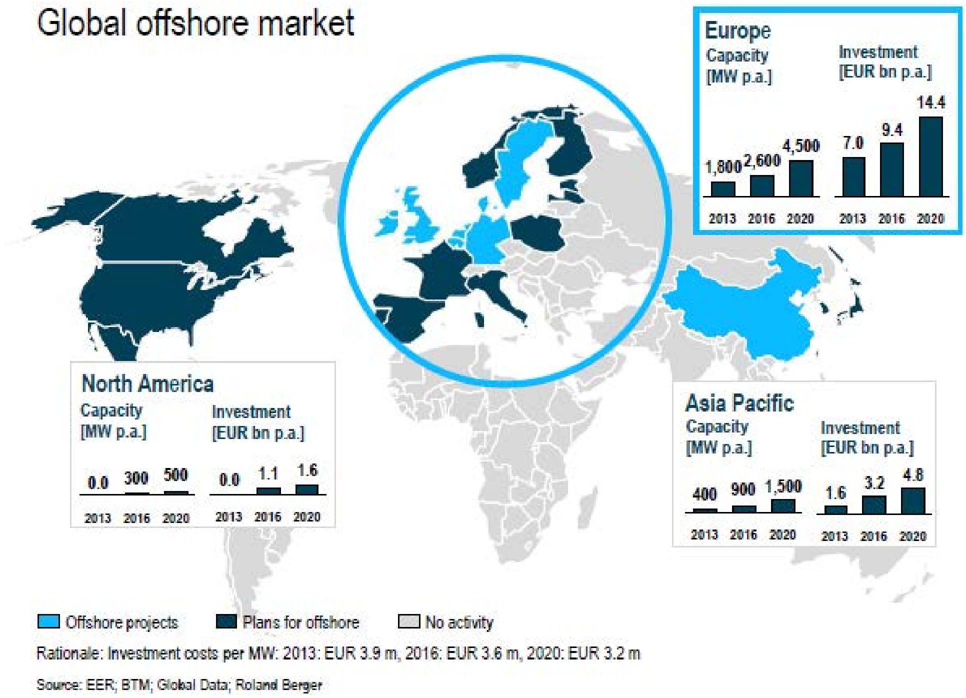

Figure 1.1: Global Offshore Market [6]

Despite the major disadvantage of OWF, it must be mentioned that a rise in the number of scheduled offshore wind farms has been observed. Mainly due to the fact that offshore wind is considered as relatively young technology that offers potential cost reduction and several European countries focused on offshore wind to achieve their energy and climate targets [6]. These are also the main reasons why a lot of research regarding the reduction of the total cost of installation and operation is conducted.

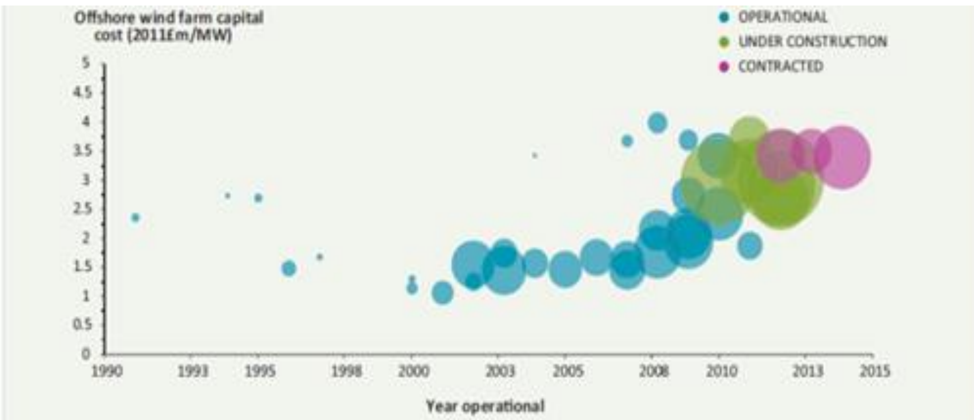

Figure 1.2: European Offshore wind farm capital costs per year [5]

1.2 Purpose of this thesis

History has proven that cable installation has contributed by 15-30% to the total investment, whose order of magnitude is in terms of billions Euros [7]. Studies have shown that there is room for improvement in cable installation in order to make it more cost effective and more reliable in order to minimize failures.

Moreover, cable installation is often characterized as difficult to plan and execute because of various reasons. Firstly, cable installation has interfaces with other installation processes, meaning that cable installation is often based on prerequisite installation operations in order to be completed successfully. Moreover, since offshore wind sector is considered to be relatively immature there are not any established methods that are used in all cases. Furthermore, each project is unique, meaning that it has its own characteristics and the most suitable method. These are the reasons why there are plenty of different methods available to perform the cable installation. Another reason that contributes in the complexity of cable installation is that the methods are sensitive to dynamic and unpredictable surrounding conditions.

Also it is worth mentioning that 70% of insurance claims involve failures during the installation and operation of submarine power cables. The main reasons of failures during installation concern the use of unsuitable vessel or equipment for the task and the inexperience of the sub-contractor. The right choice of vessel or equipment and the detailed diligence of installation logistic, installation vessels and installation equipment are crucial [8].

Therefore the industry is calling for innovation in order to reduce the risk and the cost of the OWF installation. A model that facilitates the concept design engineer's choice of the most economical and efficient design concepts could be an answer. The purpose of this thesis is the design of a decision support tool to help professional engineers in simulating and comparing different scenarios of infield cable installation, in order to decide which alternative is the most efficient. This tool could also be used by concept design engineers, in order to help them propose new or improved technologies, such as vessels and equipment, in order to improve the time needed to complete the operation.

This thesis is performed within the wider research program 'Far and Large Offshore Wind (FLOW)' which is subsidized by the Dutch government. It is a public-private partnership that includes thirteen companies and knowledge institutions that collaborate on innovation to reduce costs for offshore wind [28].

1.3 Research objectives

The goal of the current thesis is to *Design a probabilistic decision support tool regarding the inter-array cable installation of an Offshore wind Farm.*

Main research questions

- How realistically can weather time series that take into account the dependence between the weather variables be produced? Why is this important?

- How to calculate the time needed for infield cable installation including uncertainties?
- Can the tool help in obtaining better insight regarding the proposed installation scenarios under the influence of uncertainties?

1.4 Research approach

The current thesis was conducted in the following steps:

- Literature study on cable installation and decision tools
- Statistical analysis to find the dependence between wind speed and wave height using Copulas theory in order to generate realistic weather time series
- Build an algorithm to calculate the time needed and indirectly obtain an insight into the cost of the installation by running Monte Carlo simulations
- Run a realistic test case provided by Van Oord

1.5 Outline of thesis

The remainder of the thesis is organized as follows:

In Chapter 2 a description of the OWF components and the operations for the installation of OWF is given. Also the vessels and the equipment used in cable installation are presented.

Chapter 3 provides a theoretical background on Copulas functions and explain how they can be used in order to find the dependence between two random variables, such as wind speed and wave height. Also it presents the analysis of historical weather data and explains how the results of the analysis can be used in order to produce random time series of wind speed and wave height by taking into consideration their dependence. Finally the validation of the produced time series is also presented.

Chapter 4 describes in detail how the designed in Matlab, cable installation algorithm works. Also explains the methods that were used in order to include the cable installation uncertainties in the model.

In Chapter 5 the test case provided by Van Oord is described and the results of the tool are presented. Lastly, Chapter 6 summarizes the conclusions of the thesis and provides some recommendations for future work.

2. Installation of Offshore Wind Farm

2.1 Description

The current thesis is focused on the inter-array cable installation of an offshore wind farm, which is an important part of the total installation. However there are definitely important, prerequisite operations which should be completed before the cable installation commences. Also there are various vessels with different equipment that take part in particular steps of the installation [10]. Therefore, in this section some basics concepts regarding the main components and installation operations of an OWF as well as the vessels and equipment are introduced. Because of the subject of this thesis, more attention is drawn to the operations and necessary equipment of cable installation.

2.2 Main Components of OWF

The main components of an offshore wind turbine as one may observe in Figure 2.1, are the following:

- **Foundations**: Support structures of the offshore wind turbines. Different types of foundations are chosen based on the seabed geology, the metocean conditions and the water depth [11]. Monopiles are the most commonly used support structure, because of their lower manufacturing cost, compared to jackets which are a more expensive solution suitable for depths larger than 30 meters [12].
- **Transition piece:** Connects the foundation to the tower and corrects any potential misalignment of the foundation happened during installation [14].
- **Tower:** It is attached to the transition piece and supports the nacelle and the rotor in the determined height. It includes a yaw motor at the top, a transformer in the base of the tower as well as communication and power cables [14].
- **Rotor**: The blades bolted to the hub compose the rotor. The blades are made of fibre glass reinforced epoxy and carbon fibre and they are designed to maximize the produced power while they are able to withstand heavy loads.[15]. The steel hub connects the blades to the generator's main-shaft in order to transform the rotational kinetic energy to electricity.
- **Rotor Nacelle Assembly (RNA):** The rotor is connected to the nacelle which contains the generator, the gearbox as well as equipment used for monitoring and control.
- **Offshore substation:** Transforms the voltage of electricity generated by wind turbines to a higher voltage, in order to minimize the transmission losses from field to shore. The arrays of wind turbines are connected by "infield cables" to the substation and the electricity is transmitted from the substation to sore, using an "export cable".

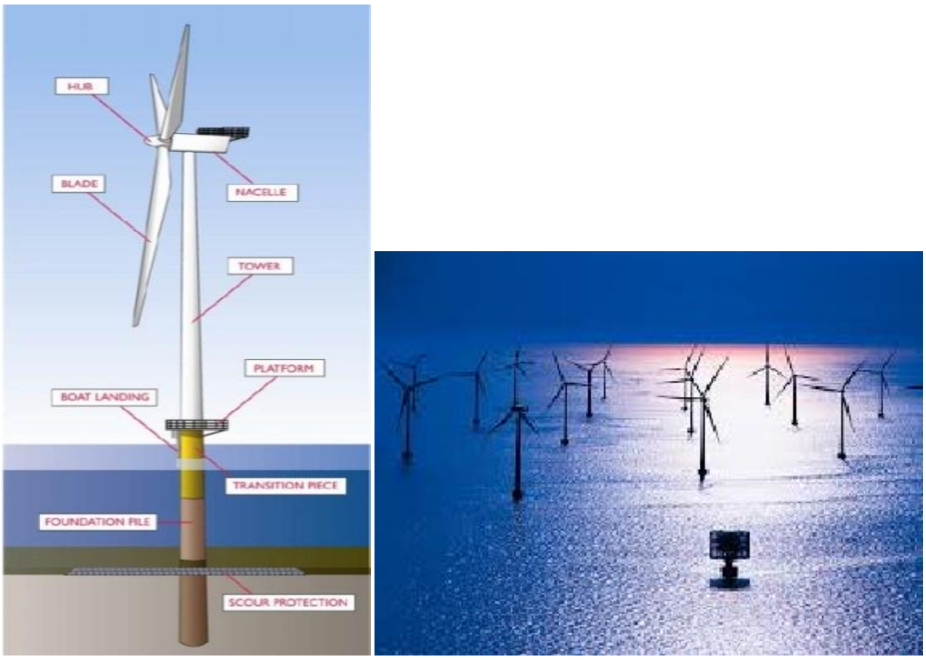

Figure 2.1: Left: Main Components of an offshore wind turbine [11] Right: Overview of OWF

2.3 Installation Operations

The installation of an OWF could be considered as a rather complex process and it could be divided in various subcategories. In order to complete the OWF installation, one may categorize the operations that should be performed as follows:

- Geophysical survey
- Foundation installation
- Cable installation
- Scour protection
- Wind turbine installation
- Substation installation

2.3.1 Geophysical Survey

Geophysical survey is already performed before the design phase of the offshore wind farm. During this survey the presence of boulders or other obstacles which could delay the installation, are investigated [12]. Based on the survey important decisions regarding the position of the wind turbines as well as the installation operations are made. Sometimes another survey operation is conducted before the installation of foundations or cables starts, in order to verify that the seabed has not changed considerably and further seabed preparation activities are not needed. Survey vessels and special designed equipment is used in order to complete this survey.

2.3.2 Foundation installation

Prior to the wind turbines' installation, the foundations are installed. There are different types of foundations which are handled in different ways. Monopiles are placed in the seabed by using a hydraulic hammer to drive them in the required depth. In case of rocky soil, the monopiles should be drilled which results in a cost increase [14]. Regarding the gravity based support structures, seabed levelling is essential before placing the support structure. Finally, as far as jackets or tripods are concerned, supporting piles are driven either before or after placing the support structures using heavy lift vessels [16].

2.3.3 Transition piece

In case of jackets or gravity foundations the transition pieces of wind turbines, are installed in port since the installation of the support structure allows it. However, as far as monopiles are concerned, the transition piece is usually transferred and installed by the same vessel which transfers the foundations. After the successful placement of the monopile, the vessel fits the transition piece on top of the monopile. Next, grouting process is performed, where grout is used to fill the gaps between the transition piece and the monopile, finalizing their attachment [14].

2.3.4 Scour protection

Scour is defined as the removal of soil around the support structure, due to currents. When a support structure is placed in erodible seabed a scour is likely to be formed due to the currents around it, and cause crucial stability issues to the turbine (Figure 2.2). Therefore, an important part of the installation of an OWF is the scour protection. There are different methods used for scour preventive actions, such as rock dumping around the support structure or installing concrete mattresses [14]. Also, it must be mentioned that although monopiles and gravity based structures require always scour protection, tripods and jackets usually do not need any [26]. The scour protection can be applied before or after the foundation installation. In case of monopiles, a rock dumping vessel is commonly used to create a layer consisted of small rocks prior to the monopile installation and then create a second layer of bigger rocks after the cable installation is completed.

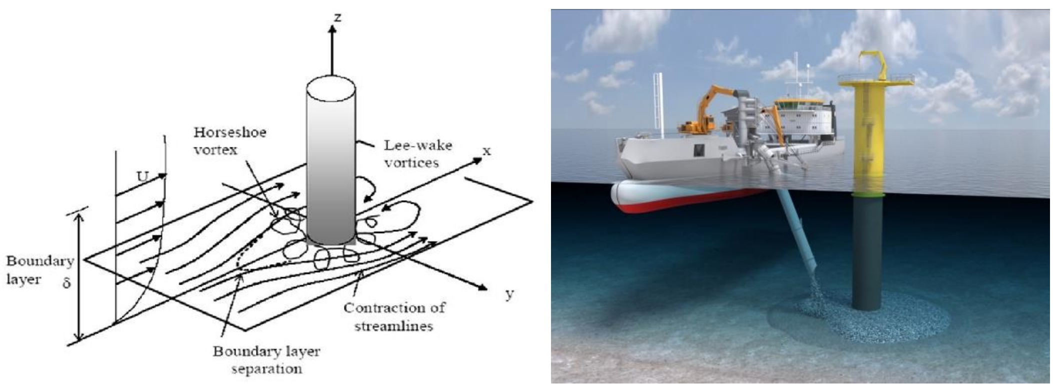

Figure 2.2: Scour formation and scour protection

2.3.5 Tower Nacelle and Rotor

There are many different methods that have been used in the past in order to install a wind turbine in offshore environment. The optimal method varies based on different characteristics of each case, such as: the available space on the installation vessel, the weather conditions on the site and the cost total cost. A number of different ways of wind turbine installation, which have been tried in the past, are listed:

- Transfer and install the components individually (nacelle, tower, blades)
- Transfer the tower in two parts and the rotor having already installed the two of the blades (bunny ears)
- Transfer the tower in one part and the rotor as bunny ears
- Transfer the tower in two parts and the rotor pre-assembled
- Transfer the tower in one parts and the rotor pre-assembled
- Transfer the whole turbine pre-assembled.

It is important to mention that each method needs different amount of time and it has different costs based on the type of vessel, the fuel consumed and the time that the vessel should wait on weather until the weather limits are satisfied.

2.3.6 Install the substation

The substation is located in the offshore wind farm site and it is used in order to either transform from AC to DC in order to be able to transfer the generated electricity to the onshore grid, minimizing the losses due to the long distance (more than 100 km), or AC to AC of higher voltage. Its installation requires large heavy lifting vessels that are capable of handling big and heavy components.

Figure 2.3: Left: Offshore substation. Right: Installation of offshore substation.

2.3.7 Cable installation

Cables are fundamental for an OWF, in order to transfer the generated power to shore and connect to the grid. For this reason cable installation is considered a very important part of the design of an OWF; however it is also quite hard to plan and optimize. A major developer stated that "80% of their problems in offshore installation are due to the cables. Because it's just very difficult to do." [18]. Cable installation is one of the few processes where the vessel should move over a specific predefined route precisely. Therefore special vessels equipped with sophisticated systems such as Dynamic positioning (DP) are needed. Also it is interesting to mention that the cost of cable installation may exceed up to 3 times the cost of the cables [18].

The cable installation of an OWF could be divided in two operations:

- Installation of the inter-array or infield cable which connects the wind turbines in arrays and then to an offshore substation
- Installation of export cable, connecting the offshore substation to the onshore substation in order to transfer the generated power to the grid.

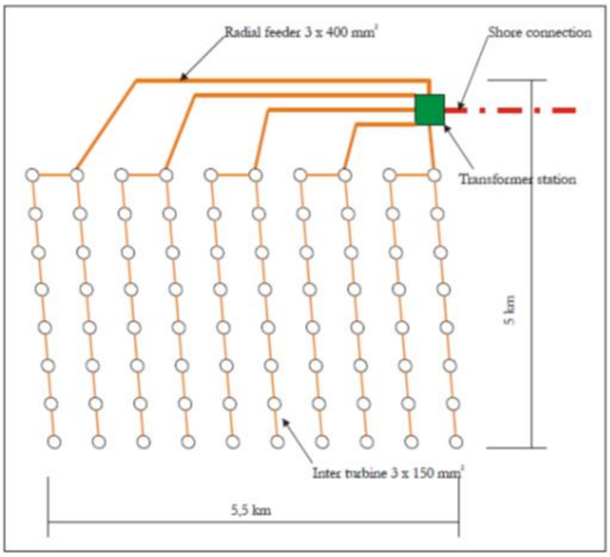

Figure 2.4 Example of Horns Rev OWF cable layout.

These two operations could be divided in different sub-processes, using different types of cables, equipment and vessels. Furthermore, the methods that are applied to install the infield and the export cable differ. All of the above are presented in detail in the following paragraphs.

2.3.7.1 Cables

There is a variety of cables that are used in offshore wind farms cable installation. First it must be mentioned that cables of different diameters are used to transfer successfully the generated current, at the predefined connection voltage. Compared to cables that connect the wind turbines in an array, cables which connect a whole array to the offshore substation has larger diameter, since it should be able to transfer the maximum total current generated by the array.

Apart from cable diameter there are other important characteristics that the engineers take into account during the cable layout design phase, such as: type and number of conductors, maximum bending radius, the insulation, the screening layer and the metallic sheathing and the armour [18]. Usually for inter-array cables as well as export cable, 3C HVAC cable is preferred. However in the future, as the OWF move further offshore, it is expected that HVDC cables will be used for export cable in order to minimize the losses when transporting current over longer distances. [20]

The physical characteristics of cables which influence most the installation operation are: the outside diameter of the cable (e.g. value for infield HVAC cables ranges between

100 – 300 mm) the weight per meter ratio (e.g. 30-60 kg/m) and the minimum bending radius which plays a significant role in cable laying process [19].

Some types of submarine cables used in offshore wind farms are presented in Table 3

Table 2.1: Types of submarine cables [8]

					
Rated Voltage	33 kV AC	150 kV AC	420 kV AC	320 kV DC	450 kV DC
Insulation	XLPE, EPR	XLPE	Oil/paper or XLPE	Extruded	Mass Impregnated
Typical Application	Connection of offshore WTG	Export cable	Crossings of rivers with large export capacity	Long distance connections of OWF	Interconnection of power grids
Max length	20-30 km	70-150 km	< 50 km	> 500 km	> 500 km
Typical rating	30 MW	180 MW	700 MW/ 3 cables	1000 MW/ Cable pair	600 MW/ cable

2.3.7.2 Cable protection

Until 1980s a common practice was to lay the submarine cables unprotected, leading to more and more failures as also the fishing equipment (anchors and trawls) was getting heavier. Appropriate subsea burial equipment was available after 1980s and a lot of studies were conducted resulting that cable burying of subsea cables is very important [21].

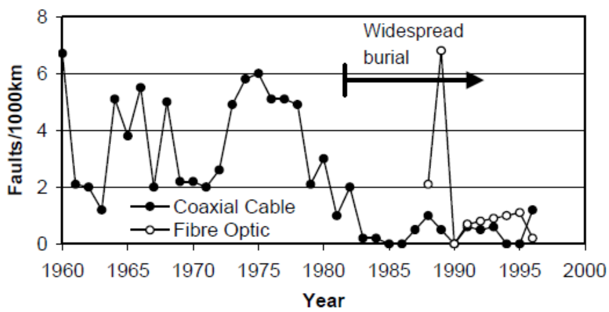

Figure 2.5: Failures of cables during previous years [22].

Cable burying is the most used method for protecting submarine cables. In order to specify the burial depth an index was introduced. This is the Burial Protection Index which indicates the burial depth in relation to the soil type (Figure 2.6).

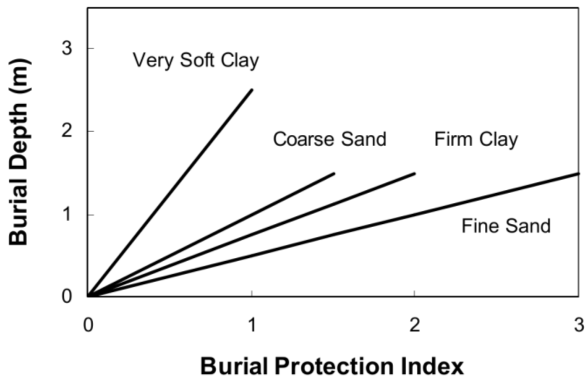

Figure 2.6: Burial Depth based on different soil types [22].

A typical cable burial can be divided in four sub processes. In Table 6 below the four processes of the cable burying as well as the different methods for each stage, are presented.

Table 2.2: Methods of burying cable

Cable Burying operation	Methods
Break cohesion	Erosion Jetting Cutting
Remove soil	Mechanical transportation Hydraulic transportation
Burial of the cable	Pre-lay trenching Post-Lay burial Simultaneous Lay and Burial
Deposition of soil	Power driven tools are used in order to backfill the trench (Active process) Natural erosion forces are used to backfill the trench (Passive process)

It is worth mentioning that in case of cable crossings a different protection method should be considered, since the cable burying is not feasible. In Europe the most common method is by placing concrete mattresses at the crossing location over the existing line prior to laying the new line. Alternative methods of protections that can be used are the rock placement and the use of articulated pipes (armouring).

2.3.7.3 Infield cable installation

Regarding the layout of the infield cables, it is worth mentioning that there are different system configurations in order to collect the AC current produced by the wind turbines to the offshore substation. The design engineers are responsible to choose one of the following configurations:

- **Radial configuration**. It is simpler and less expensive than the other two, mainly due to a smaller amount of required cable. However, it is considered as the least reliable as in case of cable failure the whole array does not function.
- **Ring configuration**. It is an extended configuration of the radial system, where two arrays are connected in a ring arrangement. It is more reliable but is more complex and expensive due to the amount of cable needed.
- **Star configuration**. The voltage is not transformed in each turbine, as in radial configuration, but in the transformer located in the centre of each star (i.e. group of wind turbines) [27]

After the design regarding the cable layout and the before mentioned characteristics, the following processes should be performed in order to install infield cable**:**
Initially, a survey takes place in order to verify that the route between the wind turbines is clear and it is possible for the cable to be laid and buried. Also pre lay grapnel run, takes place to ensure the suitability of the seabed for the cable installation. Furthermore, in the event that sand waves are observed, the use of a suction hopper dredge could be used in order to prepare the cable route.
Afterwards, the installation of the cable takes place. Regarding the installation of the inter-array cable, the following processes should be performed in order to install all the cable interconnections infield:

- CLV is loaded with cable and the burial tool is prepared
- Transport to the site and positioning
- Pull-in first end using a messenger wire and fixation of the cable head
- The cable is laid until the next WT
- The cable is connected to the next turbine performing second Pull-in through a j-tube using a messenger wire and fixating the second end.
- Burying of the main length of the cable using one of the following methods
    - Post lay burial is performed by a separate vessel using trenching/ jetting equipment
    - Bury simultaneously the cable using a plough or a burial sled which is towed by the vessel
    - A self-propelled ROV is used to simultaneously bury the cable.
    - A separate vessel is used in order to open a pre-cut trench. Then the cable is laid inside the trench by the cable laying vessel. It must be mentioned that this method is not used often because of difficulties in coordinating the two vessels as well as in maintaining the trench [19]

In order to complete the infield installation, sometimes a diving support vessel and a rock dumping vessel could also be used. The diving support vessel contributes in pull-in activities and burial of the transition part of the cable between the exit of the j-tube and the buried by the burial tool, part of the cable. The rock dumping vessel places rocks over the “transition zone” installing the upper layer of scour protection. [13]

2.3.7.4 Export Cable Installation

Concerning the export cable connection, a route survey as well as a grapnel run should be performed before the installation starts. Simultaneously, the cable is prepared by using pull-heads and become ready to be paid out.

Regarding the installation of the export cable, the following activities should be performed by the cable laying vessel:

- Load-out of vessel with cable length and preparation of burial tool
- Sail to site and take up position at shore connection point
- Pull-in offshore landing section
- Deploy burial tool and lay cable and simultaneously bury towards wind park
- Take up position for pull-in at central collection point
- Pay out rest of the cable with floatation at the cable tail end
- Pull in of cable tail at central collection point
- Remove floatation and complete burial of remaining cable section

Then in order to land the export cable to the shore, a duct has already been drilled on the beach so that the cable can be pulled ashore through the duct, by a winch. The landing of the cable is performed by following the subsequent steps [13]:

- Cable lay vessel takes up position just offshore of the landing point.
- Winch cable is brought from the beach to the cable vessel and connected to cable pull-head
- The cable is paid out, fitted with floaters and pulled onto the beach
- The cable gets connected to the messenger wire and transferred into the duct and pulled to the grid connection manhole.
- The floaters are removed from the cable
- The burial tool is placed on the cable as close to the beach manhole as possible and burial of the cable to intended depth commenced
- Cable lay vessel continues laying and burying the cable towards the wind park, or to where the cable has already reached the required depth.

A more detailed description of the cable laying and pull in for both infield and export cable can be found in Table 2.3 and Table 2.4.

Table 2.3: Details of infield cable installation.

Infield cable processes	**Information**
Pull in first end	Winches on the transition piece of the WT or winches on the CLV (pull-back). Diver or ROV
Cable hang off first end	Clamps used to fixate the cable.
Cable laying methods	Cable being paid out slowly when the vessel moves slowly ahead.
Cable pull-in second end	Methods: Quadrant, Dog leg and Floating

Hang off second end	Strip the cable armouring and fixate the second cable end in the hang off system using the armouring
Electrical connection	Cable connected to the terminal of the WT
Testing	Optical fibres are tested in site. Test end terminations

Table 2.4: Details of export cable installation.

Export cable processes	**Information**
Horizontal Directional Drilling (HDD)	Drill a hole under the beach into the open water. Hole is lined with steel or plastic pipes for the later pull in of cables.
Cable pull in shore end	Direct: the vessel approaches the beach. Then the pulling wire is used to pull the cable (with floats attached to it) to shore. Preinstalled: a low draft vessel is used to preinstall a separate shore end cable and the main CLV joints the cables.
Cable hang off shore end	Strip the cable armouring. Subsequently fixate the first cable end in the hang-off system using the armouring.
Cable laying	Usually the cable length is not enough to cover the distance from the substation to shore. Therefore the vessel need to return to the quay to load the cable carousel
Cable pull in second end	After installing the pull-in winch the CLV gets in position in order to create slack. Then the cable is cut at appropriate length and get clamped to the bending restrictor
Hang off second end	Strip the cable armouring and fixate the second cable end in the hang off system
Electrical connection	Cable connected to the offshore substation
Testing	Test end terminations

2.3.7.5 Cable installation vessels

Diverse vessels, such as cable laying vessels, cable laying barges, support vessels and rock dumping vessels are often used to perform the cable installation. Also in some cases, different CLV could be used in infield and export cable installation because the export cable is more stiff and of larger diameter among other reasons [13]. Obviously, the most complex and essential for the cable installation are the vessels which transfer and install the cables. Therefore, a description about the cable laying vessels and the cable laying barges is following.

- **Cable Laying Vessels (CLV)**

Specially designed vessels used in cable installation are called cable laying vessels or cable layers and they have been deployed since 1870's. They are available in various sizes with all kind of equipment. However an important distinction should be made between the CLV suitable for power cable installation and the CLV that are designed for installing telecom cables. The latter are lacking the required cable handling equipment, since they are designed to work with smaller and lighter cables.

One of their main properties of CLV is the presence of one or more carousels/ turntables, which are capable of storing large amounts of cables (up to 10000 tons) by taking into account the maximum bending radius of the cable. Usually cable layers also have cable guiding sheaves, loading arm, tensioners and appropriate installation devices like Remotely Operated Vehicles (ROVs). The majority of modern CLV are equipped with Dynamic positioning (DP) systems which have the ability to maintain their position under rough weather conditions [25].

- **Barges**

In order to reduce the cost of cable installation, the use of a non-self-propelled barge properly equipped for the operation, which is driven by tugs or using anchoring, may be considered as an alternative solution. This solution may seem appealing but it must be noted that there are drawbacks. Firstly there is need of highly experienced personnel since the majority of the automated processes of a CLV are not available (e.g. the cable laying system is not linked to the positioning system). Moreover if the barge needs to be stopped to joint another section of cable it must be immobilized while that activity takes place, which leads to be subject to weather conditions [8]. However regarding the export cable, barges are mainly used for shallow waters near shore, where the CLV cannot operate. In this case it is important that sufficient cable to cover the route in one run, can be loaded, avoiding joints.

Figure 2.7: Left: Cable laying vessel, Right: Cable laying barge

2.3.7.6 Cable installation equipment

The more important special designed equipment that exist in a Cable laying vessel or barge in order to perform successfully the cable laying, consists of:

- **Turntable or Carousel:** It is suitable for storing large power cables which won't be possible to be stored in a fixed tank. Usually it is loaded in horizontal layers starting from the base. The most recent turntables can store up to 10000 tons of cable.
- **Cable drums:** They are appropriate for storing cables purposed for project where little cable length is needed, such as infield cable installation in a small wind farm. Also they can be installed in cable laying vessels or barges when extra amount of cable is needed.
- **Cable Tensioners:** They are also called as "linear machines" and they are responsible for gripping the cable in order to apply necessary tension during cable laying operation. Usually they include pairs of wheels, although sometimes they may have belts called "caterpillars".
- **Emergency cutter:** It is responsible for performing rapid cutting in case of emergency.

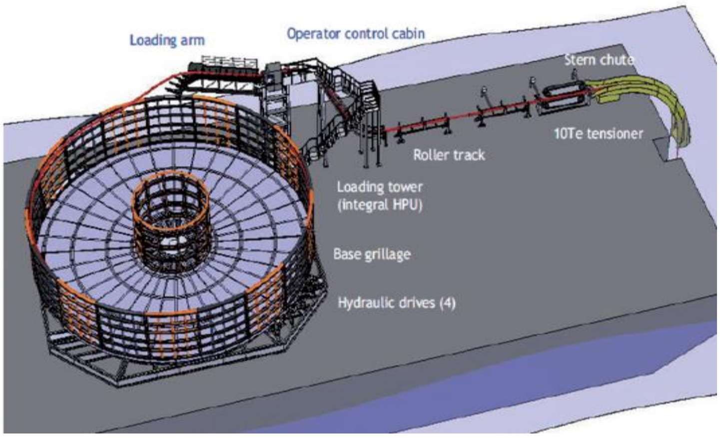

Figure 2.8: Cable laying equipment on CLV deck [23]

There are different types of equipment used in every aspect of the cable installation. As it was mentioned before, the burying of cables is essential. Therefore, it is important to present the equipment used in burying the cable. Available burial equipment consist of [24]:

- **Ploughs:** A plough digs a trench and places the cable simultaneously in the sea floor, before the removed soil backfills the trench naturally due to gravity. Ploughs can be used for different types of soil and from shallow water to 1500 m depth. There are various types of cable ploughs such as narrow share cable ploughs, advanced cable ploughs, modular cable ploughs rock ripping ploughs and vibrating share ploughs. It worth mentioning that this method is typically used in export cable installation and that the vessel used in the burying should have sufficient bollard pull in order to be able to tow the plough ensuring that the simultaneously laying and burying is performed correctly.
- **Tracked cable burial machines:** They are vehicles controlled by an umbilical cable connected to the support vessel. Based on the soil type, they use jetting or mechanical cutting tools to bury the already laid cable. Usually they are deployed for shorter lengths of cable burial. Divers are often used to

assist the installation in shallow waters. They can operate form shallow waters up to 2000 m water depth. There are various types that have different parts such as: jetting systems, rock wheel cutters, chain excavators, dredging systems.

- **Free swimming ROVs with cable burial capacity:** They are remotely operated from the host vessel in order to bury the already laid cable by using jetting or dredging systems. They can be used only for clay and sandy soils, from 10m to 2500 m water depth.
- **Burial Sleds:** They are often used in shallow waters and they can use a variety of different tools such as jetting systems, rock wheel cutters, chain excavators and dredging systems in order to be able to operate in different soil types. They either have subsea power or utilise the power system of host vessel.

Plough

Tracked cable machine

ROV

Burial Sled

Figure 2.9: Burying equipment

2.4 Need of simulation tool

Trying to optimise and make optimal decisions concerning the planning of such a complex process as the installation of an offshore wind farm, is practically impossible without using a specially designed tool. The common practice to install the transmission system is planning the required operations using deterministic methods considering the worst cases [9]. However, the conditions and processes that influence the decision are stochastic and contain a large level of uncertainty. These uncertainties and the random nature of the environment (boundary conditions for the system) need to be taken into account in the optimization process.

Therefore, simulation and optimization tools have been developed over the past years, in order to address the major disadvantage of the OWF (i.e. the capital cost) and help professionals in the decision making (e.g. SIMO tool or ECUME tool used by EDF group).

The purpose of such tools is to simulate different proposed scenarios and propose an optimal solution in terms of cost and time. It is expected that this trend will continue as long as the offshore wind sector continues to grow and the decisions to be taken are based on money and time involved.

Although some simulation and optimization tools for the installation of OWF already exist, the majority of them do not include the uncertainties regarding the met-ocean conditions or the risk of failures, which may influence the installation. For that reason the designed tool in the current thesis aims to incorporate the uncertainties of the cable installation and provide to the user a better insight on the required time to complete the activities.

3. Construction of weather time series including dependence

In order to create the simulation tool for the logistics of the cable installation in an OWF, first the time series of the significant wave height and the average wind speed during one-hour intervals must be constructed. The tool will calculate the installation time of each proposed solution based on these weather conditions. Therefore, as far as the simulation's results are concerned, it is crucial to find a way to produce, in a computationally efficient way, a large number of time series that represent the weather conditions in the site realistically.

There are several different methods found in literature to produce time series of weather conditions, such as Markov chains and Monte Carlo simulations [29]. In the current thesis a different and relatively new method was chosen; in order to find the dependence between the wind speed and the wave height, Copulas functions were used. Copulas have been used in the past in order to find the dependence between two or more random variables and it is stated that this approach has benefits over traditional Markov chains [30]. In this chapter the basic statistical concepts needed for the copula approach, the methodology applied for the analysis, as well as the results of the weather data analysis are presented.

3.1 Basic concepts

In this paragraph some basic statistical concepts are defined and presented. These concepts are essential to the copulas approach.

A random variable (r.v.) was described by Gnedenko (1962) as follows "a random variable is a variable quantity whose values depend on chance and for which there exists a distribution function."

The cumulative distribution function of a random variable X is defined as a function F such that $F_X(x) = P[X \leq x]$ [31].

The probability density function of a continuous random variable X is defined as the derivative of the distribution function as follows:

$$f_X(x) = \frac{dF_X(x)}{dx}$$

The mean value of a random variable X is defined as:

$$E(X) = \int_{-\infty}^{\infty} x f_X(x) dx$$

The variance of a random variable X is defined as follows [32]:

$$Var(X) = {\sigma_X}^2 = E\{(X - E(X))^2\}$$

Random variables $X_1, \dots X_n$ are independent if for any interval $I_1, \dots I_n$,

$$P\{X_1 \in I_1, \ldots, X_n \in I_n\} = \prod_{i=1}^{n} P\{X_i \in I_i\}$$

In order to measure the dependence between random variables, the most used measure is Pearson's correlation coefficient or product moment correlation. The product moment correlation of random variables X, Y is defined for finite expectations *E(X), E(Y)* and finite variances $Var(X), Var(Y)$ is:

$$\rho(X,Y) = \frac{E(XY) - E(X)E(Y)}{[Var(X)Var(Y)]^{1/2}} = \frac{E[(X - E(X))(Y - E(Y))]}{[Var(X)Var(Y)]^{1/2}} = \frac{Cov(X,Y)}{[Var(X)Var(Y)]^{1/2}}$$

The basic properties of product moment correlation are:

- Range: $-1 \leq \rho(X,Y) \leq 1$
- Independence: if X, Y are independent, then $\rho(X,Y) = 0$
- Invariance under linear transformations:
  for $a, c \in \mathbb{R}\backslash\{0\}, b, d \in R, \rho(a X + b, c Y + d) = sgn(a c)\rho(X,Y)$
- Linear dependence: if $\rho(X,Y) = 1$ then for $a > 0, b \in R, X = aY + b$

Product moment correlation measures the linear dependence between random variables (i.e. is the geometric mean of the best linear predictor of $X(Y)$ given $Y(X)$). When high values of a r.v. match high values of another r.v. while small values of the same r.v. match small of the other one these random variables are positively correlated and the Pearson correlation has positive value. On the other hand when low values of a r.v. matches high values of another r.v. while high values of the first match low values of the second, then Pearson's correlation has negative value [33].

Pearson's correlation fails to capture the dependence of r.v, whose relationship is not necessarily linear but monotonic. Spearman rank correlation overcomes this barrier by measuring the correlation between the ranks of the values of r.v. In this way the monotonic relationship between the random variables is taken into consideration. One could say that the rank correlation is a more flexible measure of dependence, because it always exists and does not depend on marginal distributions [41]. Marginal distributions of the random variables are transformed into ranks by applying the cumulative distribution function.

Spearman's rank correlation coefficient of random variables X, Y with cumulative distribution functions (cdf) F_X and F_Y is defined as:

$$\rho_s(X,Y) = \rho(F_X(X), F_Y(Y))$$

with the following properties:

- Range: $-1 \leq \rho_s(X,Y) \leq 1$
- Independence : if X, Y are independent, then $\rho_s(X,Y) = 0$
- Invariance under non-linear monotonic transformations:
  if $G: \mathbb{R} \rightarrow \mathbb{R}$ a strictly increasing function, then $\rho_s(X,Y) = \rho_s(G(X),Y)$
  if $G: \mathbb{R} \rightarrow \mathbb{R}$ a strictly decreasing function, then $\rho_s(X,Y) = -\rho_s(G(X),Y)$

- Monotonic dependence: if $\rho_s(X,Y) = 1$ then there exists a strictly increasing function $G: \mathbb{R} \to \mathbb{R}, X = G(Y)$

Finally, it must be mentioned that although usually Pearson correlation and Spearman correlation are different, for uniform variables they are the same. It must be mentioned that rank correlation is not enough to represent the dependence between random variables [33]. Therefore, Copulas approach should also be used to describe the dependence of r.v.

Another useful concept that should be defined is tail dependence. One could describe tail dependence as the limiting proportion that the value of a r.v exceeds a certain threshold with a certain probability given that the value of another r.v. has already exceeded threshold with the same probability. The upper tail dependence coefficient for a two dimensional random vector $X = (X_1, X_2)$ with marginal distribution functions F_1 and F_2 is given by:

$$\lambda_U = \lim_{u \to 1} P\{X_1 > F_1^{-1}(u) \mid X_2 > F_2^{-1}(u)\}$$

while for lower tail dependence of X:

$$\lambda_L = \lim_{u \to 0} P\{X_1 \leq F_1^{-1}(u) \mid X_2 \leq F_2^{-1}(u)\}$$

One can say that X is upper tail dependent if and only if $\lambda_U > 0$ and lower tail dependent if and only if $\lambda_L > 0$. Moreover, X is upper or lower tail-independent when $\lambda_U = 0$ and $\lambda_L = 0$ respectively [34].

3.2 Copulas

Copulas are functions that join or "couple" multivariate distribution functions to their one-dimensional marginals. Alternatively, copulas are multivariate distribution functions whose one-dimensional margins are uniform on the interval [0,1] [31].

The most important theorem regarding the copulas is the Sklar's theorem. Sklar's Theorem states that any multivariate joint distribution can be written in terms of univariate marginal distribution function and a copula which describes the dependence between the variables. For the multivariate case, concerning n variables, it is defined as following:

$$F(y_1 \dots y_n) = C\{F_1(y_1), \dots, F_n(y_n)\}$$

For the two dimensional case let $H_{XY}(x,y)$ be a joint distribution function with marginal distribution $F_X(x)$ and $G_Y(y)$. Then there is a Copula C such that for all x, y in I^2 (meaning the interval $[0,1] \times [0,1]$).

$$H_{XY}(x,y) = C\{F_X(x),\ G_Y(y)\}$$

If F and G are continuous then C is unique; otherwise, C is uniquely determined on $RanF \times RanG$. Conversely if C is a copula and $F_X(x)$ and $G_Y(y)$ are CDFs then $H_{XY}(x,y)$ is the joint CDF with margins $F_X(x)$ and $G_Y(y)$.

Any copula C represents a model of dependence which is bounded by two extremes named "Frechet - Hoeffding bounds" and translates into the following inequality:

$$C_L \leq C \leq C_U$$

where $C_L = \max(0, u + v - 1)$ and $C_U = \min(u, v)$ are copulas that represent perfect negative and positive dependence respectively [35][33].

There is a large variety of different copulas functions. The most common families of copulas are the following:

3.2.1 Gaussian (Normal)

Using the bivariate Normal distribution and applying the standard normal cdf to the standard normal marginals one can transform the standard normal marginals into uniforms. Subsequently one can obtain the Gaussian copula.

$$C(u, v) = \Phi_\rho\left(\Phi^{-1}(u), \Phi^{-1}(v)\right),$$

where $\Phi_\rho(x, y) = \int_{-\infty}^{x} \int_{-\infty}^{y} \frac{1}{2\pi\sqrt{1-\rho^2}} e^{\frac{2\rho st - s^2 - t^2}{2(1-\rho^2)}} ds\, dt$ and Φ the standard normal CDF [36].

Although Gaussian copula is the most used copula, it does not represent the dependence between the extreme values of random variables (i.e. tail dependence). For that reason other copulas families which allow tail dependence can be used.

3.2.2 Archimedean Copulas

Archimedean copulas constitute another very popular family of copulas that may be used in different applications, mainly due to their many different sub-families and the ease of construction. There are one-parameter families or two-parameter families of Archimedean copulas.

An Archimedean Copula is defined as:

$$C(u, v) = \varphi^{-1}(\varphi(u) + \varphi(v))$$

where φ is the generator of Archimedean copula, a strictly decreasing, continuous, convex function. The pseudo-inverse of φ is defined as:

$$\varphi^{-1}(u) = \begin{cases} \varphi^{-1}(u), & 0 \leq u \leq \varphi(0) \\ 0, & \varphi(0) \leq u \leq \infty \end{cases}$$

Gumbel copula and Clayton copula are two of the most used one-parameter Archimedean Copulas. For example, the generator of Gumbel copula is $\varphi(u) = (-\ln(u))^\theta$, $\theta \in [1, \infty)$, while the generator of Clayton copula is $\varphi(u) = (u^{-\beta} - 1)/\beta$, $\beta \in [-1, \infty)$ [36][43].

So the Gumbel copula is defined as:

$$C(u, v; \theta) = \exp\{-[(\ln(u)^\theta + ln(v)^\theta]^{\frac{1}{\theta}}\}$$

and the Clayton copula is defined as:

$$C(u,v;\beta) = (u^{-\beta} + v^{-\beta} - 1)^{-\frac{1}{\beta}}$$

In Figure 3.1 the density functions of the three before mentioned copulas are presented. The rank correlation of both Gumbel and Clayton plots is equal to 0.8. Regarding the density function plots of the Gumbel copula and the Clayton copula, it is apparent to the observer that there is upper tail dependence and lower tail dependence respectively.

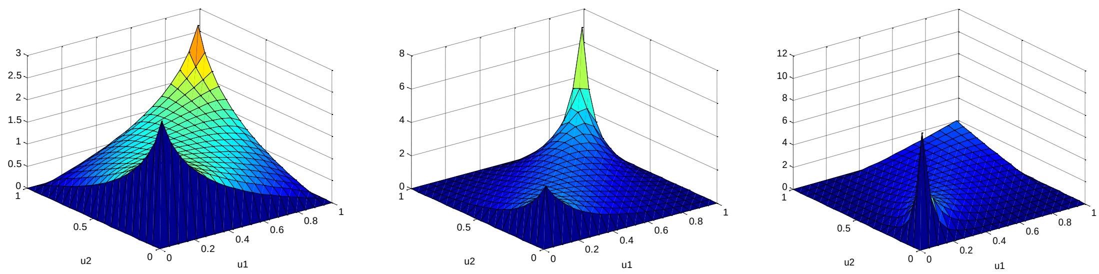

Gaussian copula ($\rho = 0.5$) Gumbel copula ($\theta = 2$) Clayton copula ($\beta = 2$)

Figure 3.1: Density functions of Gaussian, Gumbel and Clayton copulas.

3.3 Weather data

Since the limits of the vessels that take part in the infield cable installation mainly concern the wave height and wind speed, historical time series containing the significant wave height as well as the average wind speed during the time interval were required. The significant wave height is defined as the mean over the upper third of the observed wave heights during the time interval [43].

In order to find the dependence between the wind speed and the wave height, two sets of measured data were investigated. The first set of historical weather observations was available on the website of National Oceanic and Atmospheric administration where values of the significant wave height and the average wind speed are provided among others. The second set of metocean historical conditions was provided from Deltares and contains wind speed and significant wave height observations.

- **NOOA data**

First the analysis of the weather data, found in NOOA website, was conducted. The first set of historical data concerns weather observations from station 41010, located in east of Cape Canaveral (indicated in Figure 3.2), over the past 21 years from 1990-2011.

Figure 3.2: Map showing the location of station 41010.

It must be mentioned that some data were missing, probably because of a failure in the measuring/recording equipment. These measurements were noted by the value 99 and they were excluded from the measurements. Furthermore, while sixteen out of twenty-one provided annual time series were in hourly basis, the rest of the annual data were in 30 minutes intervals. Since it is known that the greater the sample size the better for the fitting of Copulas [37] instead of not including those years, it was decided to transform the measurements of the years containing 30-minutes intervals by choosing the greater value observed during one hour. The reason behind this decision was based on the fact that the weather data analysis will be used to produce random time series of significant wave height and average wind speed which will determine whether the vessels can operate or not. Therefore by choosing the maximum value observed during the one hour period, the prediction of the produced time series will be a conservative one. In Figure 3.3 the scatter plot of wind speed (in m/s) and significant wave height (in m) is presented. One can observe positive rank correlation of the order of 0.64.

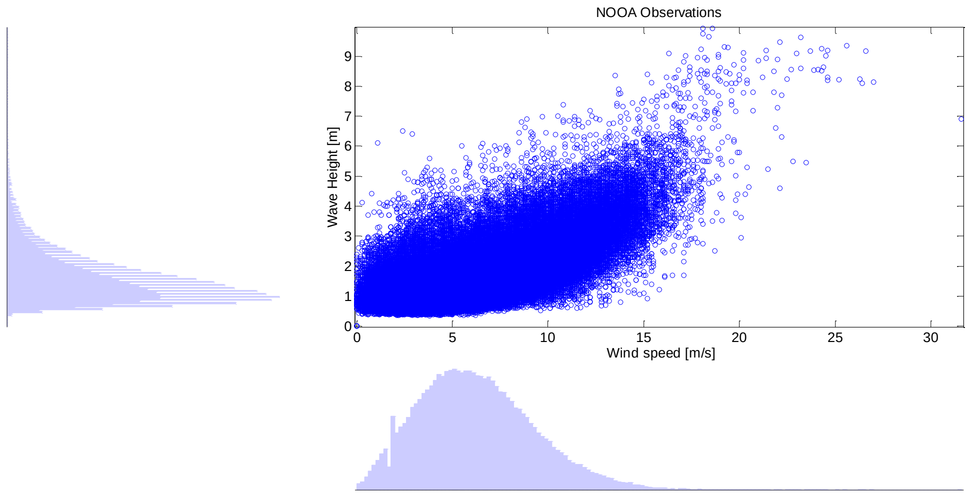

Figure3.3: Scatter plot of average wind speed and significant wave height observations from NOAA.

- **Deltares weather data**

The second set of weather data was provided from Deltares which is also involved as a contributor in FLOW project. The observations were collected from area A121 located in the North Sea (indicated with a red dot in Figure 3.4), during a 3 year period from 2010 to 2013 in 10 minutes interval. Since the simulation will be in hourly basis, the measurements of the years containing values in 10-minutes intervals were transformed in one hour intervals by choosing the greater value observed during one hour.

Figure 3.4: Map showing the location of area A121 in North Sea.

In Figure 3.5 the scatter plot of wind speed and significant wave height is shown. As one may observe there are very high values of significant wave height for very small values of wind speed (around zero). This fact could be characterized as contradictory to reality. Further investigation was conducted and showed that there were large differences between two successive wind speed measurements. For example there were cases where the wind speed was raised from 0.2 m/s to 13 m/s in 10 minutes period. These events are not realistic and they indicated that there was probably a failure in the anemometer. For that reason, it was decided to exclude the samples which appeared wave heights larger than 3 m and wind speeds smaller than 1 m/s. The scatter plot of the corrected data is presented in Figure 3.6.

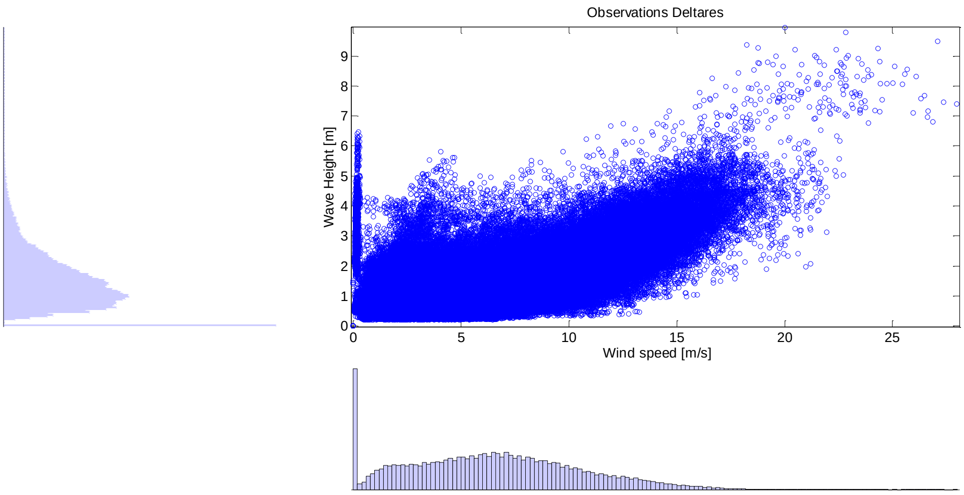

Figure 3.5: Scatter plot of average wind speed and significant wave height observations provided by Deltares, before corrections.

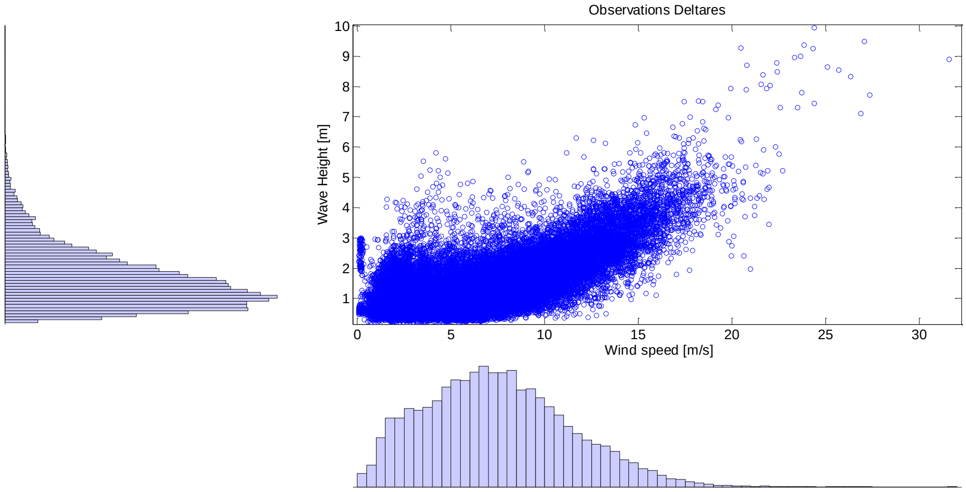

Figure 3.6: Scatter plot of corrected average wind speed and significant wave height observations provided by Deltares.

In this section the scatter plots of the two available weather data sets were presented in order to get a first impression regarding the behavior of wind speeds and wave heights. One can observe for both weather data sets that large values of wind speed do not encounter small values of wave heights and vice versa. Another interesting remark that should be mentioned is that although the weather data were measured in different locations, they are similar. The observed extreme values of wind speed and wave height regarding both weather data sets, have the same level. Also the rank correlation of the two data sets are similar, with values equal to 0.64 and 0.61 for NOOA and Deltares data respectively. The rank correlation can vary from -1 to 1 for perfect negative and perfect positive correlation respectively. Both weather data sets have positive correlation which means that large values of wind speed are more likely to encounter large values of wave height.

3.4 Methodology of analysis

In order to find the dependence structure of the wind speed and the wave height, through the parametric copulas described in section 3.2, based on both sets of available measurements, an analysis consisting of different tests was performed for the whole set of observations as well as for each month separately. In this section the performed tests as well as the results for the total number of available weather data from NOOA and Deltares, are presented.

The following procedure was followed for the weather data analysis:

- Transformation of observations into ranks.
- Calculate square differences based on Cramer von Mises statistics.
- Calculate Semi-correlations.
- Calculate exceedance probabilities for different percentiles.

First the before mentioned analysis was conducted for the entire weather data sets in order to acquire a first impression on the dependence of wind speeds and wave heights. Following the same analysis was conducted for each month separately in order to take into account the seasonality of weather data.

3.4.1 Transforming observations into ranks

The underlying copula of a random vector is invariant by continuous, strictly increasing transformations. Therefore the observations (X_{ij}), when i reffers to the r.v. and j to the number of the sample, can be safely transformed to pseudo-observations, using the ranks. The pseudo-observations are defined as:

$$U_{ij} = \frac{R_{ij}}{n+1} = n\hat{F}_j(X_{ij})/(n+1)$$

where

n the number of the observations and

$\hat{F}_j$ the empirical cumulative distribution function defined as: $\hat{F}_j(t) = \frac{1}{n}\sum_{i=1}^{n} \mathbf{1}(X_{ij} \leq t)$

First, the values of observations are transformed into ranks by adjusting for ties using tiedrank Matlab function and then the ranks are divided by $(n+1)$, producing the pseudo-obseravations. The pseudo-observations can be characterized as a sample of the underlying copula [37]. In Figure 3.7 the calculated pseudo-observations for both sets of available data are presented.

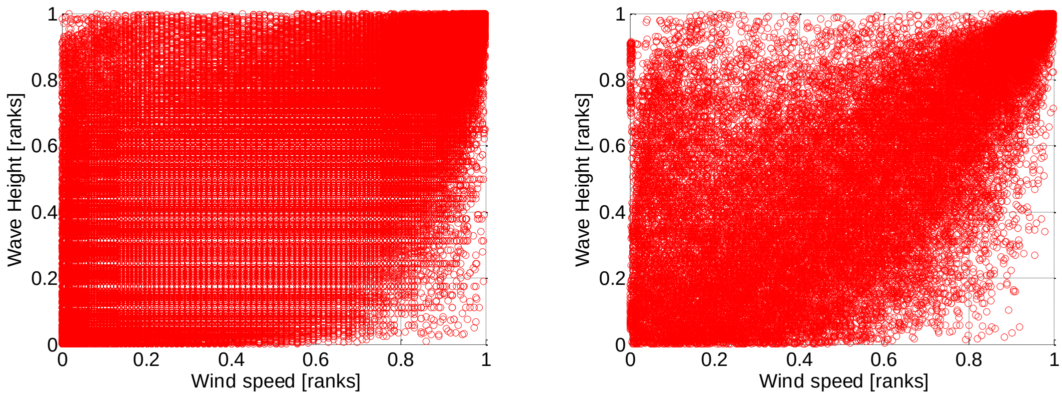

NOOA data transformed into pseudo-observations

Deltares data transformed into pseudo-observations

Figure 3.7: Pseudo-observations plots

3.4.2 Square differences based on Cramer - von Mises statistics

It was decided to investigate three of the most used Copulas: Gaussian, Gumbel and Clayton Copula. In order to find which Copula fits the data best, "blanket tests" are usually utilized. The "blanket tests" are favored compared to other methodologies due to the fact that they do not involve parameter tuning or other strategic choices [37]. There are various types of "blanket tests" but in this study the test that focus on calculating the sum of square differences between the empirical C_n and the parametric copula C_{θ_n}, based on Cramer-von Mises statistic was exploited. The empirical copula is a non-parametric estimator of the true Copula and it summarizes the information of pseudo-observations. The empirical copula for the multivariate case with d r.v. is defined as:

$$C_n(u) = \frac{1}{n}\sum_{i=1}^{n} \mathbf{1}(U_{i1} \le u_1, \dots, U_{id} \le u_d), \qquad \boldsymbol{u} = (u_1, \dots, u_d) \in [0,1]^d$$

The Cramer-von Mises type statistic for an empirical process $A_n = \sqrt{n}(C_n - C_{\theta_n})$, is defined as [54]:

$$S_n = \int_{[0,1]^d} A_n^2(u) dC_n(u) = \sum_{i=1}^{n} \{C_n(U_{i,n}) - C_{\theta_n}(U_{i,n})\}^2$$

The sum of the square difference between the Empirical and the parametric copula was calculated for every copula under consideration (i.e. S_N for Gaussian, S_{Gum} for Gumbel and S_{Cl} for Clayton). These values, calculated for both available weather data sets are presented in Table 3.1.

Table 3.1: Sum of square differences for each copula under consideration

	S_N	S_{Gum}	S_{Cl}
NOOA	1.2848	0.5084	9.7843
Deltares	2.1420	0.9587	11.2876

One may observe that for both weather data sets the Gumbel copula has the smaller square difference compared to Gaussian and Clayton copula; meaning that the Gumbel copula has the smallest "distance" between empirical copula and the estimation represented by the parametric copula. This indicates clearly that the Gumbel copula is the copula that fits the data best among the copulas under consideration. However more tests were conducted in order to verify that result.

3.4.3 Semi-correlations

Another approach to estimate which copula describes better the joint distribution of wave height and wind speed, concerns the calculation of Pearson correlation for upper and lower quadrant of the actual observations transformed to standard normal N(0,1) margins. Let Φ denote the standard normal cumulative distribution function, then $Z_j = \Phi^{-1}(U_j)$, for $j = 1 \dots, d$ are the standard normal transforms of the pseudo-observations [44]. In Figure 3.8 the scatter plots for the transformed weather data are presented.

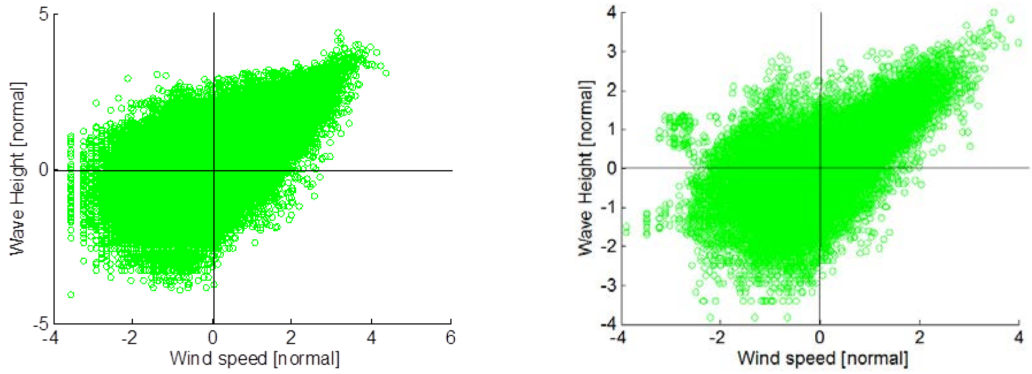

NOOA Deltares

Figure 3.8: Scatter plots of transformed weather data

After dividing the standard normal transforms of observations into four quadrants, for positive correlation the upper semi-correlation is defined as:

$$\rho_{ne} = \rho(Z_1, Z_2 \mid Z_1 > 0,\ Z_2 > 0)$$

and the lower semi-correlation is defined as:

$$\rho_{sw} = \rho(Z_1, Z_2 \mid Z_1 < 0,\ Z_2 < 0).$$

The upper and lower quadrant correlations indicate whether or not there is tail asymmetry. When there is tail asymmetry, the two semi correlations present an obvious difference [44]. Also, these values could be compared to the product moment correlation of all quadrants ρ. If the values of semi-correlation are larger than the overall Pearson correlation, then there is tail dependence.

In Table 3.2, the calculated semi-correlations as well as the overall Pearson correlation for both available weather data sets are presented. The calculated values of semi-correlations clearly show that there is tail asymmetry. Also, it can be seen that the upper quadrant semi-correlation regarding Deltares data is larger than the overall correlation when the upper quadrant semi-correlation regarding NOOA data are very close. This result suggests that a model with upper tail dependence is more preferable. Considering the three copulas under investigation, only Gumbel Copula has upper tail dependence. Therefore this test also indicates that Gumbel Copula expresses the dependence of wind speed and wave height best.

Table 3.2: Semi-correlations for upper and lower quadrants

	ρ	ρ_{ne}	ρ_{sw}
NOOA	0.6412	0.6322	0.1531
Deltares	0.6123	0.7092	0.1278

3.4.4 Conditional exceedance probabilities for different percentiles

Finally, another test was conducted in order to further support the decision of choosing the Gumbel Copula. During this test the conditional exceedance probability is calculated for different percentiles of the observations. Then it was plotted in a graph with the conditional exceedance probabilities for each different Copula under investigation, in order to evaluate which Copula describes better the extreme cases of high wind speeds and wave heights. Also it must be mentioned that since the purpose of this study is to find the right copula that will be used to produce weather time series which will help to find whether or not the vessels are able to operate during the time intervals, the percentiles (u_p) that are investigated should correspond to values close to the limits of the vessels. Therefore it was decided to investigate percentiles from 0.8 to 0.99 with 0.01 step. Following this approach it is safe to assume that these percentiles include the limits of the vessels.

The conditional exceedance probability of the observations is defined as the conditional probability of events A and B as follows:

$$P(A|B) = \frac{P(A \cap B)}{P(B)}$$

where A the case that the wave height exceeds the u_p of the significant wave height observations and B the case that the wind speed exceeds the u_p of the wind speed observations. Since the number of observations is the same, the calculation of conditional exceedance probability for a particular percentile is simplified to:

$$P\left(X_2 > u_p \mid X_1 > u_p\right) = \frac{\sum_{i=1}^{n} \mathbf{1}(x_{p1} > u_p \,, x_{p2} > u_p)}{\sum_{i=1}^{n} \mathbf{1}(x_{p1} > u_p)}$$

where $x_p = {F_X}^{-1}(u_p)$

The calculation of the joint exceedance probabilities for each Copula under consideration is described by the following formula [45]:

$$P\left(U > u_p, V > u_p\right) = 1 - 2u_p + C\left(u_p, u_p\right)$$

Therefore the calculation of the joint conditional exceedance probabilities for each Copula under consideration is:

$$P\left(U > u_p \mid V > u_p\right) = (1 - 2u_p + C\left(u_p, u_p\right))/(1 - u_p)$$

In order to calculate the joint conditional exceedance probabilities for each Copula under consideration, two Matlab functions were utilized: *copulacdf* and *copulaparam*. *Copulacdf* returns the cumulative probability of a defined copula family with a parameter evaluated for the data by *copulaparam* function.

In Figure 3.9 both graphs present the exceedance probability versus different percentiles for the Copulas families under consideration for the available weather data. Gaussian, Gumbel and Clayton Copula are shown by magenta, blue and black line respectively, while the red dots indicate the exceedance probability of weather data for different percentiles. As may be seen the Gumbel Copula (blue line) underestimates the exceedance probability less than the other investigated families of Copulas, as far as percentiles smaller than 90% and 96% are concerned for NOOA and Deltares data respectively. For percentiles higher than the before mentioned values, the exceedance probabilities of the data tend to be closer to that of Gumbel copula. Therefore one can safely conclude that based on the conducted tests on the whole set of data Gumbel Copula is an appropriate model for the joint probability distribution for wind speed and significant wave height.

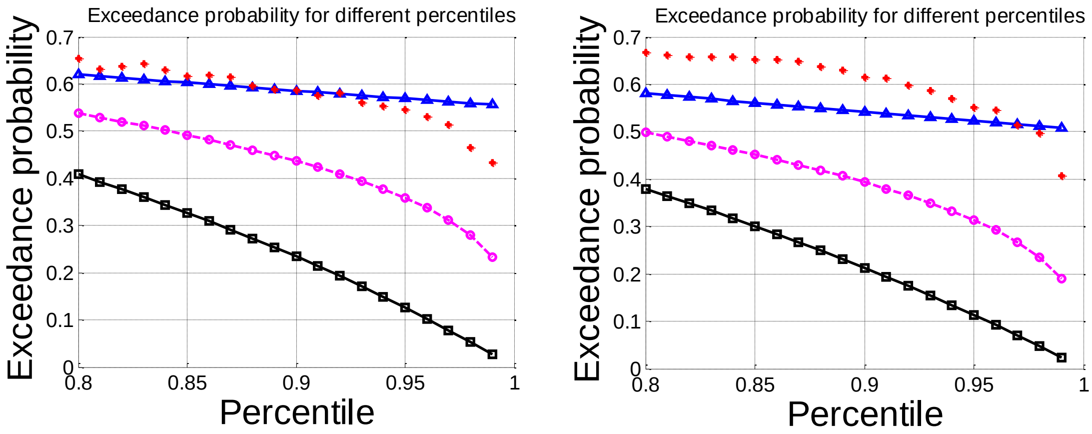

NOOA weather data   Deltares weather data

Figure 3.9: Exceedance probability for different percentiles

3.5 Monthly analysis

It is known that the values of wind speed and wave height present a considerable diversity during different months. Thus by analyzing each month to find the best fitting Copula, the seasonality of the produced metocean conditions will be secured [38]. Monthly analysis goal is to confirm that Gumbel copula is still the best among the investigated families. Also it gives the opportunity to calculate a different value of the parameter for each month, which allows producing time series including monthly characteristics. Therefore the described analysis was performed for each month and the generated graphs are presented in the current section.

The scatter plots of the actual observations on June for both NOOA and Deltares weather data are shown in Figure 3.10 and Figure 3.11 respectively. The scatter plots for all months can be found in Appendix A. The red and green areas of the graph show the 95th percentile of the wind speed observations. Also the green area represents the 95th percentile of both wind speed and wave height observations. These graphs visualizes the area needed to calculate the conditional exceedance probability for the 95th percentile $P(X \geq 95\%ile \mid Y \geq 95\%ile)$ using the before mentioned relation, where X refers to the significant wave height and Y refers to the wind speed.

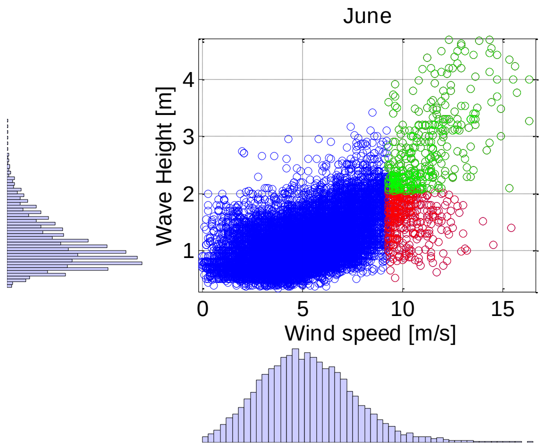

Figure 3.10: Scatter plot of NOOA weather data for June

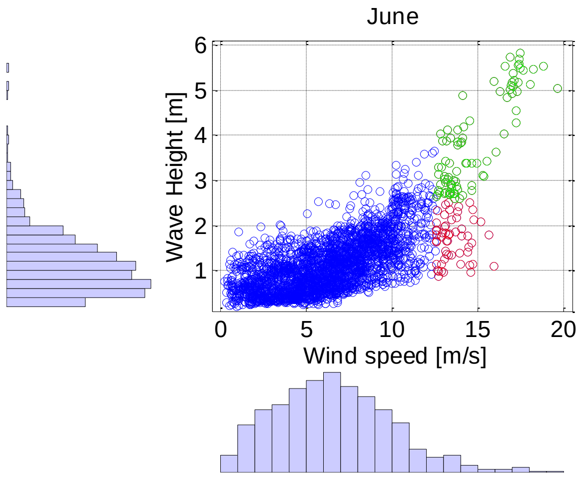

Figure 3.11: Scatter plot of Deltares weather data for June

Also, the values of semi-correlations as well as the sum of square differences for each copula under consideration were calculated in a monthly basis and they are presented in Table 3.3 and Table 3.4, for NOOA and Deltares data respectively. As one may observe there are differences between the calculated values. However none of these values suggests that a different copula than Gumbel is more appropriate to describe the data.

Table 3.3: Semi correlation and square differences for each month of NOOA weather data

	ρ	ρ_{ne}	ρ_{sw}	S_N	S_{Gum}	S_{Cl}
January	0.6902	0.6136	0.2212	0.8363	0.4121	9.1647
February	0.6542	0.6496	0.1442	1.1522	0.4223	9.7625
March	0.6478	0.6491	0.1560	1.0725	0.3716	9.5076
April	0.6359	0.5650	0.2167	0.8785	0.4471	8.1363
May	0.5527	0.5319	0.0414	1.0332	0.4371	7.7375
June	0.5595	0.5692	0.1232	1.0443	0.4731	6.8582
July	0.4968	0.4578	0.1943	0.9539	0.4715	5.1752

August	0.5017	0.5834	0.0597	1.7210	0.7554	7.9654
September	0.5586	0.6000	0.2156	1.2304	0.7992	5.9006
October	0.6528	0.6812	0.1770	0.9633	0.4482	8.4139
November	0.6596	0.5348	0.2145	1.0873	0.8096	9.0153
December	0.6721	0.5978	0.2511	0.6863	0.3539	8.3034

Table 3.4: Semi correlation and square differences for each month of Deltares weather data

	ρ	ρ_{ne}	ρ_{sw}	S_N	S_{Gum}	S_{Cl}
January	0.5475	0.4936	0.3611	1.5216	1.2075	6.8278
February	0.6486	0.6479	0.2536	2.5932	1.3222	12.3801
March	0.5859	0.7119	0.1439	3.7731	2.3459	12.3004
April	0.4507	0.5705	0.2709	1.8690	1.1050	7.3280
May	0.5530	0.6253	0.2649	2.0274	0.9568	7.9704
June	0.6750	0.6431	0.3244	0.8740	0.3189	9.3321
July	0.6070	0.7566	-0.0098	2.4120	1.0628	13.1585
August	0.6228	0.6301	0.1983	0.8853	0.2726	8.6733
September	0.6463	0.7613	0.3396	4.0080	1.9200	17.2957
October	0.6874	0.6725	0.1741	1.4045	0.7921	10.4398
November	0.6507	0.6466	0.1382	2.2902	1.0791	9.6532
December	0.5253	0.7495	0.2675	4.5913	2.9380	14.1674

Finally the plots showing the exceedance probability for different percentiles were produced for each month. The plots of June are presented in Figure 3.12 and Figure 3.13 for NOOA and Deltares data respectively.

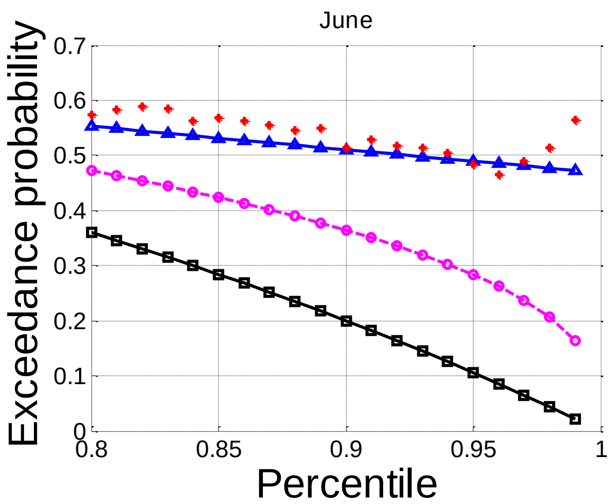

Figure 3.12: Exceedance probability for different percentiles concerning NOOA weather data of June

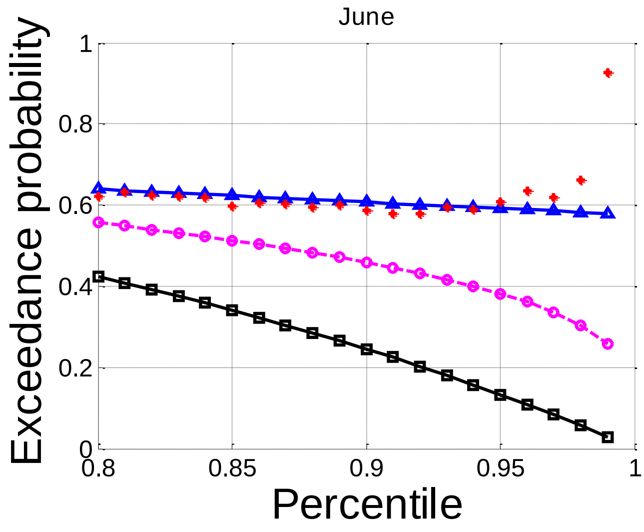

Figure3.13: Exceedance probability for different percentiles concerning Delares weather data of June

As it can be seen in the exceedance probabilities plots (Appendix A.3 and A.4), for the majority of the months, Gumbel copula has a lower degree of underestimation than the other families. However using Gaussian instead of Gumbel copula, for some months such as November (NOOA) and October (Deltares) could also be an alternative. Nevertheless choosing Gaussian copula would lead to a significant underestimation in the extreme values if wind speed and wave height, which are the most crucial for the logistics tool. Therefore Gumbel copula was chosen to produce the weather time series for each month in order to follow a conservative approach. Also it is worth mentioning that this result was also expected based on the literature, since Gumbel exhibits upper tail dependence, which can be clearly seen in the pseudo-observations scatter diagrams, and it is the most commonly used copula for extreme dependence [30] [39].

3.6 Physical explanation of analysis

The described statistical analysis investigates the dependence between the wind speed and the wave height by treating them as variables and analyzing the observations of those two variables. However these two variables represent physical characteristics of the weather. Therefore based on the results of the conducted analysis, useful information can be derived regarding those physical quantities.

As it was noted in similar studies the wind speed and the significant wave height present some worth mentioning trends [55] [56]. Firstly the cases where large values of wind speed and small values of significant wave heights encounter small values of significant wave height and large values of wind speeds respectively are sporadic. This observation shows that the probability of those cases is small. For example the calculated conditional probabilities, of the case where the wind speed has a value larger than the 90th percentile of wind speed observations and the wave height has a value smaller than the 10th percentile of the wave height measurements, are equal to $6.3 \cdot 10^{-4}$ and $8.1 \cdot 10^{-4}$ for Deltares and NOOA weather data sets respectively.

Also the analysis showed that there is tail dependence on the measured weather data. This observation demonstrates that higher values of wind speed are correlated to higher values of wave heights. Consequently the conditional probability of the case where large values of wind speed encounter large values of significant wave heights is high. That is an important remark since choosing a Copula that does not capture the tail dependence observed in the weather data may lead to underestimation of the weather windows and consequently to inadequate estimation of the duration of the cable installation. The Gumbel Copula was chosen because as it can be seen in Figures 3.10 and 3.12, it supports the observation that given high values of wind speed (above 9 m/s) are observed, high values of wave height (above 1.8 m) will occur with a probability equal to 0.55 which is very close to the probability of observations and higher than the probability of Gaussian Copula which is equal to 0.35. The physical explanation of this observation is that the non-deterministic component of waves is driven to a large extent by the wind.

3.7 Production of random time series

3.7.1 Methodology for generating weather time series

Having found the copula that describes the weather data best, is sufficient to generate couples of wind speed and significant wave height that encompass the same dependence as the observations in the specific site. However, in order to generate time series the dependence between the wind speed and the wave height is not enough. The autocorrelation of the r.v., which is the degree of similarity between a given time series and a lagged version of itself, is also needed. It was found, through a procedure similar to the one described in section 3.4 that the autocorrelation of the wind speed could be represented with the Gaussian copula.

Therefore, in order to produce the weather time series the following procedure was conducted for each month:

- Generate the first wind speed value f in [0,1] using random number generator.
- Calculate the values of wind speed in [0,1] based on the previous value (f) by solving the inverse h-function of Gaussian copula [46]:

$$h^{-1}(u, f, \rho) = \Phi\{\Phi^{-1}(u)\sqrt{1-\rho^2} + \rho\Phi^{-1}(f)\}$$

  where Pearson correlation $\rho = 2\sin(\frac{\pi}{6} r_s)$ and r_s: Spearman correlation.

- Next, the inverse conditional Gumbel copula function written in Matlab by Patton [40] provides the value of wave height (v) in [0,1] for each of the generated wind speed values (u). Using the calculated parameter k of Gumbel Copula the following formula [44] is solved numerically using bisection method. The inverse conditional Gumbel copula is described by the following relation:

$$C(v|u;k) = u^{-1} \exp\left\{-[x^k + y^k]^{\frac{1}{k}}\right\} \cdot [1 + (y/x)^k]^{\frac{1}{k}-1}$$

  where $x = -\ln u$ and $y = -\ln v$.

- Finally the values of wind speed and wave height are transformed back to the original units through the inverse cumulative distribution function of each separate variable.

After completing the above mentioned procedure for each month, the time series for the whole year are generated.

3.7.2 Graphs of produced time series

In this section the graphs of the produced time series for March are presented and compared to the actual observations. In Figure 3.14 the plots of the observed and generated wind speed time series for March, based on NOOA data set, are presented while in Figure 3.15 one may find the observed and generated time series concerning the significant wave height.

As it can be observed from these figures, the produced time series seem to have a similar behavior to the observed data. Furthermore the extreme values of the generated time series are very close to the extreme values of the observations. Finally it must be mentioned that the produced time series of wind speed and wave height are random and they are different for each realization. However as a general remark one could say that the produced time series represent adequate the weather conditions that have been observed in the site.

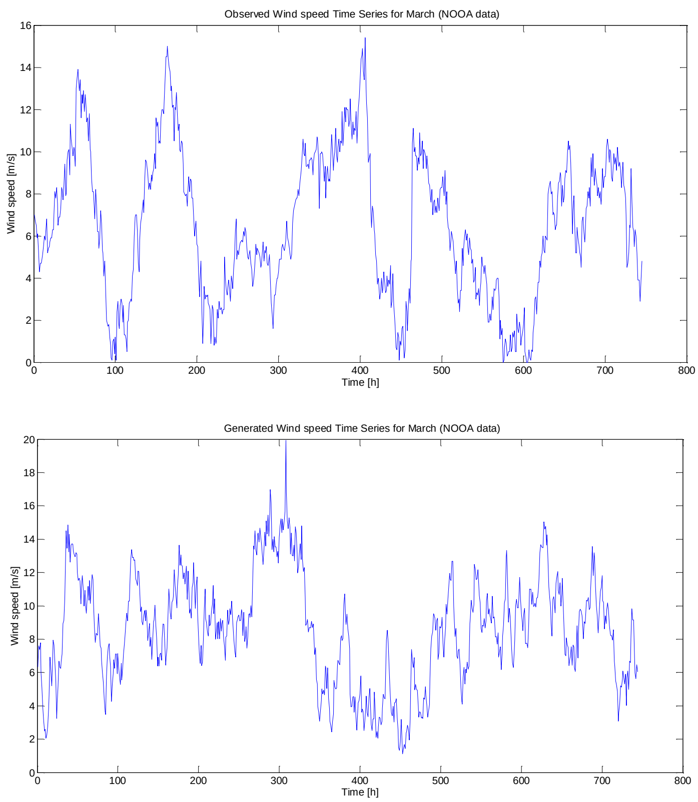

Figure 3.14: Observed and generated wind speed time series for March (NOOA data)

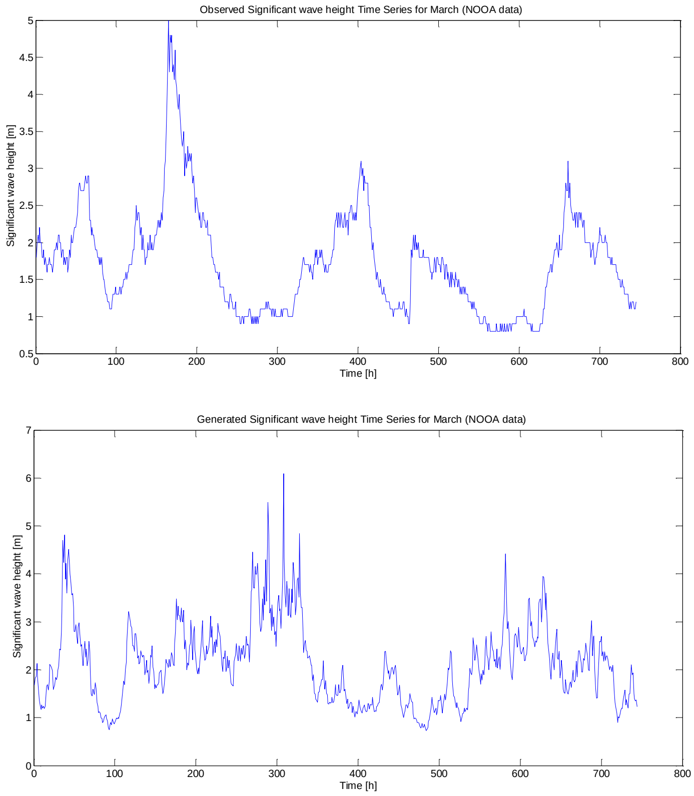

Figure 3.15: Observed and generated significant wave height time series for March (NOOA data)

3.8 Validation of produced time series

In order to validate that the produced time series were produced correctly following the Gumbel copula, the same analysis was conducted for 100 years of generated time series based on Deltares data. The time series are in hourly basis, consequently the total number of the produced couples is equal to 876000 and it is considered sufficient for the analysis. The analysis was conducted for the whole set of produced time series as well as for each month separately. The plots of this analysis can be found in the Appendix in sections A.5 and A.6.

In Figure 3.16 it is evident that the exceedance probabilities for different percentiles of the produced time series, which are presented with the red dots, approximate the exceedance probabilities of the Gumbel copula (blue line). Also it can be seen in Table 3.5 that the values of Pearson correlation for upper quadrant is always bigger than the lower quadrant and closer to the overall Pearson correlation ρ. Moreover the values of the square differences of Gumbel copula are smaller compared to those of Gaussian and Clayton copula. These results indicate that the generated time series follow the Gumbel copula as it was expected.

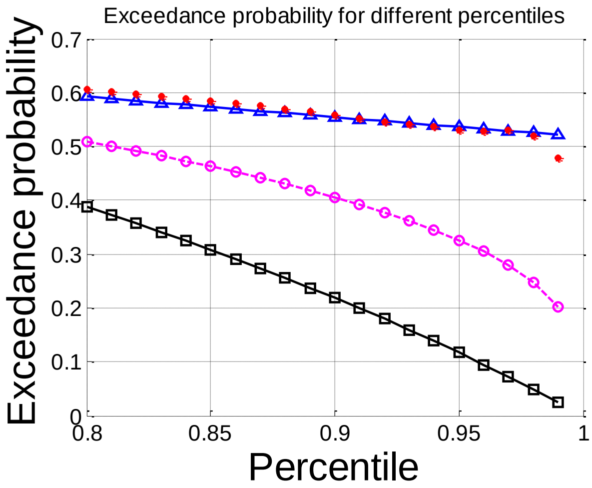

Figure 3.16: Exceedance probabilities of generated time series.

Table 3.5: Semi correlations and square differences of produced time series

	ρ	ρ_{ne}	ρ_{sw}	S_N	S_{Gum}	S_{Cl}
Overall	0.6148	0.5970	0.2362	0.5819	0.0795	6.7565
January	0.5965	0.5770	0.2442	0.3452	0.0095	5.3233
February	0.6455	0.6443	0.2651	0.6302	0.0657	7.1842
March	0.5553	0.5813	0.2463	0.4272	0.0225	5.0920
April	0.4866	0.4884	0.1746	0.2969	0.0109	3.8401
May	0.5282	0.5253	0.2375	0.3567	0.0089	4.3785
June	0.6901	0.6707	0.3150	0.4827	0.0225	7.3261
July	0.6428	0.5856	0.2990	0.2758	0.0153	5.4528
August	0.6419	0.6091	0.2901	0.3121	0.0085	5.7935
September	0.6778	0.6485	0.3611	0.3710	0.0146	5.8696
October	0.7073	0.6778	0.3627	0.3020	0.0124	6.3006
November	0.6316	0.6013	0.2928	0.3030	0.0057	5.5525
December	0.5582	0.5357	0.2383	0.3119	0.0085	4.8494

Furthermore, it must be mentioned that the values of Pearson correlation and semi correlations, presented in Table 3.5, are very similar to the respective values of the observations, presented in Table 3.4. This remark indicates that the dependence of wind speed and wave height of the produced time series is similar to the dependence of observations.

In order to further validate that the produced time series are similar to the observations the scatter plot of the produced time series should be examined. In Figure 3.17 the scatter plot of 100 years of generated time series based on Deltares observations is presented. As it can be seen, the scatter plot of the generated time series presents similarities to the scatter plot of the observations (Figure 3.6). The extreme values of wind speed and wave height are close to the observed. Moreover the samples where large values of wind speed encounter small values of wave height and the samples where large values of wave height encounter small values of wind speed are scarce.

However it must be noted that the level of skewness observed in the scatter plot of observations (Figure 3.6) is not observed in the scatter plot of the generated time series.

This can be explained by the fact that Gumbel copula is not able to capture well the skewness. In order to include the observed skewness in the generated time series, Copulas families with more parameters should be used.

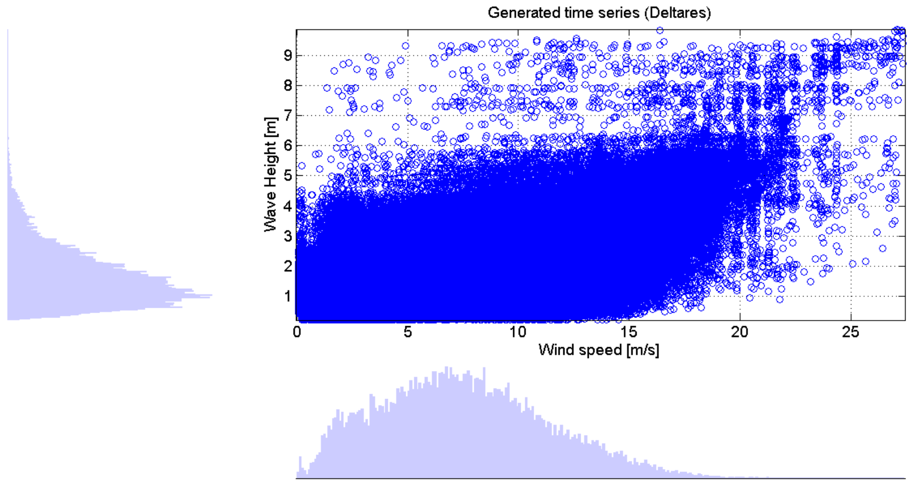

Figure 3.17: Scatter plot of produced time series based on Deltares observations.

4. Cable installation algorithm

4.1 Introduction

The goal of the current Master thesis is the design of a decision support tool which will be used by professional engineers to compare different solutions regarding the infield cable installation in an OWF. The user will be able to simulate different installation scenarios by entering the values that describe the solution under consideration. Based on the inputs entered by the user the tool will calculate the time needed for the cable installation for a number of different met-ocean time series and provide a CDF curve of the duration.

The probabilistic approach of this tool is considered to help the user, by providing the CDF curve, in order to determine the time needed of an installation scenario within a confidence level. This is different from the deterministic approach that is currently used by the majority of the planners.

In this section the designed decision support tool is described.

4.2 Tool architecture

The decision support tool will help the professional user decide for a certain confidence level, among different installation scenarios, by providing the cumulative distribution function plot of the time needed to complete the infield installation. A general flow chart of the probabilistic decision support tool is presented in Figure 4.1.

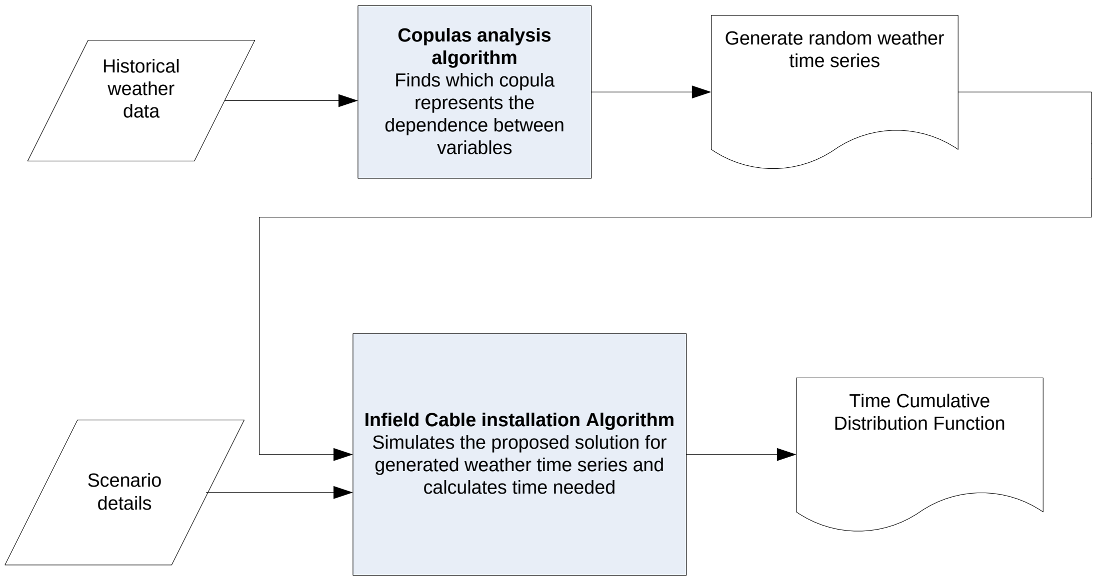

Figure 4.1: Flow chart of probabilistic decision support tool.

First, as many weather time series as the number of simulations should be generated. As it was described in Section 3.6, the values of average wind speed and significant wave height are produced in hourly basis by using the autocorrelation observed in the historical measurements in the site, provided by the user. Using this method the generated values will have dependence similar to the observations. Then the cable installation scenario described by the required inputs is simulated using the infield cable installation algorithm, which is written in Matlab, for every one of the produced weather time series. Finally the cumulative distribution function of the time needed is obtained.

4.3 Probabilistic approach

Probabilistic modeling concerns a form of modeling that utilizes probability distributions of certain inputs in order to calculate the implicit probability distribution of the output. In contrast to deterministic modeling which assumes the values of inputs as constant, probabilistic modeling provides an output distribution that includes the uncertainties. The most commonly used method of probabilistic planning is that of Monte Carlo simulations. The Monte Carlo method is roughly a technique that solves mathematical problems by solving their statistical analogues, by subjecting random numbers to numerical processes [47]. The method of Monte Carlo simulations is used to understand the impact of uncertainties in forecasting models.

In order to acquire a good estimate on the time needed for the completion of the installation, a large number (e.g 100 - 1000) of Monte Carlo simulations should be performed. For that reason, different random hourly time series of the average wind speed and the significant wave height are generated, taking into account historical weather data of observations in the particular site of installation. For each generated time series, the tool can simulate the proposed solution for the cable installation and calculate the time needed to complete it.

4.4 Model assumptions

It is impossible to create a model that is able to simulate reality perfectly. Therefore a number of simplifications and "educated assumptions" are required. The most important assumptions and simplifications regarding the infield cable installation algorithm were based on cable installation experts' opinion and they are listed below:

- Offshore Wind farm layout is already defined in the design phase, including the number of turbines and their place.
- Offshore wind farm layout is divided in sections (or edges, according to graph theory) where one vessel can operate and installation operations can take place.
- The working hours during a day are important to calculate the duration of the operation. It was assumed that operations take place during 24 working hours per day and 7 days per week.
- During installation, the vessel will stay at the site. The vessel is considered to leave the section (or edge) where it is working only for the following reasons:
    - vessel needs to refill fuel
    - reload components (e.g. cable)
    - go to next section (or edge)
- Different ports are taken into consideration since the cable installation operation usually starts from cable factory's quay.

- There are cases where a difference between the time needed to install the first cables compared to the last was observed. This is an example of "learning by doing", which is often observed due to lack of experience. In this model, “learning by doing” will be neglected since it is assumed that the crew is experienced and well trained.
- It is assumed that there are always available component resources in the quay. Therefore there is no need of modeling the stock level in the port.
- In case of emergency, traveling to safe port is always possible.
- The transit speed of a vessel is considered constant.
- When the simulation starts all the vessels are located in the port or quays and they are filled to their capacity (fuel, cable etc).
- A vessel starts the operation only if there is enough time available to complete it.

The infield cable installation consists of the following sub-operations:

- Pre-lay grapnel run: Performed by a support vessel to prepare the seabed for a successful cable installation.
- Pre-lay survey: the CLV performs a survey in order to confirm that it is safe to start the cable laying operation.
- Transfer crew: The crew transfer vessel (CTV), transfers the crew to the transition piece.
- Pull-in first end: A cable laying vessel (CLV) loaded with cable approaches the wind turbine (WT) and by using a messenger wire, the crew pulls-in the cable through the j-tube and fixates it on the WT.
- Cable laying: After the first end pull-in, CLV moves slowly towards the next WT paying out the cable.
- Transfer Crew: The CTV transfers the crew to the transition piece of the second wind turbine.
- Second end Pull-in: CLV connects the cable to the second WT.
- Pre burial survey: The burying vessel (BV) performs a survey in order to confirm that the cable laying was completed successfully and the it may proceed to the burying operation.
- Burying: The BV buries the cable by using an ROV.
- Post burial survey: A final survey is performed by the BV in order to confirm that the burying was completed successfully

4.5 Inputs of infield cable installation algorithm

In order to estimate the time needed for the infield cable installation, the user should enter a number of inputs that describe the installation scenario under consideration. In this section the required inputs for the cable installation simulation are presented. Also it must be mentioned that appropriate forms were created in Excel sheets, in order to facilitate the user in entering the required inputs.

The required inputs consist of:

- Matrices of Nodes and Edges of the OWF

The conventional graph theory describes that any graph is formed by a pair of sets (V, E) where V is the set of vertices or nodes and E is a multiset of edges which are formed by the pairs of nodes that connect. [49] Using these basic graph components, the user is able to provide the algorithm with the OWF graph. An example of OWF graph is presented in Figure 4.2. Each node of the OWF graph represents every place where the vessels should reach in order to perform an operation (i.e. wind turbines and offshore substation for pull-in operations, and ports for fuel and cable refill). The edges represent the cable connection between the wind turbines, as it is determined by the OWF cable layout, by showing the starting and the ending node of the edge.

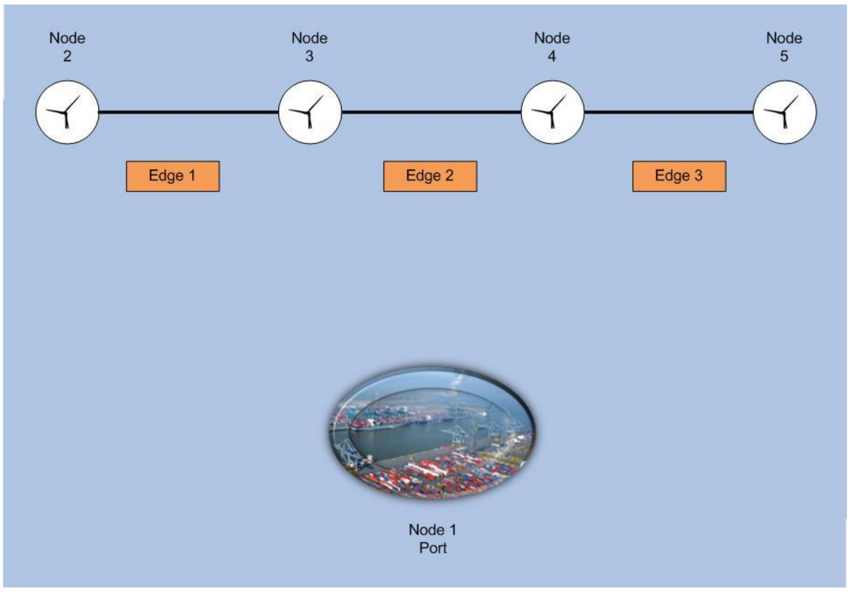

Figure 4.2: Example of nodes and infield section

Thus the user should provide a matrix containing the number of each node of the OWF graph, as well as its coordinates (i.e. longitude and latitude). The coordinates of each node are essential because they are used in the calculation of the distance between the nodes. Also the user should provide a matrix containing the number of each edge as well as its starting and ending node, based on the cable layout of the offshore wind farm. Figure 4.3 presents an example of the Excel sheet created to help the user to enter the information about the OWF graph as well as the cable layout.

Name

Matrix of nodes' coordinates

Description

The user should enter the coordinates (longitude and latitude) of each area where a vessel may perform an operation (i.e. ports and wind turbines)

	Number of node	Longitude	Latitude	Unit
Port	e.g. 1			degrees, or decimal form
Cable reload port	e.g. 1			degrees, or decimal form
Fuel refill port	e.g. 1			degrees, or decimal form
Wind turbine 1	e.g. 2			degrees, or decimal form
Wind turbine 2	e.g. 3			degrees, or decimal form
Wind turbine 3	e.g. 4			degrees, or decimal form

Name

Matrix of infield sections

Description

A table that shows the cable layout of the wind turbines. The first column is the number of the section, while the second column and third column refer to the first and second wind turbine of this section, respectively.

Number of Section	Number of starting node	Number of ending node
1	e.g. 2	e.g. 3
2	e.g. 3	e.g. 4

Figure 4.3: Example of excel sheet concerning OWF graph inputs.

- Number of simulations

The proposed installation scenario will be simulated for different generated weather time series, based on the weather data analysis of the installation site. The user should enter the number of simulations for the cable installation scenario. It must be mentioned that a large number from 100 - 1000 should be used in order to simulate the proposed scenario under different possible weather realizations.

- Starting hour

Usually the cable installation is scheduled for summer period because of better weather conditions. However the user could simulate the proposed cable installation scenario, starting on different months by entering the hour of the year that the infield cable installation starts. For example, if the user would like to simulate a cable installation scenario starting on January 1st or June 1st, he/she should enter the starting hour variable equal to 1 or 3625 respectively.

- Transit speed

When a vessel travels from one node to another without performing any operation, the transit speed, which is assumed constant, is needed in order to calculate the time that it will take to reach its destination. Therefore the user should provide the transit speed for every vessel that takes part in the infield cable installation process.

- Performance of each operation

The performance of a vessel regarding a specific operation is used to determine the time needed to complete the operation. However it must be noted that the performance and consequently the time needed, are not constant. Therefore two kinds of performances were introduced in order to incorporate this attribute in the simulation algorithm. Each operation is performed by a vessel with maximum or normal performance based on two sets of weather limits.

- Limits of each operation

The most important reasons for delays in cable installation are due to harsh weather conditions [50]. However the weather conditions which limit the operations vary for different operations and they are also influenced by the characteristics of vessels that are used. The user should enter the maximum wind speed and maximum wave height that limit each operation by taking into account the characteristics of the installation vessels. Above these maximum limits the vessel is not able to perform the operation. Moreover, as it was mentioned before, the user should also provide the weather limits that correspond to the maximum performance for every operation. For weather values below these limits the vessels operate in maximum performances while for a value that exceeds either the limit regarding the wind speed or the wave height but it is still lower than the maximum limits, the vessel operates with normal performance. Figure 4.4 presents an example of the Excel sheet created to help the user enter the weather limits as well as the performance values for each operation.

	CLV												BV			
	First end Pull -in				Cable laying				Second Pull - in				Burying			
Limits	max wind (in m/s)	max wave (in m)	normal wind (in m/s)	normal wave (in m)	max wind (in m/s)	max wave (in m)	normal wind (in m/s)	normal wave (in m)	max wind (in m/s)	max wave (in m)	normal wind (in m/s)	normal wave (in m)	max wind (in m/s)	max wave (in m)	normal wind (in m/s)	normal wave (in m)
Performance	(h/WT)		(h/WT)		(in m/h)		(in m/h)		(h/WT)		(h/WT)		(in m/h)		(in m/h)	

Figure 4.4: Excel sheet example regarding the weather limits and the performances.

- Fuel capacity

Each vessel has different characteristics. The most important characteristic concerning the time needed for the infield cable installation is the fuel capacity. This characteristic influences the availability of the vessels and in combination with the fuel consumption is used to estimate when fuel refill is needed for each vessel.

- Fuel consumption

The fuel consumption of each vessel varies significantly during different states of the vessel. Therefore three different states are included in the algorithm, idle, working and sailing state. The idle state refers to the situation when the vessel has to wait on weather, while the working and sailing states refer to the situations when the vessel is performing an operation and travels from one node to another respectively. The values of each vessel, concerning the fuel consumption for different states are considered constant.

- Cable capacity

Another important characteristic that is vital for the simulation of the cable installation is the cable capacity of the cable installation vessel. There is a variety of cable laying vessels which have different cable capacities which typically range from 2000 tons to 10000 tons for the largest available vessels.

- Fuel refill and Cable reload performances

These variables represent the equipment characteristics and methods used to refill the vessels with fuel and reload the CLV with cable when it is needed, in the appropriate ports. These variables are used to calculate the time that a vessel needs to spend in the port or the quay in order to refill fuel or reload cable respectively. In Figure 4.5 an example of the created Excel sheet, which will be used to enter the rest of the required cable installation inputs, is presented.

Variable name	Value	Description
Starting hour of the simulation	e.g. 1	It shows the hour that the simulation is considered to start. E.g. the value is equal to 1 if the scenario under consideration starts on Jan 1 at 1.00 am. Range: [1, 8760].
Fuel refill	(in l/h)	This value shows how many litres per hour can be refilled in each vessel and it is used to calculate the time needed to
Cable reload	(in m/h)	This value shows how many meters of cable per hour can be reloaded in each vessel and it is used to calculate the time needed to reload the CLV
Cable capacity	(in m)	The cable capacity of the CLV is usually measured in tons, so for cables with different diameter the capacity of CLV in meters can be calculated using its density
Pull - in cable	(in m)	Amount of cable used in pull in operations.

Variables	SV	CTV	CLV	BV	Unit
Fuel capacity					litres
Fuel consumption (idle state)					litres/hour
Fuel consumption (working state)					litres/hour
Fuel consumption (transit state)					litres/hour
Transit speed					knots

Figure 4.5: Example of Excel sheet used by the user to enter the required inputs.

The following Table 4.1 summarizes the required inputs provided by the user in order to run the simulations.

Table 4.1: Inputs of cable installation algorithm.

Name	Description	Units
N_sim	Number of simulations of the scenario under consideration.	-
Starting_hour	The starting hour of the simulation. Range: [1, 8760].	h
type_vessel	Number of different types of vessels that perform the installation.	-
Nodes	Number of nodes (Figure 5).	-
cable_node	The node where the CLV refills cable.	-
fuel_capacity(type_vessel)	Fuel capacity of each type of vessel, in litres.	L
fuel_c(type_vessel, state)	Fuel consumption of each type of vessel for different vessel states.	L/h

cable_cap	The amount of cable that can be stored on the CLV.	m
cable_pli	Cable consumed in pull in operation in meters.	m
Sec [edge, starting node, end node]	Matrix containing the infield edges and nodes of each edge. In this way the user can simulate different cable layout connections.	-
Map [node, longitude, latitude]	Matrix containing the longitude and latitude of each node. Based on this matrix the distance between two nodes can be calculated.	degrees
limits(operation) [max wind speed, normal wind speed, max wave height, normal wave height]	Matrix containing the weather limits of each operation. If either of the values of weather time series exceed the maximum value of wind speed or wave height, then the vessel cannot perform any activity. Otherwise, if the values are both lower than the normal wind speed and wave height limits, then the performance of the vessel will be maximum.	m/s for wind speed and m for wave height
Performance(operation) [maximum performance, normal performance]	Matrix containing the normal and maximum performance of the each operation. Performances of pull in and crew transfer operations given in hours while performances of cable laying, cable burying, survey operations given in m/h	m/h or h
fuel_refill	The rate of refilling fuel	L/h
cable_refill	The rate of reloading cable	m/h
Speed(type_vessel)	Matrix containing the transit speed of each type of vessel	knots

4.6 Infield cable installation algorithm

It was mentioned before that after the generation of a large number of random weather time series the cable installation scenario is simulated by an algorithm written in Matlab. In this section it is explained how the algorithm regarding the infield cable installation, works. Firstly, a simplified flowchart regarding the infield cable installation algorithm is presented in Figure 4.6. The green arrows in the flow chart represent the case where the statement of the decision box is positive, while the red arrows represent the case that the statement is false.

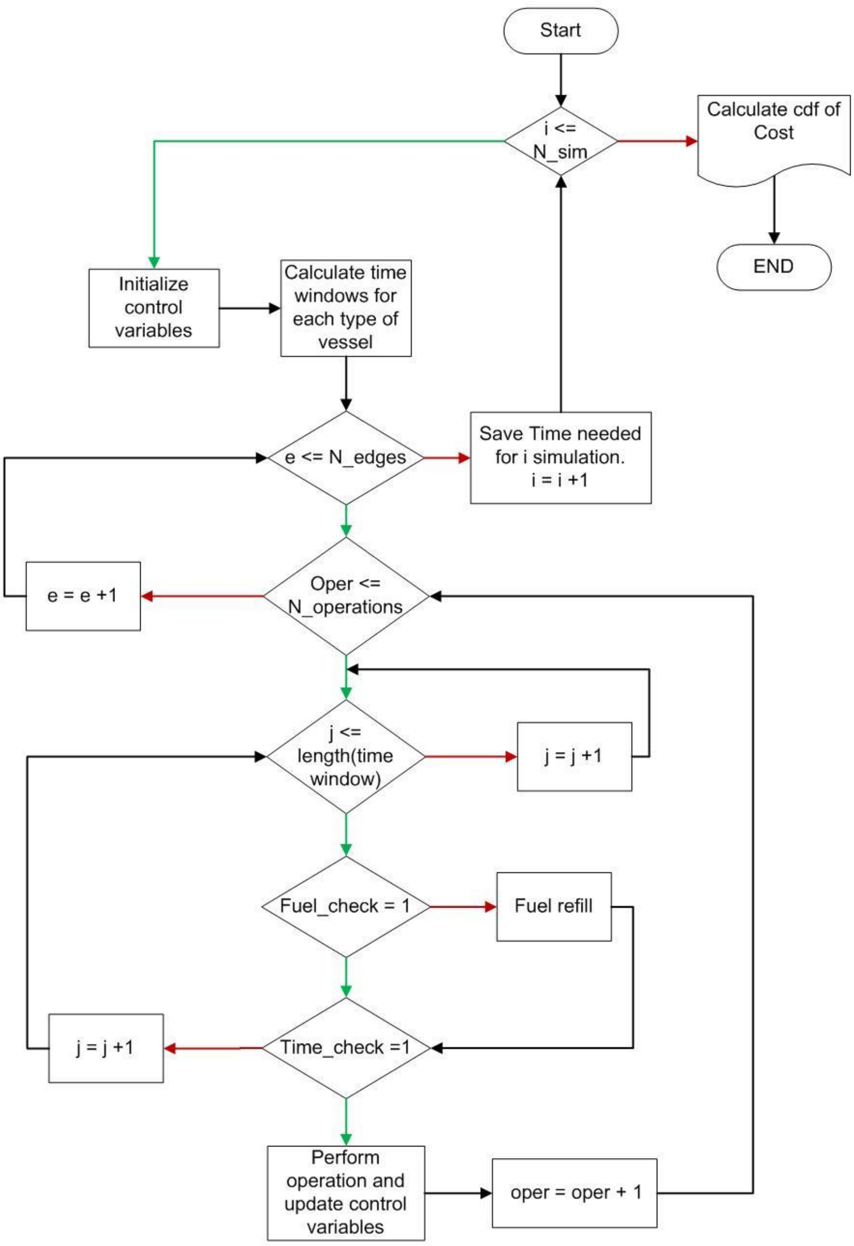

Figure 4.6: Simplified flow chart of infield cable installation algorithm.

As it can be seen in the flow chart the infield cable installation consists of the following steps:

1. Start i simulation for ith generated weather time series
2. Initialize control variables
3. Calculate weather windows for every operation of the cable installation
4. If the index e concerning the edges is smaller than the total number of edges go to 5, else save the time and set $i = i + 1$ and go to 1
5. Switch to next operation using the *progress* variable. If all operation in this edge are completed, set $e = e + 1$ and go to 4
6. If the fuel is sufficient continue to 7, else travel to appropriate node and refill fuel

7. If the time needed to complete the operation is sufficient perform the operation and update *progress* variable, else proceed to next available weather window
8. Proceed to next operation, go to 5
9. If all operations on the edge e are completed, set $e = e + 1$ and go to 4

4.6.1 Control variables

In order to simulate correctly the cable installation, a number of variables were introduced. In this paragraph these necessary variables (i.e. control variables) are described.

- *clock(vessel)*

The cable installation algorithm will calculate the time needed for the infield cable installation. Therefore one of the most important control variables is the *clock* variable which shows the time when the last operation was completed. This variable has as an argument the type of the vessel. Thus every type of vessel has a different value showing the specific hour, when the last operation performed by this particular vessel was performed. Using this variable it is possible to simulate operations that are performed simultaneously by different vessels in different locations. Finally, it must be mentioned that at start of each simulation for different weather time series, this variable is initialized by assigning its value equal to one for every vessel.

- *location(vessel)*

Another important control variable which has as argument the type of vessel, is the *location* variable. This variable is used in order to save the node where the last operation took place. Also, *location* variable is updated when the vessel moves from one node to another. It must be also mentioned that during initialization in the beginning of each simulation the location variable is set equal to the port node for all vessels except the location of cable laying vessel whose location is set equal to the cable reload node.

- *progress(edge)*

Progress is matrix having two columns and as many rows as the edges of the OWF graph. The first column shows which operation has been completed in a specific edge while the second column shows the hour that this operation was completed. *Progress* variable is used in order to find which operation was completed in the specific edge and determine which operation will be performed next. Also based on this variable the while loop concerning the cable installation in an edge, is terminated when the last operation (i.e. post burial survey) is completed. When the last installation operation on the last edge is completed, the vessels return to the port and the algorithm is terminated.

- *fuel(vessel)*

Fuel variable shows the fuel level of each vessel in litres. This variable is used to monitor the level of fuel in every vessel and facilitates the identification of a required fuel refill. At start, the variable is initialized by setting its value equal to the fuel capacity of each vessel. This variable is updated after the completion of a vessel movement, the end of an operation or when the wait on weather period has passed, by taking into consideration the three before mentioned fuel consumptions according to the vessel state.

- *cable*

Cable variable works in a similar way as the fuel variable. It illustrates the meters of cable that there are on the CLV's carousel. The information that this variable provides is used to monitor the amount of cable (in meters) that exists in the CLV and it is used to identify when cable reload is needed. In the beginning of the simulation the *cable* variable is initialized and its value is set equal to the cable capacity of the CLV.

4.6.2 Calculation of weather windows

The first part of the algorithm consists of the calculation of weather windows regarding every operation of the infield cable installation. The weather window is defined as the amount of hours that the weather conditions do not exceed the maximum weather limits of each operation. The weather window matrices are denoted by *tw(operation)* and consist of two columns. The first shows the amount of hours in one weather window while the second shows the specific hour that this weather window has started.

In order to calculate the time windows the weather time series are investigated in hourly basis and the amount of weather conditions that satisfy the maximum weather limits is noted. Weather windows are essential to determine whether or not an operation has enough time to be completed during the weather window. Otherwise the next weather window should be investigated.

4.6.3 Update clock variable

As it was mentioned before, clock variable is the most important control variable of the algorithm. This variable shows the exact hour when the last activity of the particular vessel was completed. Thus as far as operations without prerequisites are concerned the clock does not need to be updated. However, most operations have several prerequisite operations, which are usually performed by different vessels. For that reason, it is important to update the clock of the vessel before it starts its current operation. The clock of the vessel is updated by setting its value equal to the value of the clock of the vessel that performed the last prerequisite operation.

By subtracting the *clock* value from the sum of the two columns of weather window matrix, the algorithm can calculate the remaining time in the weather window (see paragraph 4.6.7). The clock variable should also be updated when the remaining time in a weather window is not sufficient for the completion of the operation and therefore the next weather window should be investigated. In that case the clock is set equal to the starting hour of the new weather window.

4.6.4 Calculate distance

A very important calculation of the algorithm is that of the distance between two nodes. Based on the distance the time needed for a vessel to move from one node to another, the algorithm can calculate the time that is needed. The distance between two nodes of the OWF graph is calculated by using the Haversine formula and using as inputs the longitude and latitude of each node [51].

$$d = 2R \arcsin\left(\sqrt{sin^2\left(\frac{\varphi_2-\varphi_1}{2}\right) + \cos(\varphi_1)\cos(\varphi_2)\,sin^2\left(\frac{\lambda_2-\lambda_1}{2}\right)}\right),$$

where φ_1 and φ_2: latitude of first and second point respectively, λ_1 and λ_2: the longitude of first and second point respectively and R: earth radius.

4.6.5 Fuel check

Before starting an operation, the fuel level of the vessel is examined. In order to start the operation, the amount of fuel in litres should be larger than the amount of fuel that the fuel it will be consumed if the vessel returns to fuel refill node, multiplied by a safety factor of 2. The minimum fuel for a vessel v, is calculated by the following formula:

$$fuel_{min,v} = (d_{fr,v} fuel_{c_{v,t}} / Speed_v) sf$$

where $d_{fr,v}$: the distance of vessels current location from the fuel refill node, $fuel_{c_{v,t}}$: the fuel consumption of vessel v when travelling, $Speed_v$: the transit speed of vessel v and sf: the safety factor.

In case that the amount of fuel is not sufficient the vessel travels back to the appropriate node to refill. The time that is needed for the fuel refill of a vessel v is calculated by:

$$time_{refill,v} = \frac{d_{fr,v}}{Speed_v} + \frac{fuel\_capacity_v}{fuel_r}$$

where $fuel\_capacity_v$: the fuel capacity of the vessel v and $fuel_r$: the fuel refill performance in litres/h.

4.6.6 Cable check

Another important investigation should be performed, before starting an operation which results in cable consumption. The amount of cable on the CLV should be larger than the amount of cable that it will be consumed during the entire cable installation in that edge. All sub-operations (i.e. 1st and 2nd pull-in and cable laying) are taken into consideration in the cable check. The minimum cable is calculated by the following formula:

$$cable_{min} = \left(2cable_{pli} + d_e\right) sf$$

where $cable_{pli}$: the amount of cable consumed during pull-in operation, d_e: the distance between the two nodes of the edge and sf: a safety factor set equal to 2.

In case that the amount of cable in the CLV is less than the minimum required cable, the operation does not start and the CLV moves to the cable reload node. The total time that is needed to reload the cable is calculated by:

$$time_{reload} = \frac{d_{cr,clv}}{Speed_{clv}} + \frac{cable\_capacity_{clv}}{cable_r}$$

where $d_{cr,clv}$: the distance of CLV from its current location to the cable reload node, $Speed_{clv}$: the transit speed of CLV, $cable\_capacity_{clv}$: the total capacity of cable in meters and $cable_r$: the cable reload performance in meters/hour.

4.6.7 Time check

If the required examinations regarding the fuel and cable are passed, then one last examination is required before the installation operation starts. The time remaining in the weather window should be more than the time needed to complete the operation; otherwise the next weather window is investigated. The time needed for the operation is estimated based on the normal performance of the operation. There are two different methods for estimating the required time, depending on the performance of the operation.

In case that the performance is given in hours then the maximum time needed for the appropriate vessel v to perform the operation z in a node n, is estimated by:

$$time_z = d_{nv}Speed_v + Performance_z$$

where d_{nv}: the distance of the appropriate vessel v from the node n, $Speed_v$: the transit speed of vessel v and $Performance_z$: the normal performance concerning the operation z.

In case that the performance is given in m/h (e.g. performance of cable laying or burying operation) then the maximum time needed for the appropriate vessel v to perform the operation z in an edge e, is estimated by:

$$time_z = d_{nv}Speed_v + d_e/Performance_{n,z}$$

where d_{nv}: the distance of the appropriate vessel v from the starting node n of the edge e, $Speed_v$: the transit speed of vessel v, d_e: the distance between the starting and the ending node of edge e and $Performance_z$: the normal performance concerning the operation z.

The check concerning whether or not there is enough time to start an operation z is expressed by the following inequality:

$$time_z \leq tw_{z,1} + tw_{z,2} - clock_v$$

where $tw_{z,1}$ and $tw_{z,2}$ are the first and the second column of the weather window matrix of the operation under investigation.

If the estimated time $time_z$ satisfies the inequality, the operation starts, otherwise the next weather window is investigated.

4.6.8 Estimate performance and perform operation

It was mentioned that the performance of an operation has a normal and a maximum value related to the weather conditions. Therefore if the estimated time needed to complete the operation satisfies the inequality, then the actual time needed by taking into consideration the weather condition should be calculated. Since the produced weather time series are in hourly basis, every hour should be investigated and calculate if the operation during this hour will be performed with the maximum or the normal performance. There are two different procedures followed in order to estimate the actual performance base on the type of performance.

In case that the performance is given in m/h, the following procedure is followed in order to calculate the actual time when the operation will be completed:

1. $i = clock_v$
2. $For\ i \leq tw_{z,1} + tw_{z,2}$
3. $if\ ts_{i,1} < limit_{n,1}\ \&\ ts_{i,2} < limit_{n,1}$
   $perf = Performance_{max,z}$
   $else$
   $perf = Performance_z$
   end_if
4. $inst = inst + perf$
5. $fuel_v = fuel_v + fuel_{c_{v,w}}$
6. $if\ inst > d_e$
   $clock_v = i + 1$
   $progress_e = z$
   $break\_for\_loop$
   end_if
7. $i = i + 1$
8. end_For

where $ts_{i,1}$ and $ts_{i,2}$: the value of wind speed and significant wave height respectively for ith hour, $limit_{n,1}$ and $limit_{n,2}$: the normal limits for wind speed and wave height respectively, $Performance_{max,z}$ and $Performance_z$: the maximum and normal performance for operation z, $fuel_{c_{v,w}}$: the fuel consumption when of the vessel v when it is performing an operation and d_e: the distance between the two nodes of edge e.

In case that the performance is given in hours, the following procedure is followed in order to calculate the actual time when the operation will be completed:

1. $i = clock_v$
2. $For\ i \leq tw_{z,1} + tw_{z,2}$
3. $if\ ts_{i,1} < limit_{n,1}\ \&\ ts_{i,2} < limit_{n,1}$
   $perf = 1/Performance_{max,z}$
   $else$

$perf = 1/Performance_z$

end_if

4. $inst = inst + perf$
5. $fuel_v = fuel_v + fuel_{c_{v,w}}$
6. $if\ inst \geq 1$

   $clock_v = i + 1$

   $progress_e = z$

   $break\_for\_loop$

   end_if
7. $i = i + 1$
8. end_For

As it can be seen from the algorithms, every hour, starting from the clock value of the appropriate vessel until the operation is completed, is investigated. If the weather conditions exceed the normal weather limits, given by the user then the normal performance is used. Otherwise the maximum performance is used. In that way the actual time needed for the operation is calculated, by taking into account the effect of weather conditions on the performance. Finally, the clock and the fuel indices of the vessel are updated.

4.6.9 Different burial method

As it was mentioned before, there are also different methods of burying the cable. The post-laying burying method which was described in the previous sections has important differences comparing to the simultaneously burying method. Since the cable is laid and buried simultaneously there is no need of a burying vessel and post-lay survey. On the other hand, this approach could have an impact on the time because the performance could be lower. The user will be able to choose which of those two methods want to simulate. In case that simultaneously burying is chosen, the operations that should be performed could be summarized as follows:

- Pre-lay grapnel run: Performed by a support vessel to prepare the seabed for a successful cable installation.
- Pre-lay survey: The CLV performs a survey to check the cable laying operation can start.
- Transfer crew: The crew transfer vessel (CTV), transfers the crew to the transition piece.
- Pull-in first end: A cable laying vessel (CLV) loaded with cable approaches the wind turbine (WT) and by using a messenger wire, the crew pulls-in the cable through the j-tube and fixates it on the WT.
- Cable laying and burying: After the first end pull-in, CLV moves slowly towards the next WT paying out and simultaneously burying the cable.
- Transfer Crew: The CTV transfers the crew to the transition piece of the second wind turbine.
- Second end Pull-in: CLV connects the cable to the second WT
- Post burial survey: A final survey is performed by the CLV in order to confirm that the burying was completed successfully

4.7 Adding uncertainty

The most important factor of delays during the cable installation of an OWF is the weather conditions. For that reason, the copulas approach was used in order to estimate various possible weather conditions. However, there are also other factors that influence the time needed to complete the cable installation of an OWF; specifically, the uncertainty of the performance of operations and the failures that may occur during the installation. For that reason, it was decided to also include these uncertainties in the algorithm, in order to take account of their impact on the final cumulative distribution of the time needed for the cable installation. In the following paragraphs the incorporation of these uncertainty aspects in the algorithm are described.

4.7.1 Performance uncertainty

Regarding the performance of the operations, deterministic values for different ranges of weather condition, are currently used. Instead of using deterministic values, random values following an appropriate distribution could be calculated by a random number generator. In that case the user could choose an appropriate distribution and provide the required inputs. Usually a triangular or a uniform distribution is used in order to estimate the value of stochastic variables in Monte Carlo simulations.

The uniform distribution refers to a probability distribution for which all the values of the random variable have an equal probability of occurring. Its probability density function is described by: $P(X = x_k) = 1/k$, where k the number of different values. As inputs the maximum and the minimum value should be provided by the user

The triangular distribution is a probability distribution that is defined by three values: the minimum (a) the maximum (b) and the peak (c) value. Its probability density function has a triangular shape and it is given by [52]:

$$f(x) = \begin{cases} \dfrac{2(x-a)}{(b-a)(c-a)} & a < x < c \\ \dfrac{2(b-x)}{(b-a)(b-c)} & c \leq x < b \\ 0 \quad elsewhere & \end{cases}$$

Using a Matlab function such as randraw which is available on Mathworks forum [53], one can choose a distribution and produce random numbers following this distribution. It must be mentioned that this method can be applied to all variables which include uncertainty. However since the crew transfer operation is the one which presents the higher uncertainty, it was chosen to apply this method only on the performance of the crew transfer vessel. The algorithm will use a randraw function to calculate the time needed to transfer the crew to the transition piece, when the vessel is in the field, from a triangular distribution. This random value is calculated in the beginning of each simulation and it remains constant for each simulation. In that case, the minimum, the maximum and the most likely value of the hours needed to transfer the crew to the TP should be provided by the user. Figure 4.7 presents the performance input form as it was included in the inputs excel sheet.

	CTV					
	Crew transfer					
Limits	max wind (in m/s)	max wave (in m)		normal wind (in m/s)	normal wave (in m)	
Performar	min (h/WT)	most likely (h/WT)	max (h/WT)	min (h/WT)	most likely (h/WT)	max (h/WT)

Figure 4.7: Crew transfer performance form in Excel inputs sheet.

Finally it must be mentioned that the user could easily modify the algorithm to apply this methodology to other variables.

4.7.2 Failure uncertainty

Apart from the performance uncertainties, there are also uncertainties regarding the occurrence of a failure that may delay the cable installation. Based on the experience of experts in the cable installation, it was stated that the failures that may occur during a cable installation are due to the human factor (i.e. mistakes of the crew). In order to include this uncertainty two characteristics are needed. First, the probability of occurrence of the failure under consideration is needed. Of course it is difficult to estimate a probability for a failure. For that reason based on the experience of past projects, the user could assign a probability equal to the failures occurred divided by the number of the performed operations. For instance, if a certain failure has occurred 2 times over the last 80 pull-in operations, a probability equal to 0.025 should be assigned by the user. The second required input of the failure uncertainty, concerns the impact on time that this particular failure would have (e.g. 5 hours to repair it). Figure 4.8 presents the form of the failure table which is included in the inputs Excel sheet.

	Probability	**Impact in time**
Failure during pull - in operation	e.g. 2,5%	(in hours)

Figure 4.8: Failure table in Excel inputs sheet.

It must be mentioned that the user could create a table containing a number of different failures. For the purpose of the current thesis, it was decided to include one failure during the pull-in operation. The procedure to estimate if a failure occurs is the following:

1. Use rand() Matlab function to calculate a random number r in [0,1]
2. If r is smaller or equal to the failure probability the failure occurs and go to 3 else go to 4.
3. The clock of the appropriate vessel is updated: $clock_v = clock_v + impact$, where $impact$: the time impact (in hours) due to the failure.

4. Proceed to the appropriate test (i.e. cable and fuel check) and perform the operation

4.8 Insight into cost of cable installation

The cost of the infield cable installation is influenced mostly by the duration of the installation. Therefore the cable installation algorithm could also provide an insight into the cost of the infield cable installation. The total cost of the infield cable installation for a simulation s could be estimated by the following relation:

$$Cost_s = \left(\sum_{v=1}^{N_v} \frac{clock_v}{24} \cdot D_v + mob_v + demob_v \right) + Fuel_s \cdot price_{fuel} + n_{fail_s} \cdot I$$

where N_v: the number of different types of vessels, D_v: day rate of vessel v, mob_v: the mobilization cost of vessel v, $demob_v$: the demobilization cost of vessel v, $Fuel_s$: the total amount of fuel (in litres) consumed during simulation s, $price_{fuel}$: the price of fuel per liter, n_{fail_s}: the number of failures occurred during pull-in operations for simulation s and I: the cost of failure.

A different cost will be calculated for every simulation and finally the CDF curve of the cost of infield cable installation will be calculated. The cost CDF curve shows the probability that the installation will cost at most a certain amount of money. Based on the cost CDF curve the user could estimate the total cost of the infield cable installation within a confidence level. Usually probability equal to 70% (P70) is used for estimations that concern the cost of a project.

Finally it must be mentioned that in order to estimate the cost of the infield cable installation correctly, there is need of accurate values regarding the inputs (i.e. day rates of vessels, mobilization and demobilization costs, price of fuel, and cost of failures). By estimating the cost accurately, the user will be able to acquire a thorough insight regarding different cable installation scenarios, since it is possible that larger and better equipped vessels may present a smaller duration of the installation but also lead to higher total cost of the installation due to their higher day rates.

5. Test cases

In order to test the developed decision support tool a test case including realistic values regarding the model inputs, was provided by Van Oord. In the current chapter the description of the test case as well as the results of the tool are presented and discussed.

5.1 Inputs of the test case

5.1.1 Graph of the OWF

The test case concerns an offshore wind farm consisting of 55 wind turbines and an offshore substation, located in the North Sea region. The cable layout of the OWF consists of 4 arrays of 10 wind turbines and one array of 5 wind turbines. Each array is connected to the offshore substation (noted as node 3). Also there is one port (noted as node 1) where the vessels, apart from the CLV, are located when the simulation starts and where the fuel refill takes place. It must be mentioned that the cable reload is performed in a separate quay (noted as node 2). Another important assumption that is worth mentioning is that in the beginning of the simulation the CLV is located already loaded to its capacity, in the cable quay. The graph of the offshore wind farm, showing the numbers of nodes as well as the cable layout, is presented in Figure 5.1.

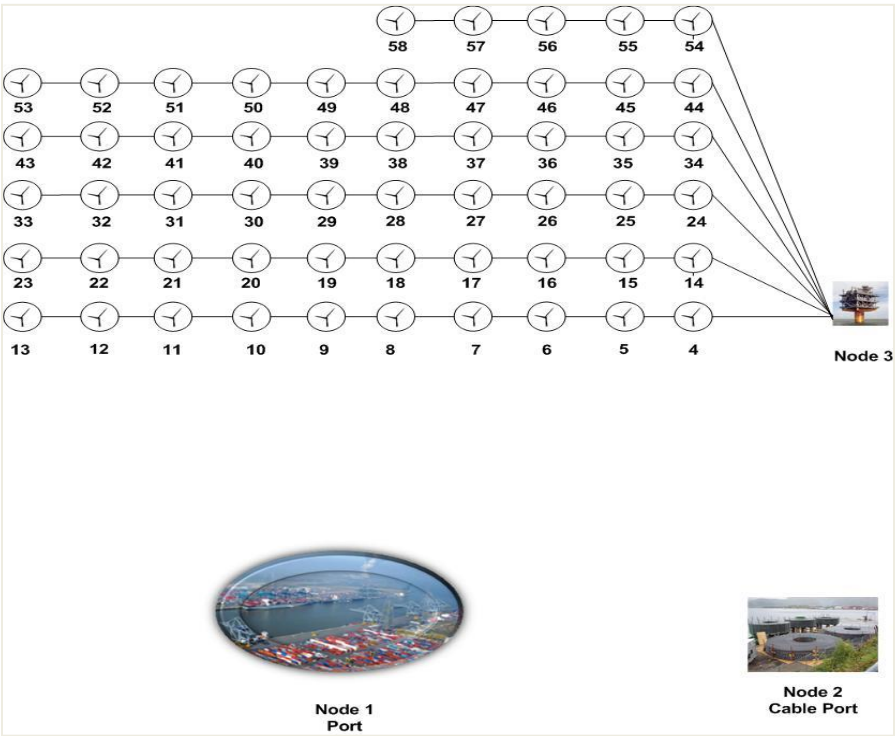

Figure 5.1: OWF graph of the test case.

5.1.2 Operations

In order to execute the cable installation, four vessels are participating. One Support vessel (SV), one vessel which is appropriate to transfer the crew in the transition piece of the wind turbines (CTV), one cable laying vessel (CLV) and on vessel (BV) that is appropriately equipped to bury the cable. As far as the method of burying the cable is concerned, post-lay burial of the cable is chosen. Therefore the operations that will be performed for the cable installation are the following:

- Pre-lay grapnel run: Performed by a support vessel (SV) to prepare the seabed for a successful cable installation.
- Pre-lay survey: the cable laying vessel (CLV) performs a survey in order to confirm that it is safe to start the cable laying operation.
- Transfer crew: The crew transfer vessel (CTV), transfers the crew to the transition piece.
- Pull-in first end: The CLV loaded with cable approaches the wind turbine and by using a messenger wire, the crew pulls-in the cable through the j-tube and fixates it on the WT.
- Cable laying: After the first end pull-in, CLV moves slowly towards the next WT paying out the cable.
- Transfer Crew: The CTV transfers the crew to the transition piece of the second wind turbine.
- Second end Pull-in: CLV connects the cable to the second WT.
- Pre burial survey: The burying vessel (BV) performs a survey in order to confirm that the cable laying was completed successfully and it may proceed to the burying operation.
- Burying: The BV buries the cable by using an ROV.
- Post burial survey: A final survey is performed by the BV in order to confirm that the burying was completed successfully

A Gantt chart of the infield cable installation operations is presented in Figure 5.2, in order to visualize the procedure of the operations. The operations are presented with different colours according to the vessel that performs them. The operations that are presented with magenta, blue, green and brown colours are performed by SV, CLV, CTV and BV respectively.

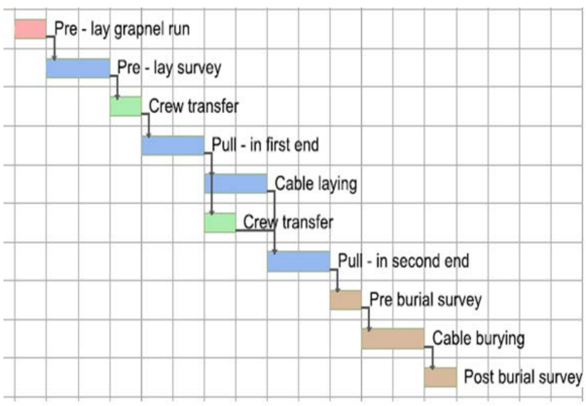

Figure 5.2: Gantt chart of infield cable installation

5.1.3 Capacity of vessels

The fuel capacities in litres, regarding the four vessels that take part in the cable installation is presented in Table 5.1.

Table 5.1: Fuel capacities of the vessels participating in the installation

SV	CTV	CLV	BV
218000 L	6000 L	374000 L	431000 L

5.1.4 Cable capacity

A cable laying vessel with 3000 tons cable capacity is considered for the installation scenario of this test case. As it was mentioned before, the cable capacity of the vessel should be given in meters, with the purpose that the algorithm would monitor the amount of the remaining cable in the CLV and calculate when cable reload is needed. Therefore, it was assumed that a power cable which weights 30 kg/m is going to be installed. This assumption results in a cable capacity of the CLV equal to 100000 m. Also it must be noted that the amount of cable that is consumed during a pull-in operation was assumed equal to 50 m.

5.1.5 Fuel consumption of the vessels

The fuel consumption of the vessels in L/h, for the different states of the vessel is presented in Table 5.2.

Table 5.2: Fuel consumption of the vessels

Vessel	idle	working	sail
SV	5 L/h	20 L/h	35 L/h
CTV	10 L/h	75 L/h	100 L/h
CLV	50 L/h	250 L/h	300 L/h
BV	30 L/h	300 L/h	300 L/h

5.1.6 Limits and performances of the operations

It must be mentioned that the test case provided from Van Oord, assumes only one value for the performance of each operation. Thus two performances and consequently two set of weather limits for each operation are not needed. However it must be noted that the performance regarding the crew transfer is calculated from a triangular distribution for every run of the simulation by using a random number generator. In Table 5.3 and Table 5.4 the weather limits and the performances respectively.

Table 5.3: Weather limits of the operations

Operation	Wind	Wave
Pre-lay grapnel run	-	1.5 m
Crew transfer	12 m/s	1.25 m
Pull-in	12 m/s	1.25 m
Pre lay survey	-	1.75 m
Cable laying	12 m/s	1.75 m
Pre-burial survey	-	1.5 m
Burying cable	-	1.5 m
Post-burial survey	-	1.5 m

Table 5.4: Performances of the operations

Operation	Performance
Pre-lay grapnel run	*** m/h
Crew transfer	min ***h peak ***h max ***h
Pull-in	*** h
Pre lay survey	*** h
Cable laying	*** m/h
Pre-burial survey	*** m/h
Burying cable	*** m/h
Post-burial survey	*** m/h

Note: The values of Table 5.4 were excluded from the report due to confidentiality reasons.

5.1.7 Transit speed

The transit speed of the vessels in knots is considered constant and it is used to calculate the required time to travel from one node to another. Table 5.5 presents the transit speed of the vessels.

Table 5.5: Transit speed of the vessels

Vessel	Speed
SV	13 knots
CTV	25 knots

CLV	6.5 knots
BV	7 knots

5.1.8 Refill fuel and Reload cable

In order to calculate the time needed to refill the fuel in a vessel or reload cable in the CLV certain values that represent the performances of the available equipment in the ports/quays are needed. The fuel is refilled in the port (node 1) with a rate of 6000 L/h while the cable is reloaded in the quay (node 2) with a rate equal to 350 m/h.

5.1.9 Failure probability

Based on the comments of experienced cable installation professionals, it was stated that it is possible that up to 2 failures in 80 operations could occur, due to mistakes of the crew. Therefore it was decided to include a failure probability equal to 2.5 % during pull-in operations. In case that a failure occurs it was assumed that the impact in time is equal to 5h.

5.1.10 Starting time

Usually the cable installation is planned to take place during summer. The main reason is that there are better weather conditions that result in larger weather windows. For that reason as a starting date of the cable installation operations the 1st of June was chosen. The constructed time series are in hourly basis, therefore the starting date should be provided in hours. Thus the starting hour of the cable installation was set equal to 3625.

5.2 Weather analysis van Oord weather data

Apart from the details concerning the cable installation, weather time series containing the average wind speed and the significant wave height were also provided by Van Oord. These weather time series were not actual observations from the installation site, but they were calculated from data available from nearby offshore stations by using a weather model in order to transform the data for the installation location. The weather time series provided by Van Oord concern 10 years and they were given in 6 hours intervals.

The same analysis as the weather data analysis presented in Chapter 3, was also performed for Van Oords' weather data. The plots and the tables produced by the data analysis can be found in the Appendix B. The weather data analysis indicated that Gumbel copula describes best the dependence of wind speed and wave height, for all months except November and December. Analysis resulted in that Gaussian copula instead of Gumbel, should be used for November and December.

5.3 Results of test case

As it was mentioned before, the output of the tool is a CDF curve concerning the time needed to complete all the operations of the cable installation. The calculated time CDF curve shows the probability that the installation will be completed in at most a certain time. This approach provides a confidence level to the user concerning the estimation of the required time of the cable installation. Usually probability equal to 80% (P80) is used for estimations that concern the time of a project.

In this section the calculated CDF curves for several runs of the tool with reference to different inputs, are presented. Based on these results some important conclusions regarding the designed tool may be drawn.

5.3.1 Deltares and Van Oord weather data

First, the cable installation algorithm was used to calculate the CDF curves by providing as weather inputs the time series provided from Van Oord and Deltares. The calculated graphs are presented in Figure 5.3. The weather observations provided by Deltares concern 3 years in a location in the North Sea

Van Oord's weather data concern 10 years of constructed time series provided in 6 hours intervals. Since the simulation performed by the cable installation algorithm is in an hourly basis, the weather data were modified in order to obtain time series in one hour intervals. The adjustment of the data to time series with one hour intervals was done by assigning the value of each interval of the data to six hours of the hourly based time series.

As it can be seen from the calculated plots, there is a significant difference between the two curves. This could be explained by the fact that the data refer to different locations of the North Sea. Specifically Deltares' weather data come from a station located faraway from shore where more harsh weather conditions are observed. Therefore the weather windows are smaller and the estimated duration of the cable installation is higher.

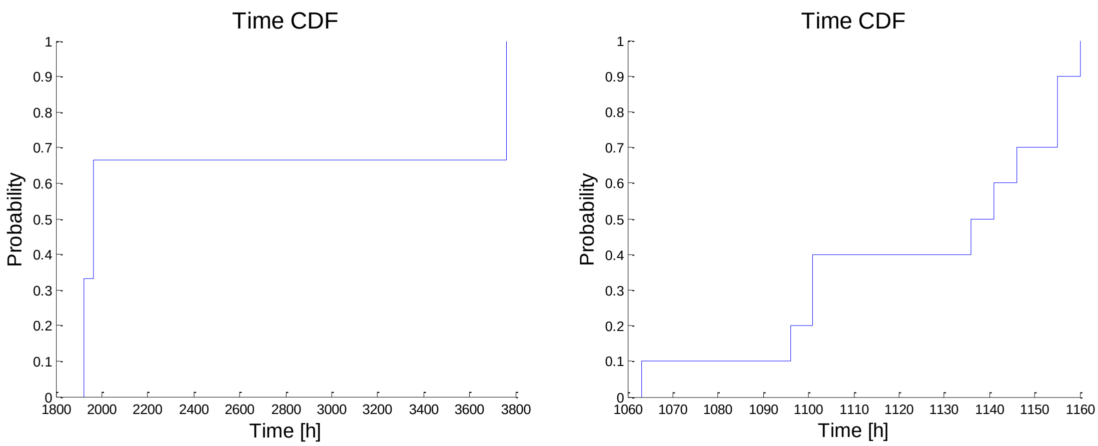

Deltares weather time series

Van Oord's weather time series

Figure 5.3: CDF curves calculated for Deltares observations and Van Oord's time series.

5.3.2 Number of simulations

Usually a large number of Monte Carlo simulations is needed to acquire a CDF curve that takes into consideration the uncertainties as much as possible. However as the number of simulations increases, the time that is needed to complete the simulations rises. Therefore it was decided to construct two sets of time series, which differ in the total number, based on Van Oord's weather data and compare them. The first set consists of

100 time series while the second consists of 1000 time series. The CDF curves obtained by the simulation of the proposed cable installation scenario for 100 and 1000 time series are presented in Figure 5.4 with blue and red color respectively. As it can been seen the obtained CDF curves are very similar and their P80 value is close to 1300 hours (i.e 55 days). The calculated duration of the infield cable installation could be considered realistic based on the statement of VBMS official website regarding the installation 111 infield cables in 4 months in Anholt OWF [57].

The P80 values of both cases are very close; for that reason it was decided that 100 time series are enough to provide a good estimation on the time needed for the cable installation, and that having a larger number of time series does not add value to the output of the tool. Since the construction of 1000 time series takes approximately 3 hours, that decision is crucial concerning the time needed to acquire an estimation by the decision support tool.

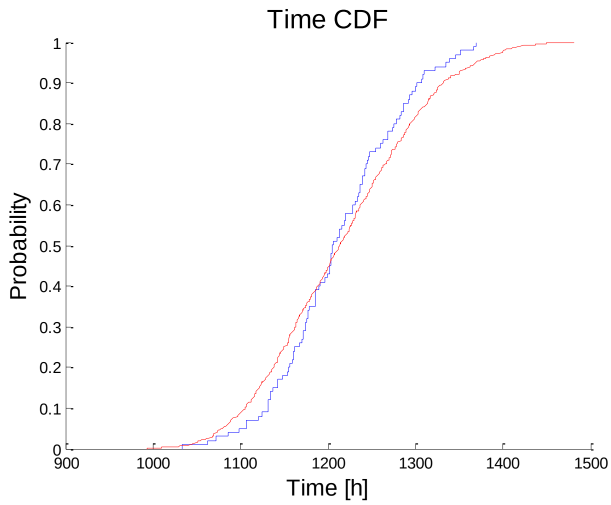

Figure 5.4: CDF curves for different number of time series

5.3.3 Constructed time series versus observed time series

One could claim that using the observed time series instead of constructing random time series, is sufficient to acquire a good estimation about the total time of the cable installation. For that reason in this paragraph the results of the cable installation algorithm, when constructed time series are taken into consideration, are compared to those of the observed data for both Deltares and Van Oord's weather data. In Figure 5.5 the CDF curves of the cable installation algorithm for the provided weather data as well as the CDF curves for constructed time series are presented.

As it can be seen in the plots for both Deltares' and Van Oord's weather data, the obtained CDF curves present a larger range in the estimation of the time, because they incorporate a larger number of possible weather conditions. Although the P80 value for Van Oord's weather data is close to that of the constructed time series, still it underestimates the required time to complete the cable installation in order of 145 hours (i.e. 6 days). It must be mentioned that although this difference seems small the impact of an underestimation such that may lead to significant impact on cost due to the high day rates of the vessels. On the other hand, this is not the case for the data provided by Deltares, where the P80 value of the data overestimates the duration in order of 1300 hours (i.e. 54 days). This result can be explained due to the limited numbers of observations and indicates that a smaller amount of time series may lead to a false estimation of the time needed to complete the installation and subsequently to false decisions (e.g. choosing better equipped and more expensive vessels to reduce the duration) that may increase the cost of the cable installation.

Another important reason why it is advised to use constructed time series based on the observations instead of using the actual observations is that often it is difficult to access a large number of a high standard weather data, since often data are missing from the observed time series due to failures of the measuring equipment. For the above reasons, it is recommended to use constructed time series, in order to include in the estimation of the time CDF as many possible conditions as possible.

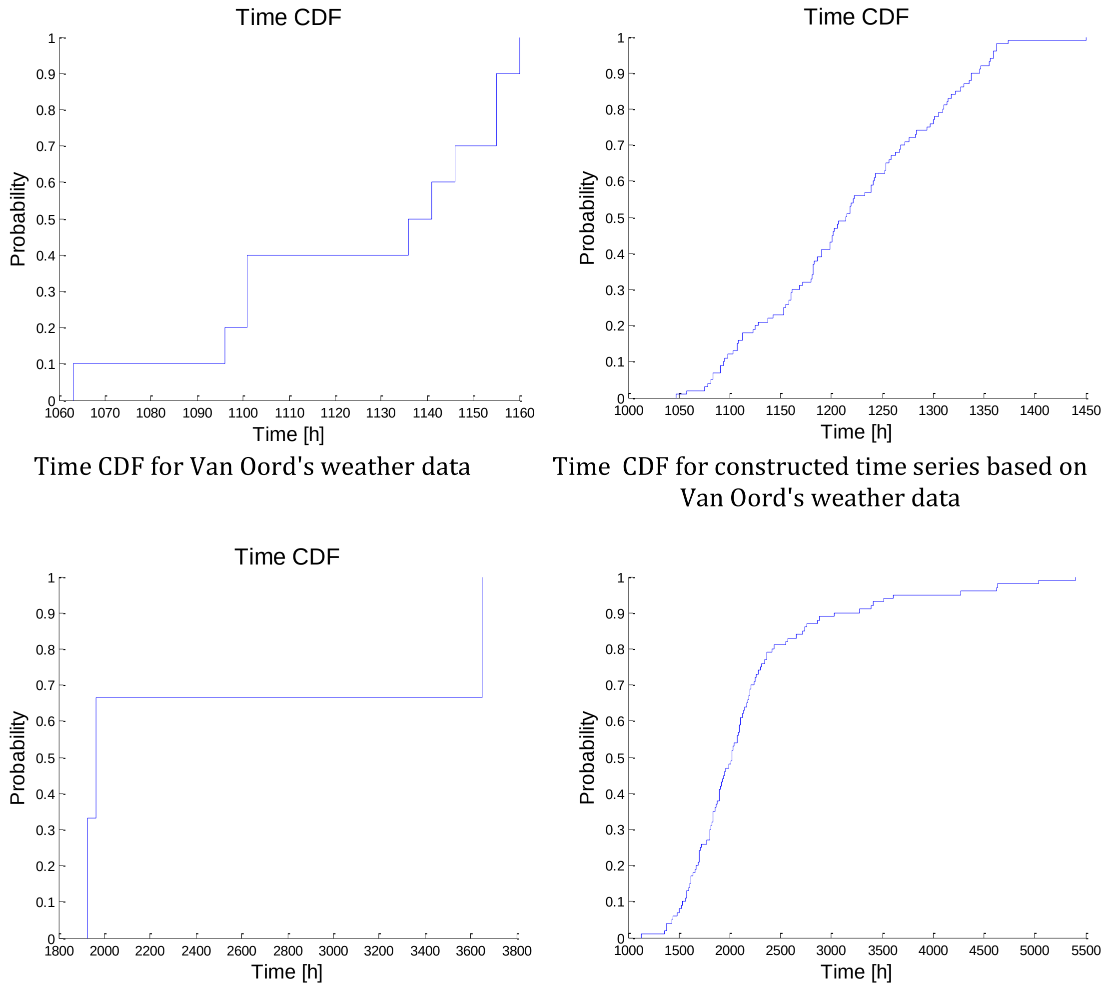

Time CDF for Van Oord's weather data

Time CDF for constructed time series based on Van Oord's weather data

Time CDF for Deltares' weather data

Time CDF for constructed time series based on Detares' weather data

Figure 5.5: CDF curves of weather data and constructed time series.

5.3.4 Independent case

Another case that is worth investigating is the case where weather time series are constructed independently, without taking into account the dependence between wind speed and wave height. In that case, the wind speed values and the wave height values are constructed independently, by calculating random numbers in [0,1] and using the empirical cumulative distribution of every month, for wind speed and wave height separately.

In Figure 5.6 and 5.7, the scatter plots of 100 years of generated time series independently and by using Copulas are presented respectively. It is clear that although the independently constructed time series present the same extreme values as the provided weather data, their scatter plot presents important differences compared to the scatter plot of the provided weather data (Appendix B.2). On the other hand although the constructed time series using Copulas have the same marginal distributions as the independently constructed time series, their scatter plot is similar to the scatter plot of provided weather data and present realistic couples of wind speeds and wave heights.

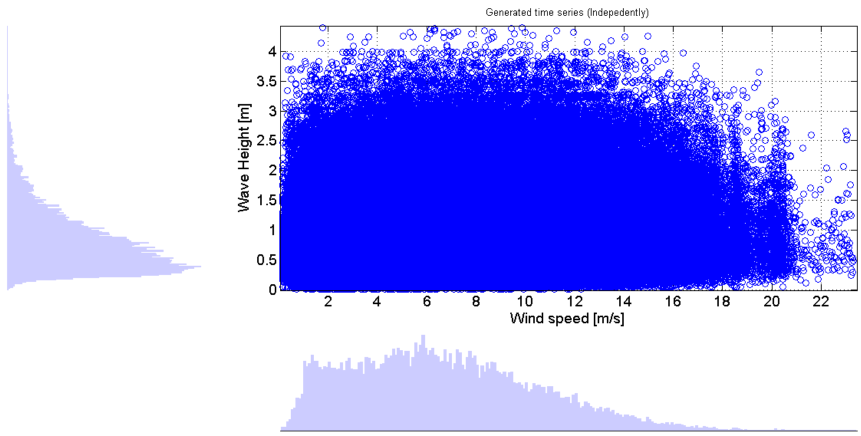

Figure 5.6: Scatter plot of independently constructed time series.

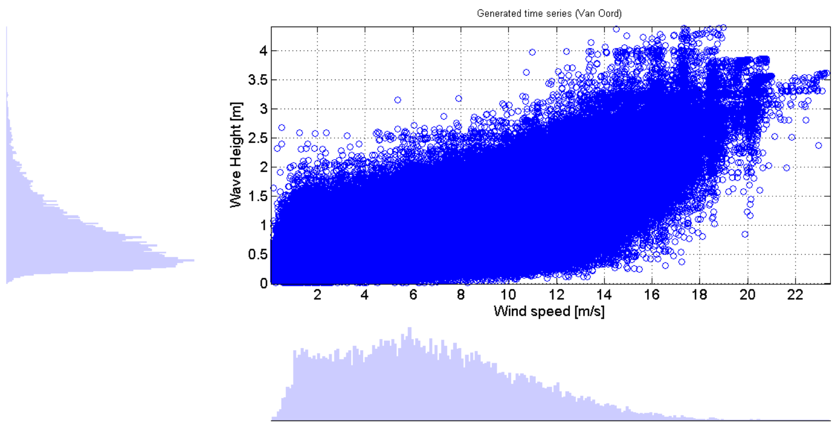

Figure 5.7: Scatter plot of constructed time series using Copulas.

In Figure 5.8 the time CDF curve for the case where time series constructed independently as well as the time CDF for the time series constructed using Copulas method, are presented. As it can be seen the time CDF curve of the independent case has a much bigger range than that of the dependent case. This result can be explained due to the fact that since the wind speed and the wave height are constructed independently, the cases where at least one of the two values exceeds the limits of the vessel are more often. This detail results in shorter weather windows and subsequently more time is needed to complete the cable installation. Therefore the P80 value of the independent case overestimates the required time in an order of 400 hours (i.e. 17 days) compared to the case of dependently constructed time series. An overestimation of that scale may lead to false decisions regarding the duration and increase the cost of the cable installation. For the above reasons, it is recommended to use constructed time series that take into account the dependence of the wind speed and the wave height observed in the site, in order to estimate more accurately the time of the cable installation.

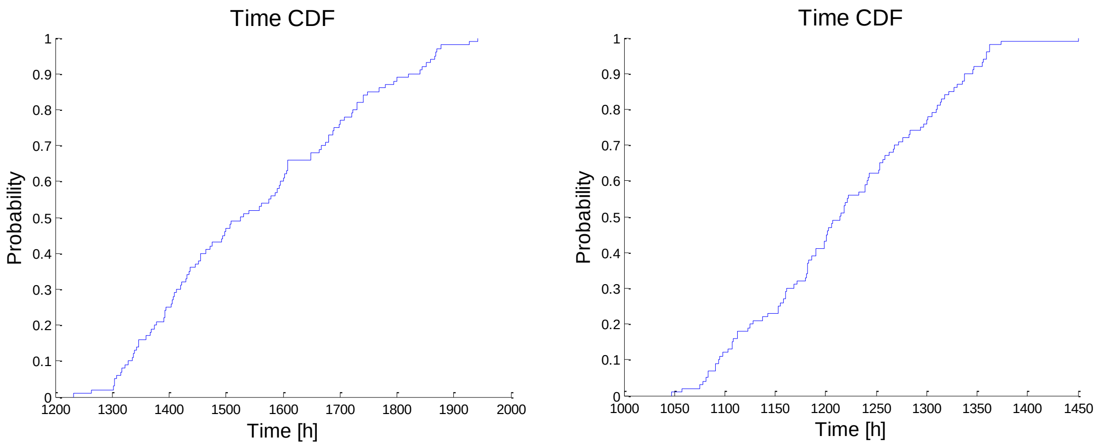

Time CDF for independently constructed time series based on Van Oord's weather data

Time CDF for constructed time series based on Van Oord's weather data, using Copulas

Figure 5.8: Time CDF for independently versus dependently constructed time series.

5.3.5 Effect of season

As it was mentioned, usually the cable installation is planned for the summer months. However the tool is able to simulate the cable installation starting on whatever date the user choose. For that reason it was decided to test the algorithm by changing the starting hour of the cable installation from 3625 (June 1st) to 8016 (December 1st). Figure 5.9 presents the obtained CDF curves considering constructed weather time series based on Van Oord's weather data and actual weather data for the two different periods.

One may observe that the time needed to complete the cable installation in winter is much larger than in summer. Specifically the calculated P80 value of the winter case is equal to 3000 hours and it is more than two times larger than the P80 value of the summer case. This outcome seems logical and it was expected since the weather windows during winter period are scarcer.

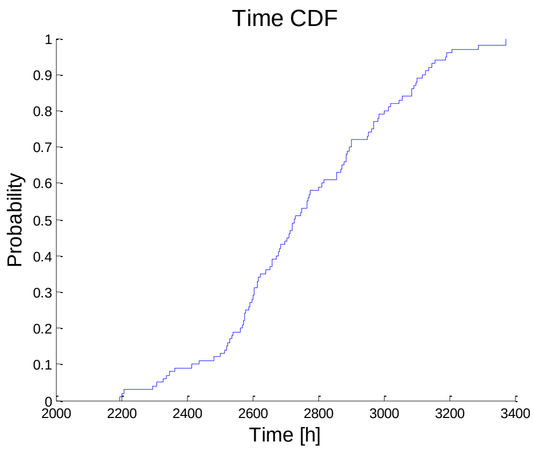

Winter case for dependently constructed time series

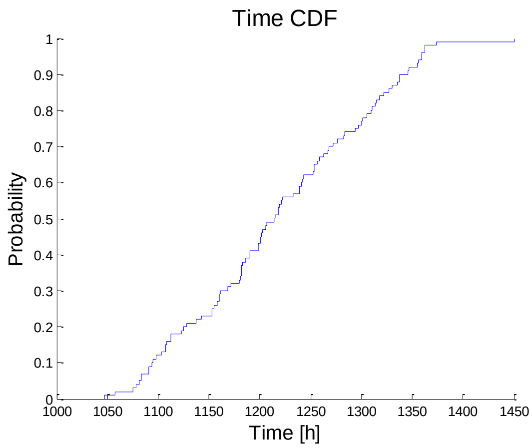

Summer case for dependently constructed time series

Figure 5.9: Time CDF curve for different starting dates.

5.3.6 Include weather effect on performances

The provided test case by Van Oord assumed that the performance of the operations is constant. However as it was explained in Chapter 4, the tool offers to the user the opportunity to include the effect of weather on the performances of the operation. For that reason the following Table 5.6 and Table 5.7, show the hypothetical case where the performance depends on weather in order to identify how the results are affected.

Table 5.6: Limits of the operations

Operation	Wind (max)	Wave (max)	Wind (normal)	Wave (normal)
Pre-lay grapnel run	-	1.5 m	-	0.8 m
Pull-in	12 m/s	1.25 m	9	0.7 m
Pre lay survey	-	1.75 m	-	0.9 m
Cable laying	12 m/s	1.75 m	9	0.9 m
Pre-burial survey	-	1.5 m	-	0.9 m
Burying cable	-	1.5 m	-	0.8 m
Post-burial survey	-	1.5 m	-	0.8 m

Table 5.7: Performance of the operations

Operation	Performance (max)	Performance (normal)
Pre-lay grapnel run	*** m/h	*** m/h
Crew transfer	min ***h peak ***h	max ***h
Pull-in	*** h	*** h
Pre lay survey	*** h	*** h
Cable laying	*** m/h	*** m/h
Pre-burial survey	*** m/h	*** m/h
Burying cable	*** m/h	*** m/h
Post-burial survey	*** m/h	*** m/h

Note: The values of Table 5.7 were excluded from the report due to confidentiality reasons.

In Figure 5.10 the output CDF distribution of the case where the performance is weather dependent is represented by the red line, while the case where the performance is assumed constant and equal to the maximum performance is represented by the blue line. As it was expected, when the performance is considered weather dependent the resulted duration of the cable installation is higher compared to that of the case where the performances are considered constant. Although this approach seems to affect the output distribution in a more realistic manner, it must be mentioned that the user should only use this when he/she is sure about the values of the normal limits and the normal performances. Otherwise the algorithm may overestimate the required time.

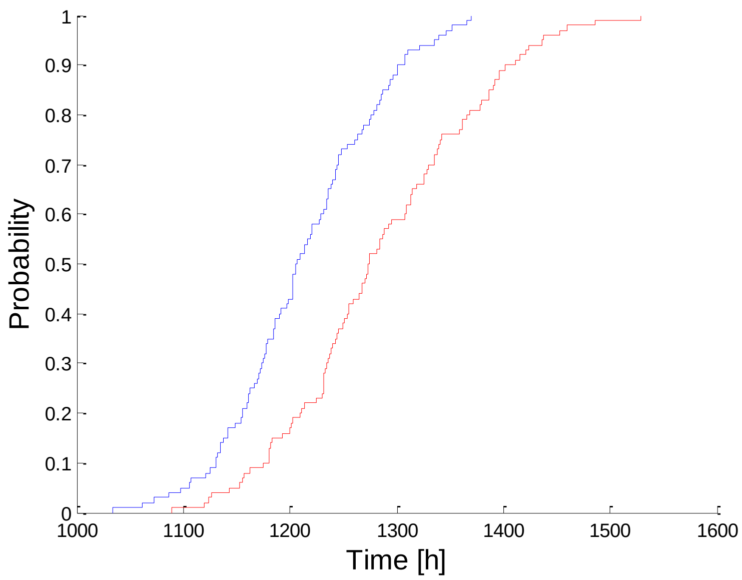

Figure 5.10: Time CDF curves for constant and weather dependent performances.

5.3.7 Comparing different scenarios

It was mentioned that the designed tool can be used to compare different installation scenarios. For that reason it was chosen to also investigate the case of simultaneously burying of the cable. This scenario was also modeled and simulated for the same set of constructed weather time series as the post-lay burial scenario. Following this approach the two different methods can be compared by the user, using their output CDF curves of the duration of the cable installation.

The main difference between the two methods is that in simultaneously burying method, the burying of the cable is performed simultaneously by a trencher as the CLV lays the cable. Therefore a separate burying vessel is not needed. The Gantt charts containing the operation of the two different scenarios are presented in Figure 5.11.

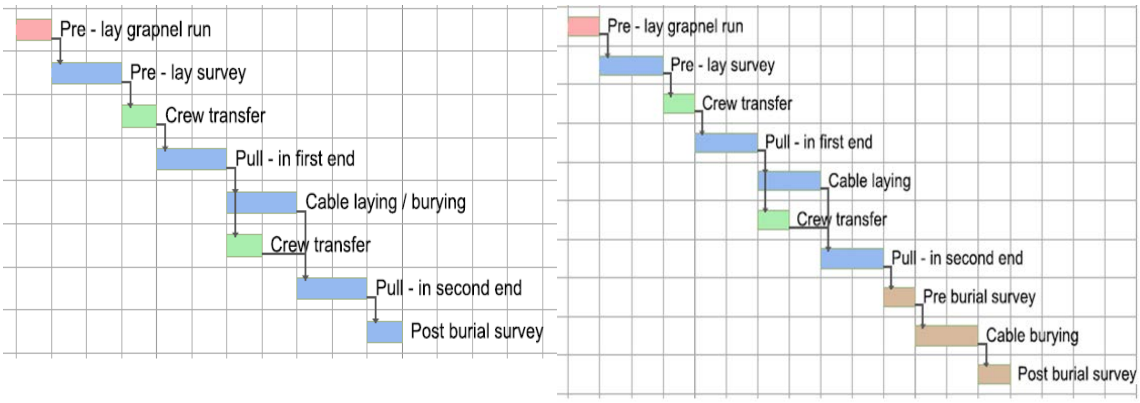

Simultaneously burying scenario Post lay burying scenario

Figure 5.11: Gantt charts of the two scenarios under investigation

In order to simulate the simultaneously burying scenario, the performances of the all operations, except cable laying performance, were kept equal to the performances of the post lay burying scenario, presented in Section 5.1. The performance of the simultaneously laying and burying of the cable was assumed equal to 150 m/h, which is slightly smaller than the burying operation of the post-lay burying scenario.

In Figure 5.12 the results of the simulation of the two cable installation scenarios, when the performances are considered constant, are presented. The simultaneously burying scenario is presented with the red line while the post-lay burying scenario is represented by the blue line. As it can be seen, the post lay burying scenario presents smaller duration for every simulation. As far as the P80 value of the two different scenarios is concerned, it can be seen that the simultaneously burial scenario has more than 200 hours larger estimated duration compared to the post-lay burying scenario. Thus based on this result the user should clearly choose the post-lay burying scenario instead of the simultaneously burying scenario.

However it must be mentioned that in order to completely evaluate the two cable installation scenarios and find the optimal, the cost must also be taken into consideration. The reason is that the simultaneously burying scenario does not require a separate vessel for burying the cable and therefore the total cost of the cable installation may be smaller.

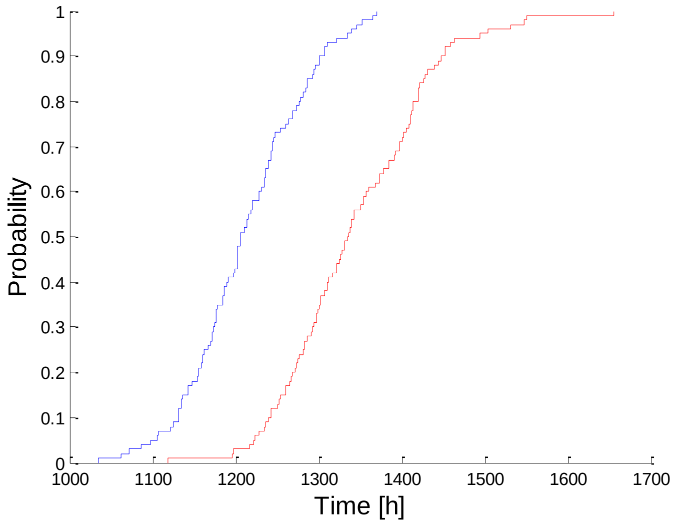

Figure 5.12: Time CDF curves for simultaneously burying and post lay burying scenarios.

6. Conclusions and recommendations

This chapter presents the conclusions derived from the work conducted for the current thesis, providing answers to the research questions. Based on the conclusions, recommendations and remarks for further future research are suggested.

6.1 Conclusions

The main goal of the thesis was the design of a probabilistic decision support tool to facilitate a professional engineer in comparing different cable installation scenarios and chose the optimal. The main research questions of the current thesis were set in the first chapter. The research questions as well as their answers provided by the conducted research, follow.

1. How realistically can weather time series, that take into account the dependence between the weather variables, be produced? Why is this important?

In order to produce time series concerning the wind speed and the wave height by taking into account the dependence between these variables, a method based on Copulas functions is proposed. This method concerns the application of a statistical analysis, which consists of different tests, on the provided historical weather data. There are various families of Copulas, for the purpose of this thesis three of the most commonly used families the Gaussian, the Gumbel and the Clayton Copula were investigated. Based on the results of the analysis, the Copula family that describes best the weather data for each month as well as its parameter can be identified. It was found that Gumbel Copula describes best the dependence between the wind speeds and the significant wave heights as far as the provided weather data sets are concerned. Moreover it was shown that Gumbel Copula supports the observation that given high values of wind speed (e.g. above 9 m/s) are observed, high values of wave height (e.g. above 1.8 m) will occur with a probability equal to 0.55 which is very close to the conditional probability of observations and higher than the probability of Gaussian Copula which is equal to 0.35. That is an important remark because it shows that not choosing the appropriate copula may lead to underestimation of weather windows and consequently to inadequate estimation of the duration of the cable installation.

After identifying the best fitting Copula function, as many time series of the wind speed and wave height as needed may be constructed, by taking into consideration the dependence between the two weather variables as well as their autocorrelation. Also it should be noted that analysing the weather observations of each month and calculating a parameter for each month ensures that the seasonality of weather observations will be preserved in the generated time series. The seasonality of the produced time series is crucial because as it was shown by the simulation of a test case provided by Van Oord, the estimation of the duration of the same cable installation scenario during winter may be more than two times larger than the estimation of the duration during summer.

Another important observation is that the generated time series using Copulas are more realistic than the independently generated time series. This observation appeared to have a significant influence on estimation of the duration and consequently the cost of the infield cable installation. Specifically it was shown that in the case where weather time series were constructed independently the estimation of the cable installation duration may be overestimated up to 400 hours compared to the case where time series were constructed by taking into consideration the dependence. Hence it is important to use constructed time series that take into account the dependence of wind speed and wave height observed in the installation site, in order to acquire better estimation of the total duration and cost of the infield cable installation or similar offshore applications.

2. How to calculate the time needed for infield cable installation including uncertainties?

In order to calculate the time needed for the installation an algorithm that simulates the proposed cable installation scenario was designed. The uncertainties of the cable installation are included in the tool by three methods. First the weather uncertainty which is considered the most important factor of delays and misestimations is tackled by generating an appropriately large number of random weather time series that take into account the dependence between the weather conditions. Secondly, the tool is able to include the dependence of weather on the performance of the installation or calculate it randomly from a provided distribution in order to include the uncertainty on the time needed to execute an activity. Finally, the tool may include certain failures and incorporate the risk of failure occurrence and the impact that it has on the total time of the cable installation.

3. Can the tool help in obtaining better insight regarding the proposed installation scenarios under the influence of uncertainties?

In order to investigate if the designed tool can help the user to get estimation including uncertainties, the provided test case was also simulated for two different sets of weather data and the output CDF curves were calculated. It was found that simulating the proposed installation scenario for a large number of constructed time series instead of a limited number of observations may lead to estimation that incorporate a higher level of uncertainty since it takes into account larger number of weather conditions.

Moreover the designed tool was used to simulate two different cable installation scenarios with different methods of cable burying using (i.e. post-lay burying and simultaneously burying). Based on the produced CDF curves of the time needed to complete the installation, it was found that the post-lay burying method is better as far as the duration of the installation is concerned.

Also it must be mentioned that in contrast to the time needed to construct a large number of random time series, the designed cable installation algorithm is able to complete hundreds of simulations in less than a minute. This attribute of the tool offers to the user the ability to test different installation scenarios in a small amount of time and obtain the required information that help in deciding which scenario is the optimal. Concluding, the designed tool can be used to simulate different cable installation scenarios or various cases considering types of vessels with different characteristic including uncertainties. Also it can assist the professional concept engineer to decide the optimal scenario and combination of vessels leading to the reduction of the duration and consequently the cost of the infield cable installation.

6.2 Recommendations

The designed tool would be useful for professional engineers who want to try different scenarios that concern the infield cable installation, by providing estimation on the time needed to complete the installation. However it must be mentioned that there still exist areas for further development. The designed tool could be improved in the following ways.

First, it must be mentioned that although wave height and wind speed are the most important weather conditions for the cable installation, there are also other met-ocean conditions, such as the speed of currents the wind direction and the temperature that may have an impact on the total time. Therefore incorporating speed of currents and temperature, in order to have a more accurate model is recommended for future study. For that case the use of Vine Copulas which are used for multivariate data, is suggested.

Moreover, the performed weather data analysis was focused on testing the most common one-parameter Copulas functions. Therefore, for future research it is suggested to investigate Copula families with more than one parameter in order to include the observed skewness of the weather data in the produced weather time series.

Also it must be mentioned that using the same methodology as the one presented in Chapter 4, a future researcher could expand the existing tool by adding more installation operations and more types of vessels, in order to simulate the entire installation of the offshore wind farm. Also an overview of the asset utilization as well as the calculation of the total time lost due to harsh weather conditions could be added to help the professional concept engineer in considering which components or operations could be improved or changed in order to reduce the duration of the installation.

Furthermore it would be interesting to apply a similar approach in order to simulate and draw conclusions regarding different scenarios concerning the operation and maintenance of the OWF.

Additionally it would be very useful for professional engineers who are used in deterministic approaches, to use the designed tool in order to calculate “factors” which represents the uncertainties. These factors could be used to incorporate the influence of uncertainties to the deterministic estimations of the duration of a cable installation scenario. However it must be noted that this process is not trivial and would require substantial research in order to provide safe results.

Finally it must be mentioned that the tool, as every simulation model, provides outputs with a quality directly related to the quality of inputs. Therefore the quality of the outputs of the designed tool could be improved by entering as accurate inputs as possible. For that reason it is recommended to investigate the use of structured expert judgment techniques in order to acquire more accurate inputs and consequently more precise outputs.

Bibliography

[1] Morandeau M., Walker R. T. , Argall R., Nicholls-Lee R. F. (2013), "Optimization of marine energy installation operations", International Journal of Marine Energy, Available from: http://dx.doi.org/10.1016/j.ijome.2013.11.002

[2] Kaiser M. J., Snyder B. F. (2013), "Modeling offshore wind installation costs on the U. S. Outer Continental Shelf", Renewable Energy, Vol. 50, pp. 676-691

[3] Gonzalez J. S. , Payan M. B., Santos J. R. (2013), "Optimum design of transmissions systems for offshore wind farms including decision making under risk", Renewable Energy, Vol. 59, pp. 115-127

[4] Esteban, M. and Leary, D., (2011), “Current Developments and Future Prospects of Offshore Wind and Ocean Energy”, Journal of Applied Energy (in print)

[5] The Crown Estate (2012), "Offshore Wind Cost Reduction: Pathways Study", www.thecrownestate.co.uk

[6] Roland Burger (2013), "Offshore Wind Toward 2020: On the pathway to cost competitiveness", Roland Berger Strategy Consultants GmbH-Presentation

[7] Junginger M., Faaij A. (2009), "Cost Reduction Prospects for the offshore Wind Energy Sector", Department of Science, Technology and Society, Copernicus Institue, Utrecht University

[8] Offshore: Risk &Technology Consulting, (2011), "Offshore Electrical Cable Burial for Wind Farms: State of the Art, Standards and Guidance & Acceptable Burial Depths, Separation Distances and Sand Wave Effect", Bureau of Ocean Energy Management, Regulation & Enforcement- Department of the Interior

[9] Dickel R., Hassanzadeh E., Henderson J., Honoré A., El-Katiri L., Pirani S., Rogers H., Stern J., Yafimava K., (2014), "Reducing European Dependence on Russian Gass: distinguishing natural gas security from geopolitics", Oxford Institute for Energy Studies

[10] Thomsen K. (2012), "A Comprehensive Guide to Successful Offshore Wind Farm Installation", Advanced Offshore Solutions, Tranbjerg, Denmark

[11] Massachusetts Clean Energy Center (2010), "Port and Infrastructure Analysis for Offshore Wind Energy Development", Tetra tech ec, Inc., Boston, Massachusetts

[12] Malhotra S. (2011), "Selection, Design and Construction of Offshore Wind Turbine Foundations", Wind Turbines, Dr Ibrahim Al-Bahadly (Ed.), Available from: http://www.intechopen.com/books/wind-turbines/selection-design-and-construction-of-offshore-wind-turbine-foundations

[13] Van Oord CZ (2001), "Cable Installation study for DOWEC", DOWEC-F1W1-RH-01-033/00

[14] Kaiser M. J., Snyder B. F. (2010), "Offshore Wind Energy Installation and Decommisioning Cost Estimation in the U. S. Outer Continental Shelf", Bureau of Ocean Energy Management, Herndon, Vol 648, pp. 340

[15] Dewan A. (2014), "Logistic & Service Optimization for O&M of Offshore Wind Farms", MSc thesis, TU Delft

[16] Dogger Bank (2012), "Dogger Bank Teeside PEI1. Appendix A: Project Description", Forewind

[18] Wright S., Rogers A., Manwell J., Ellis A., (2002) "Transmission option for offshore wind farms in the United States", Renewable Energy Research Lab University of Massachusetts

[19] The Crown Estate (2012), "Submarine cables and offshore renewable energy installations", www.thecrownestate.co.uk

[20] Johansson S., Liljestrand L, Krogh F., Karlstrand J., Hanson J. (2005), "AC Cable solutions for Offshore Wind Erergy"

[21] Worzyk th. (2009), "Submarine Power Cables. Design, Installation, Repair, Environmental Aspects", Springer

[22] Allan P. (1998), "Selecting appropriate cable burial depths a methodology", IBC Conference on Submarine communications.

[23] Magazine for the offshore wind industry (2010), "Subsea cable installation a technical guide"

[24] Haskoning R., BOMEL Ltd (2008), "Review of cabling techniques and environmental effects applicable to the offshore wind farm industry", Berr (department for Business Enterprise & Regulatory Reform), UK

[25] Bard J., Thalemann F. (2012), "Offshore Infrastructure: Ports and Vessels", Orecca, Fraunhofer IWES

[26] Seidel M. (2007), "Jackets substructures for the REpower 5 MW wind turbine", European Offshore Wind Conference, Berlin

[27] Aardal Flo R. (2009), "Configuration of large offshore wind farms", MSc thesis, Norwegian University of Science and Technology

[28] http://flow-offshore.nl/

[29] Negra, Barberis N, Holmstrom, Bak-Jensen, Sorensen (2006), "Comparison of different techniques for offshore wind farm reliability assessment" Aalborg University

[30] Dorey, Joubert, "Modelling Copulas: An overview", The Staple Inn Actuarial Society

[31] Nelsen, "An introduction to Copulas", Springer Series in Statistics, second ed., 2006

[32] Papoulis and Pillai, "Probability, Random Variables and Stochastic Processes", Electrical and Computer Engineering, McGraw-Hill, fourth ed., 2002

[33] Papaefthymiou (2006), "Integration of Stochastic Generation in Power Systems", PhD thesis, TU Delft

[34] Grobmab (2007), "Copulae and tail dependence", Diploma thesis, Center for Applied Statistics and Economics

[35] Genest C., Favre (2007), "Everything you always wanted to know about copula modeling but were afraid to ask", Journal of Hydrologic Engineering

[36] Kort (2007), "Modeling tail dependence using copulas-literature review", TU Delft

[37] Genest, Remillard, Beaudoin (2007), "Goodness-of-fit tests for copulas: A review and a power study", Insurance: Mathematics and Economics

[38] Morandeau M., Walker R. T. , Argall R., Nicholls-Lee R. F. (2013), "Optimization of marine energy installation operations", International Journal of Marine Energy

[39] Morales-Napoles, Steenbergen (2014), "Analysis of axle and vehicle load properties through Bayesian Networks based on Weigh-in-Motion data", Reliability Engineering and System safety

[40] Patton (2012),"Copulas Methods for Forecasting Multivariate Time series", Duke University

[41] Kurowicka D., Joe. H. (2011), "Dependence Modelling, Vine Copula Handbook", World Scientific Publishing Co. Pte Ltd.

[42] Nelsen R. B. (2003), "Properties and applications of copulas: A brief survey," Proceedings of the First Brazilian Conference on Statistical Modelling in Insurance and Finance, University of São Paulo

[43] Bauer E., Staabs C. (1998), "Statistical properties of global significant wave heights and their use for validation", Journal of Geophysical Research, Vol 103, NO. C1. Pages 1153-1166, January 15, 1998

[44] Joe H. (2015), "Dependence Modeling with Copulas", CRC Press, Taylor & Francis group

[45] Fischer M., Klein I. (2007), "Some Results on Weak and Strong Tail Dependence Coefficients for Means of Copulas", Lehrstuhl für Statistik und Ökonometrie

[46] Aas K., Czado C., Frigessi A., Bakken H. (2007), "Pair-copula construction of multiple dependence", Insurance: Mathematics and Economics 44 (2009) 182-198

[47] Marks R. E. (2014), "Monte Carlo Method", Palgrave Encyclopedia of Strategic Management

[49] Ruohonen K., (2013), "Graph Theory", Tampere University of Technology

[50] Unosson O. (2009), "Offshore Cable Installation - Lillgrund", The Swedish Energy Agency

[51] Mwemezi J., Huang Y. (2011), "Optimal Facility Location on Spherical Surfaces: Algorithm and Application", Logistics Research Center, Shanghai Maritime University

[52] http://www.math.wm.edu/˜leemis/chart/UDR/UDR.html

[53] http://nl.mathworks.com/matlabcentral/fileexchange/7309-randraw

[54] Remillard B., (2010), "Goodness-of-fit test for copulas of multivariate time series", HEC Montreal

[55] Yang X., Zhang Q. (2013), "Joint probability distribution of winds and waves from wave simulation of 20 years (1989-2008) in Bohai Bay", Water Science and Engineering, pages: 296-307

[56] Norouzi M., Nikolaidis. (2013), "Modeling dependence between Wind and Wave in an Offshore Wind Turbine Site", International Offshore and Polar Engineering Anchorage, Alaska, USA, June 30 - July 5, 2013

[57] http://www.vbms.com/en/projects/detail/anholt-offshore-wind-farm-array-cable-installation

Appendix A

A.1 Scatter plots of NOAA weather data

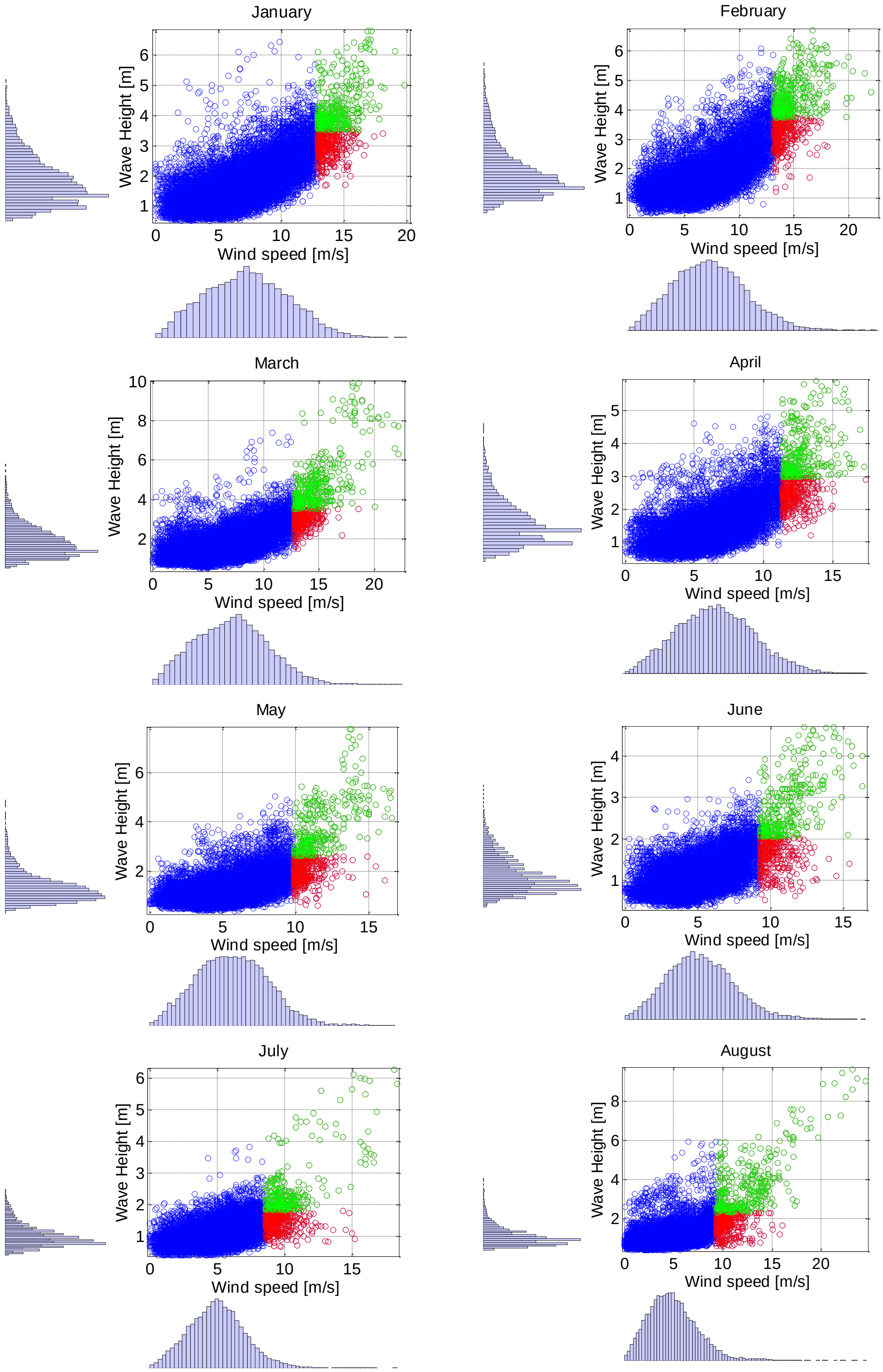

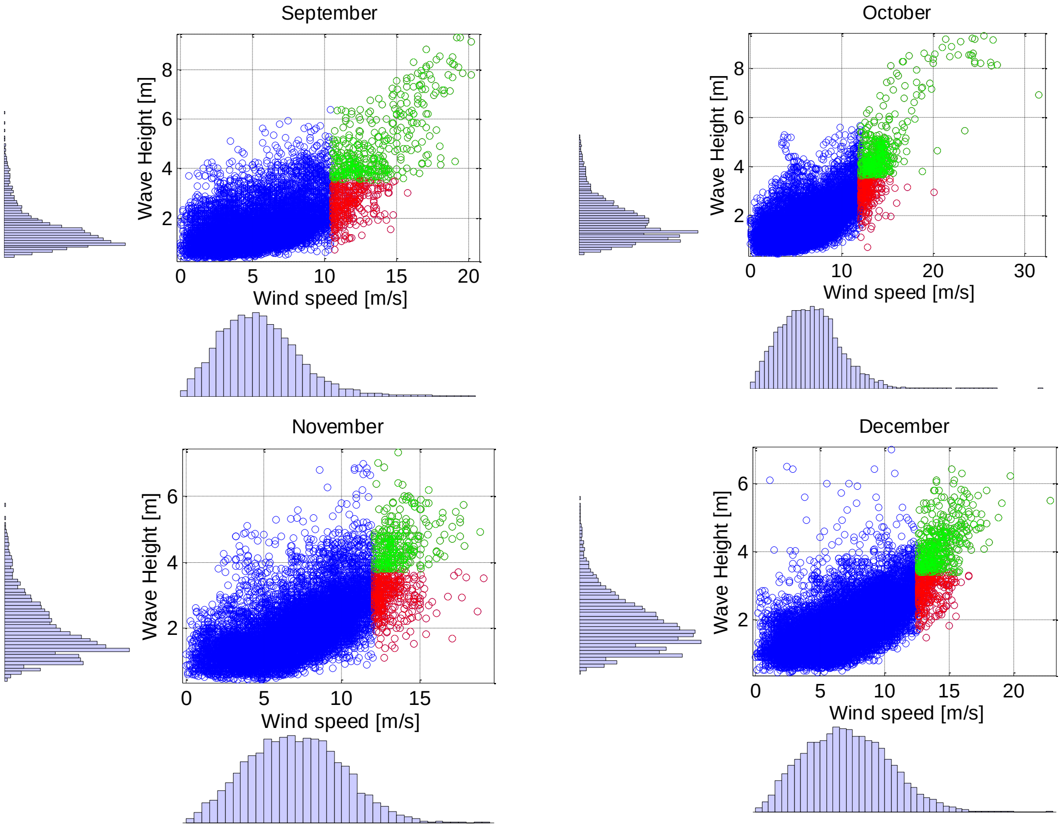
September
Wave Height [m]
Wind speed [m/s]
October
Wave Height [m]
Wind speed [m/s]
November
Wave Height [m]
Wind speed [m/s]
December
Wave Height [m]
Wind speed [m/s]

A.2 Scatter plots of Deltares weather data

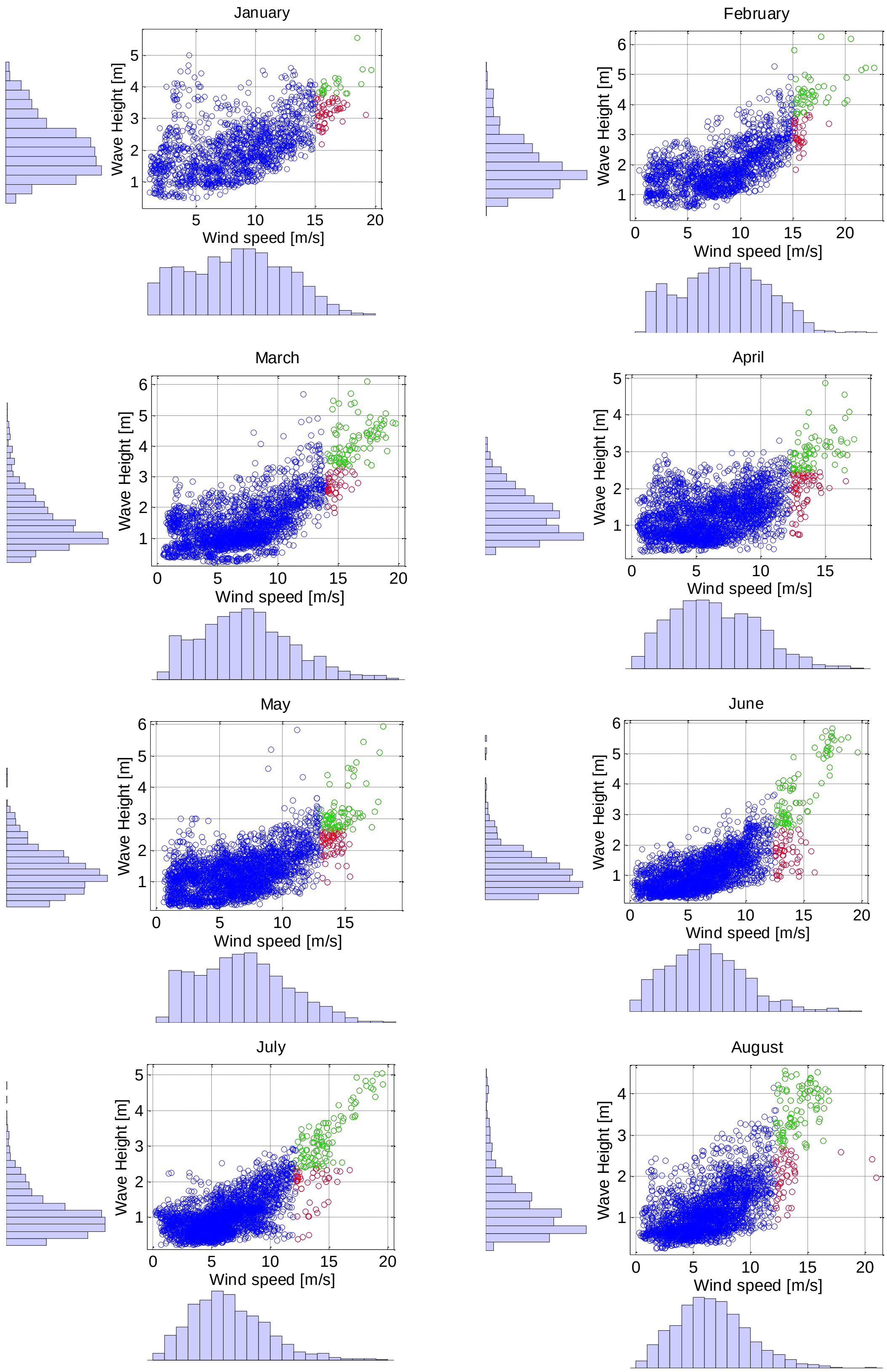

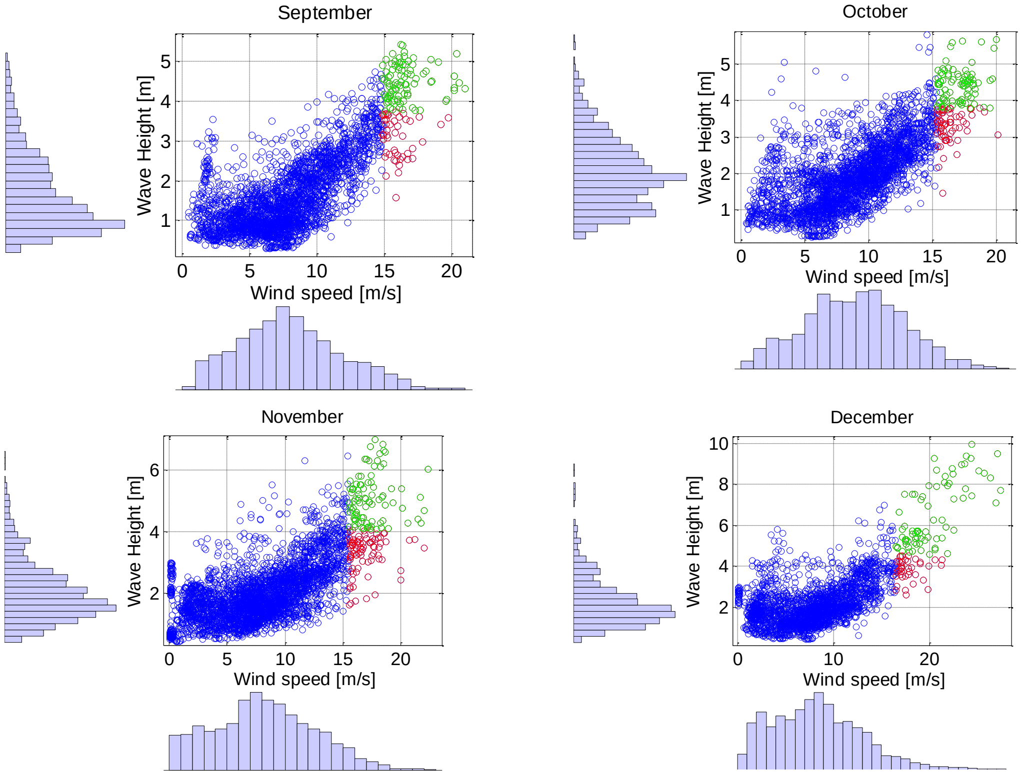
September
Wave Height [m]
Wind speed [m/s]
October
Wave Height [m]
Wind speed [m/s]
November
Wave Height [m]
Wind speed [m/s]
December
Wave Height [m]
Wind speed [m/s]

A.3 Exceedance probability for different percentiles (NOOA weather data)

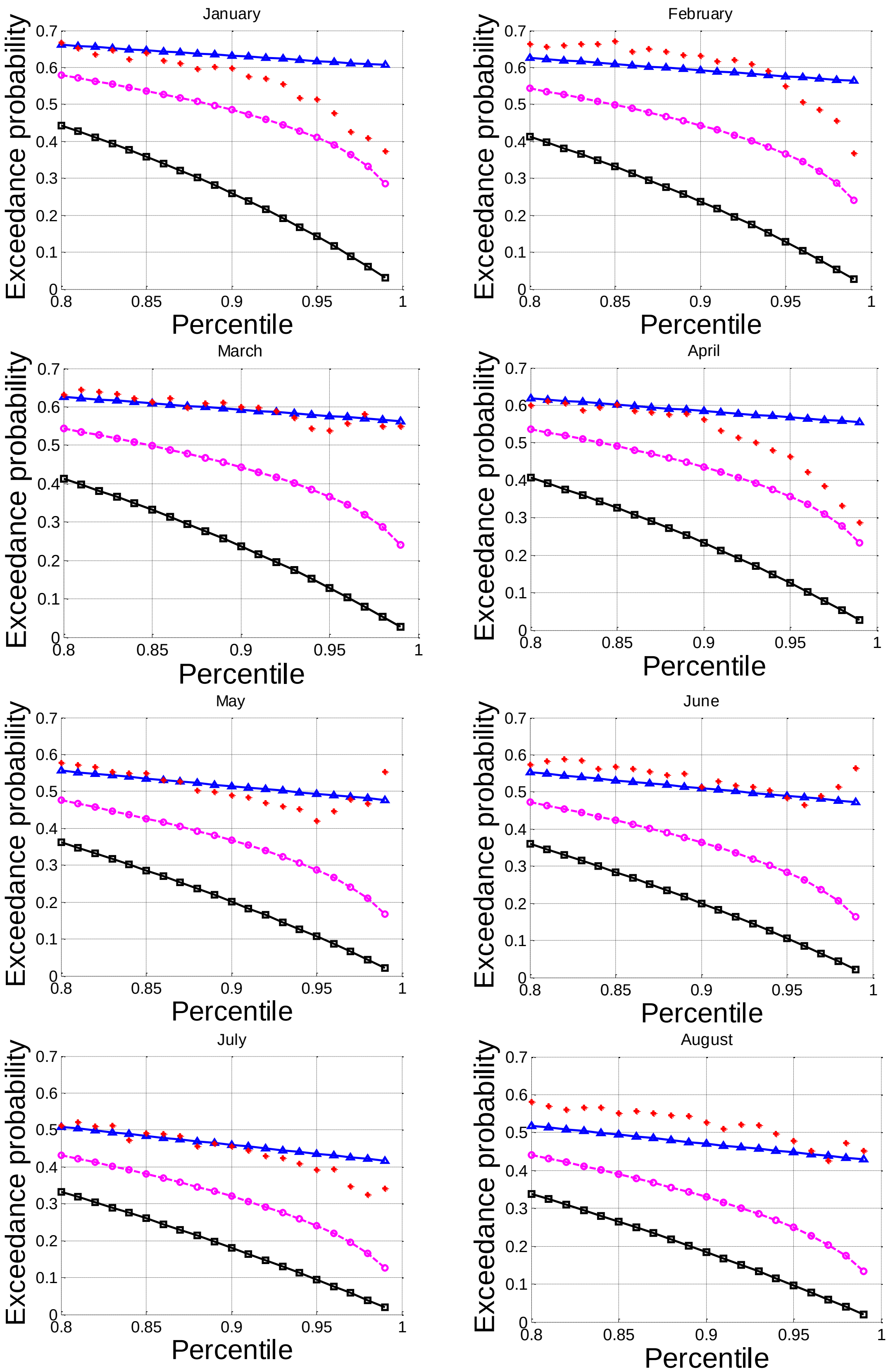

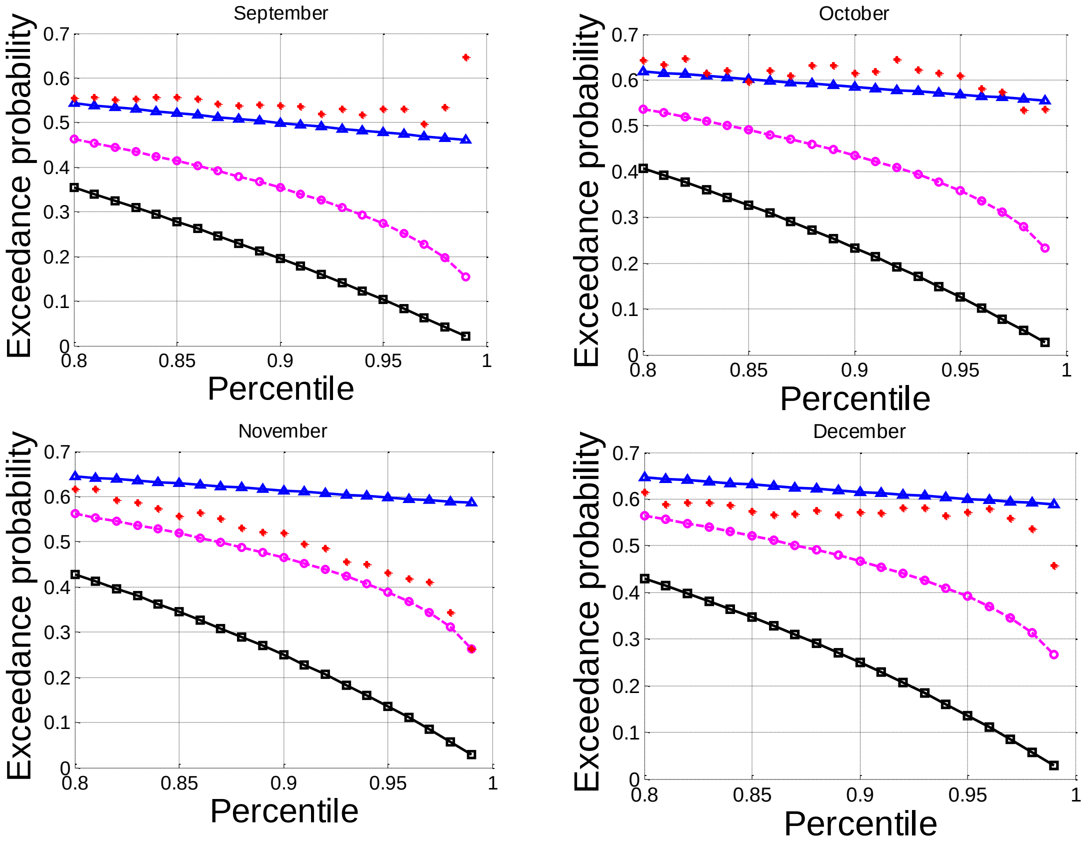
September
October
November
December
Exceedance probability
Percentile
0.7
0.6
0.5
0.4
0.3
0.2
0.1
0
0.8
0.85
0.9
0.95
1

A.4 Exceedance probability for different percentiles (Deltares weather data)

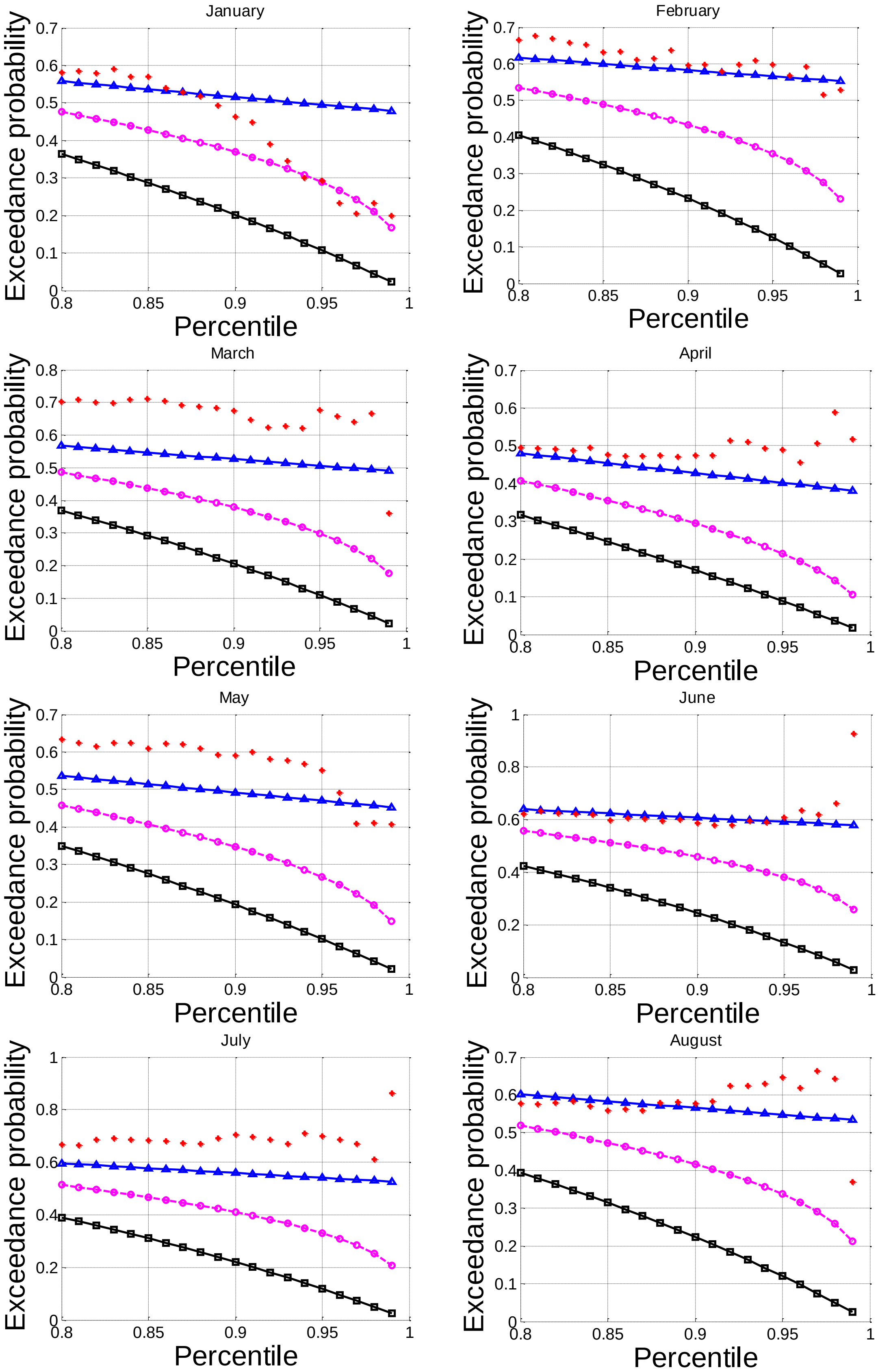

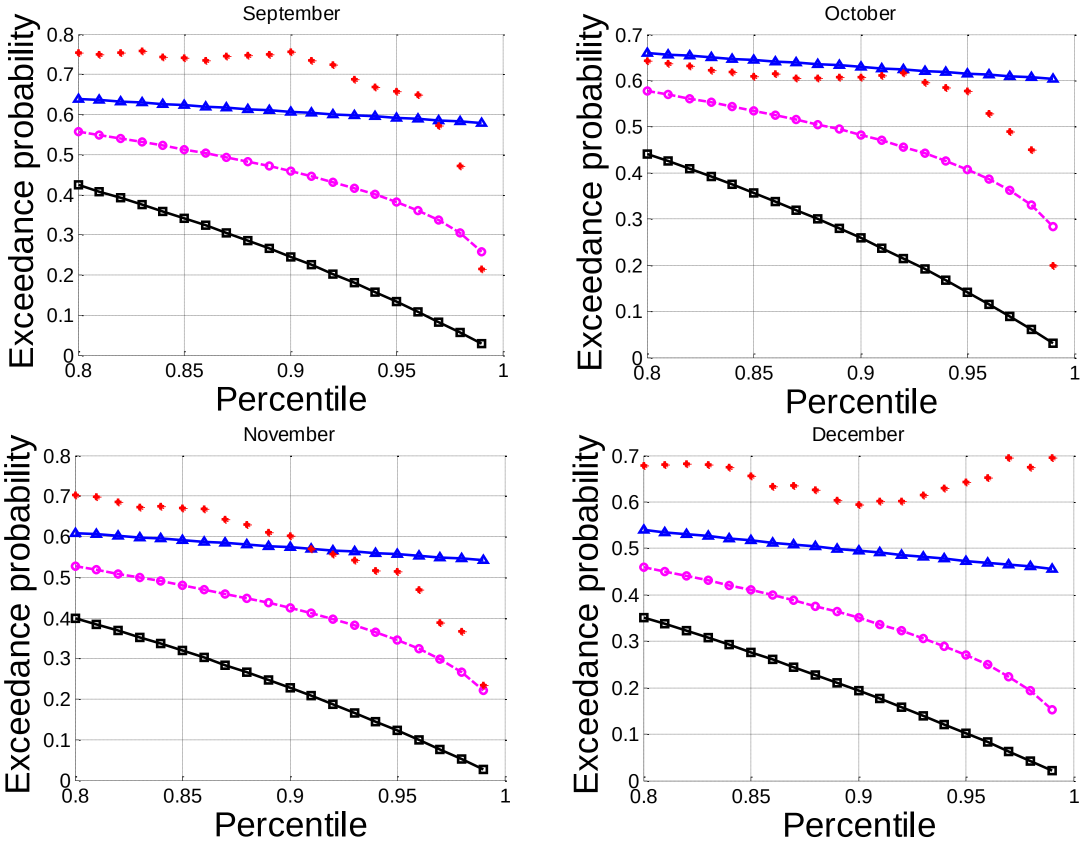
September
October
November
December
Exceedance probability
Percentile
0.8
0.85
0.9
0.95
1
0
0.1
0.2
0.3
0.4
0.5
0.6
0.7
0.8

A.5 Scatter plots of generated time series based on Deltares observations

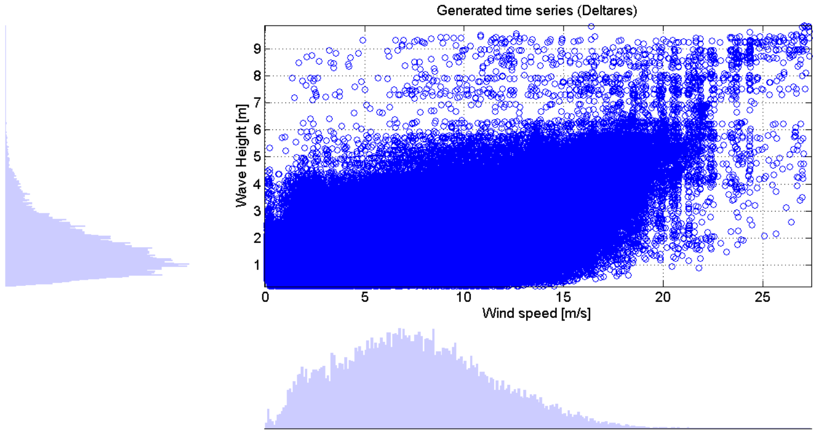

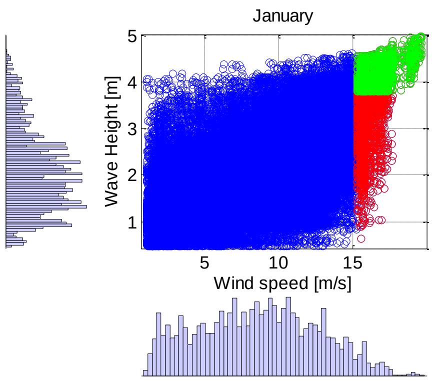

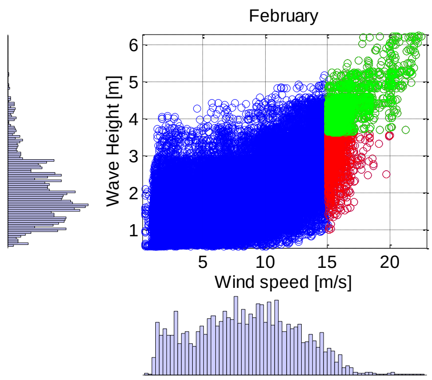

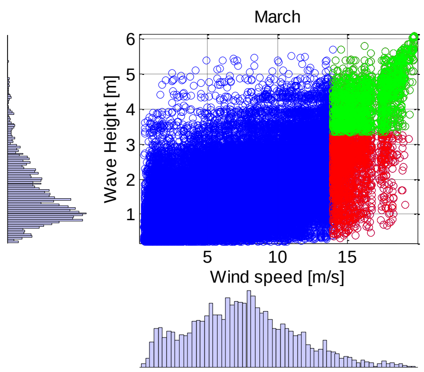

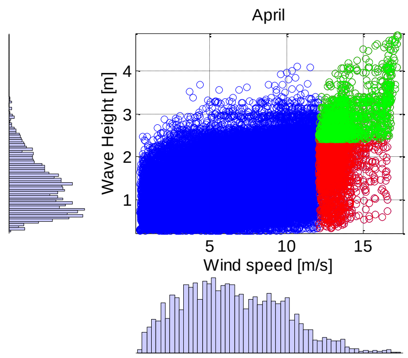

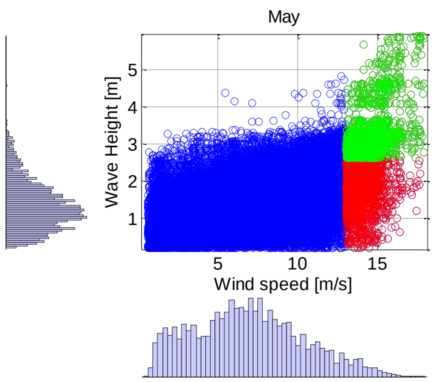

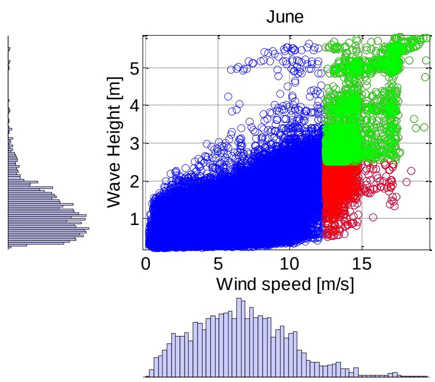

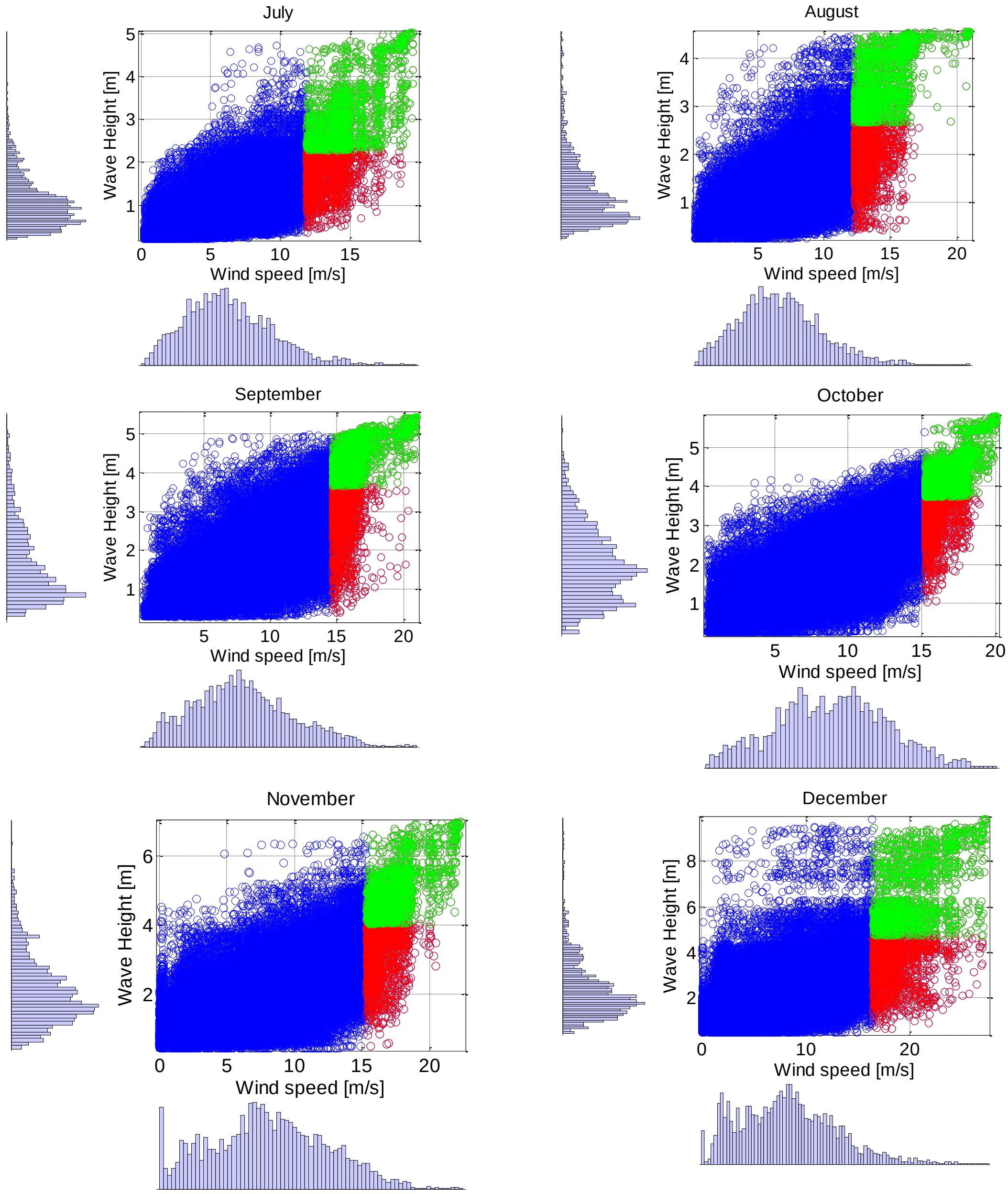
July
Wave Height [m]
Wind speed [m/s]
August
Wave Height [m]
Wind speed [m/s]
September
Wave Height [m]
Wind speed [m/s]
October
Wave Height [m]
Wind speed [m/s]
November
Wave Height [m]
Wind speed [m/s]
December
Wave Height [m]
Wind speed [m/s]

A.6 Exceedance probability for different percentiles (Generated time series based on Deltares observations)

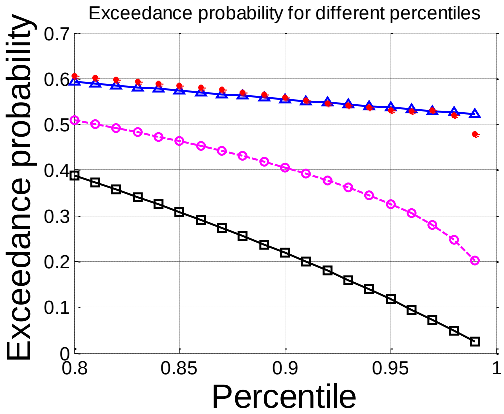

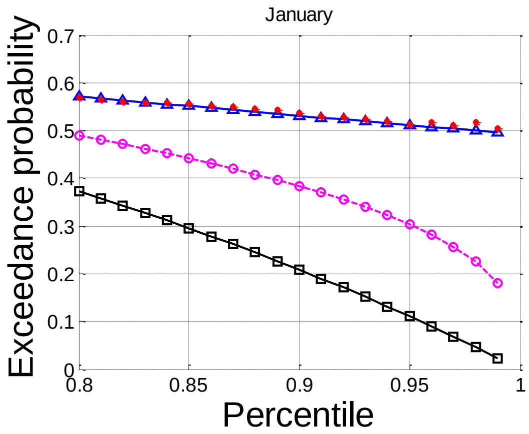

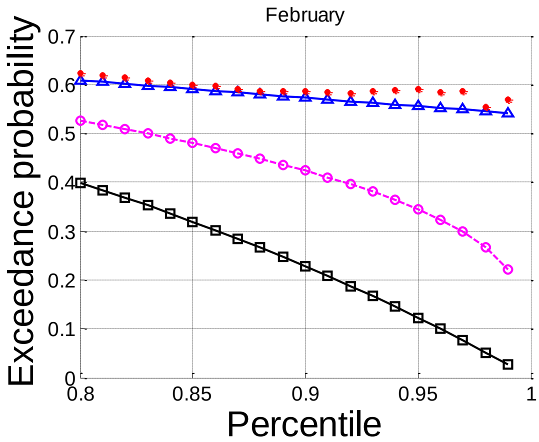

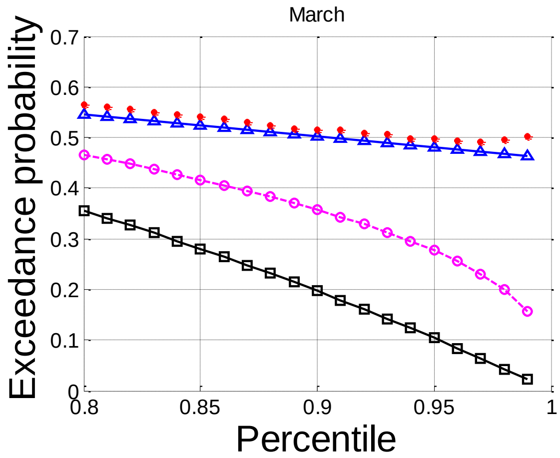

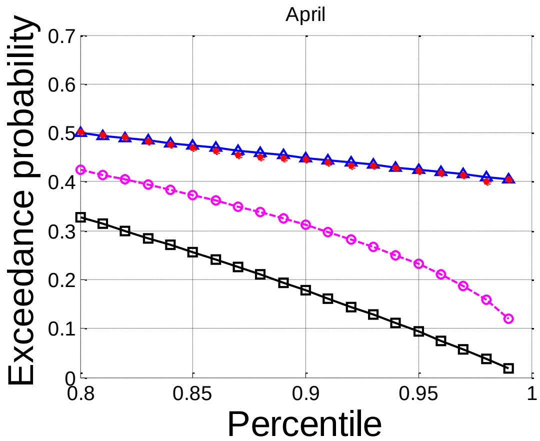

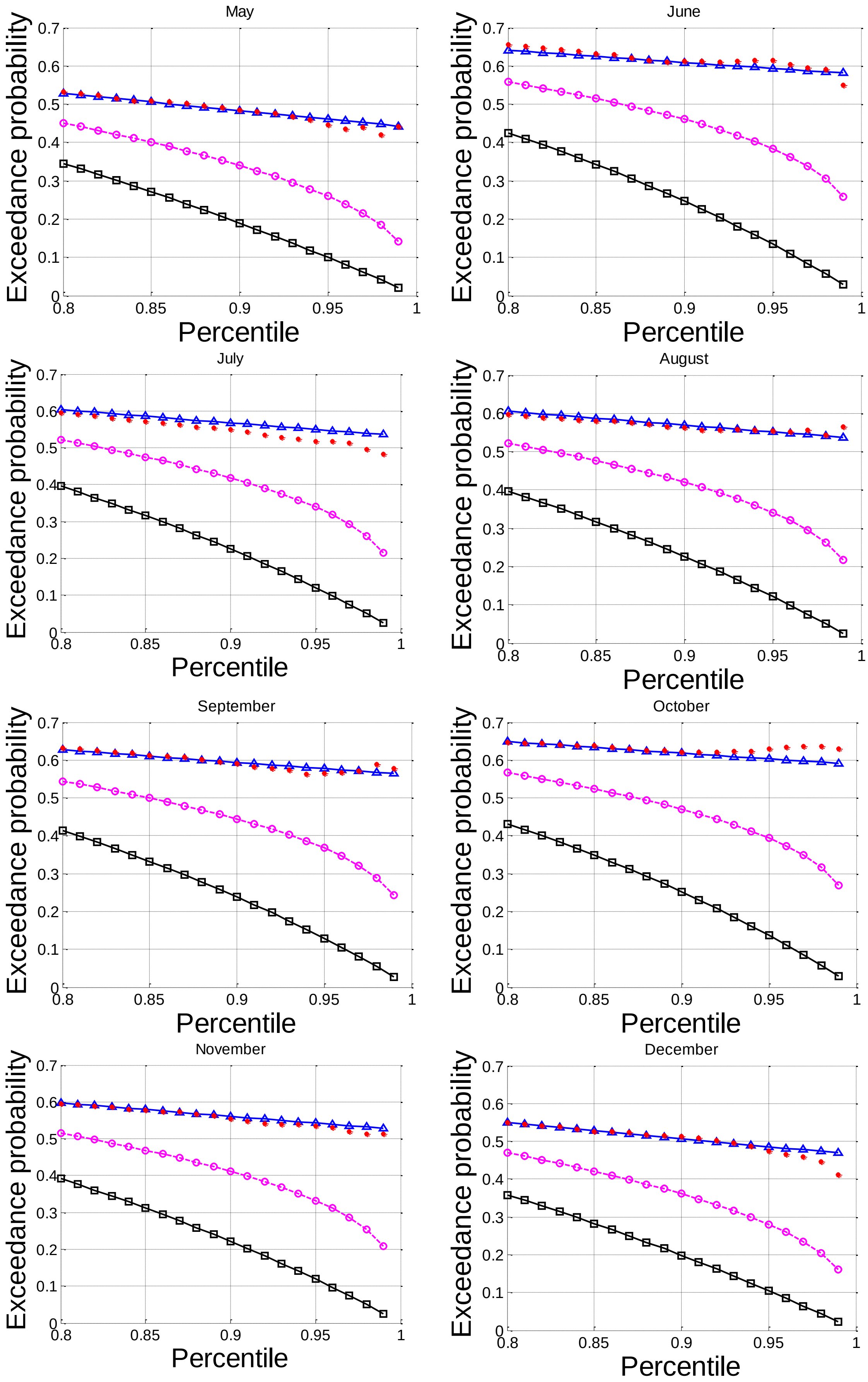
May
June
July
August
September
October
November
December
Exceedance probability
Percentile
0.7
0.6
0.5
0.4
0.3
0.2
0.1
0
0.8
0.85
0.9
0.95
1

Appendix B

B.1 Table of observations Vaan Oord weather data

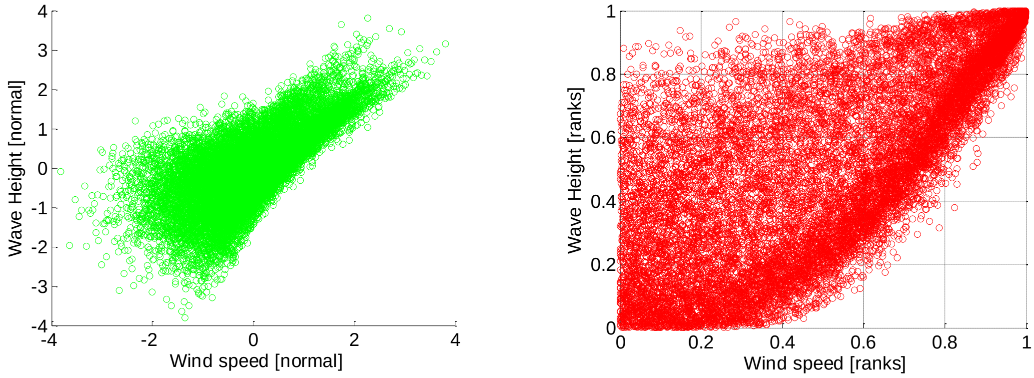

B.2 Scatter plots of Van Oord's weather data

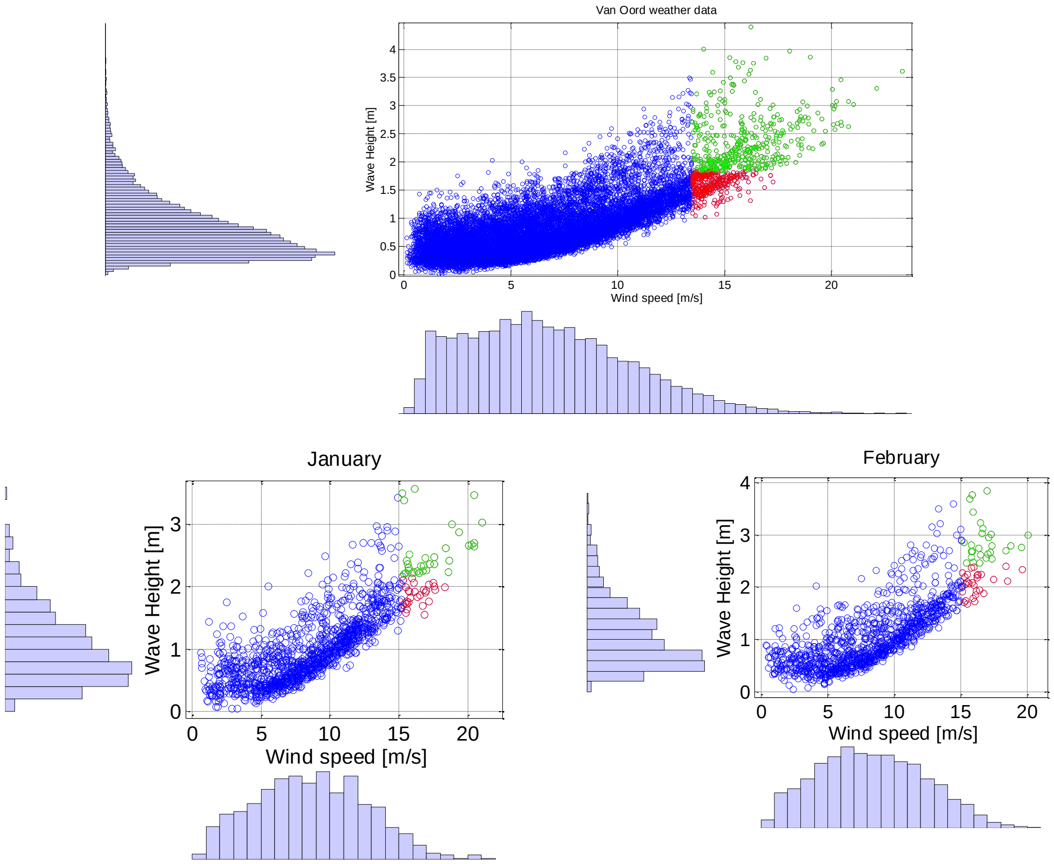

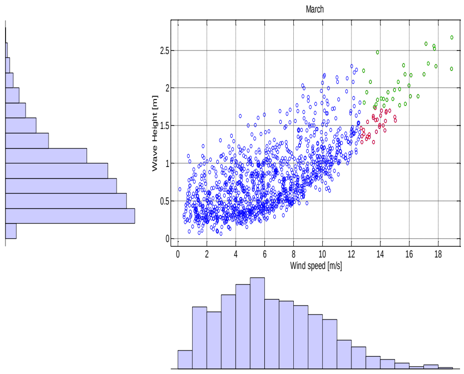
March
Wave Height [m]
Wind speed [m/s]

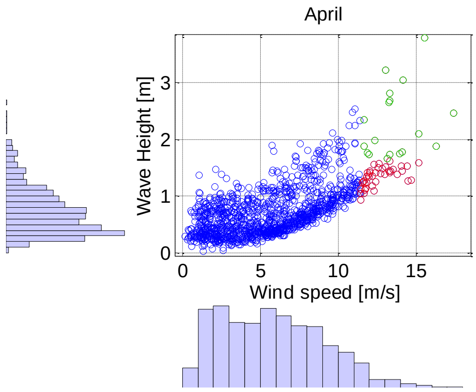
April
Wave Height [m]
Wind speed [m/s]

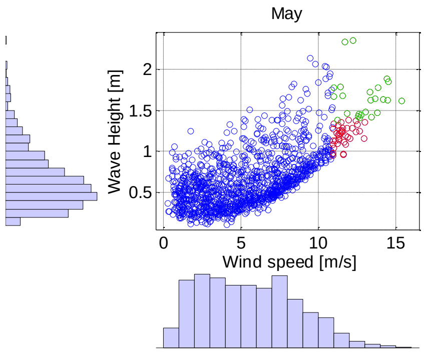
May
Wave Height [m]
Wind speed [m/s]

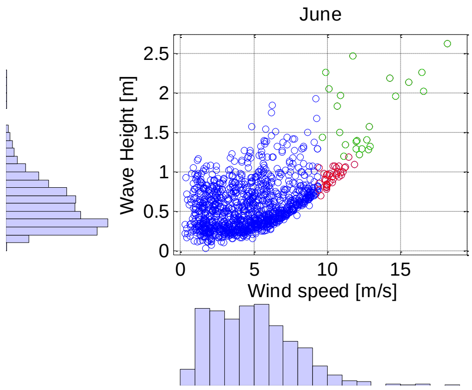
June
Wave Height [m]
Wind speed [m/s]

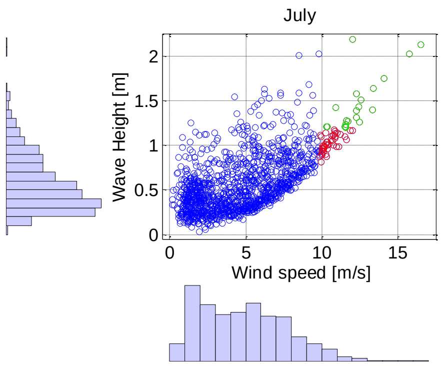
July
Wave Height [m]
Wind speed [m/s]

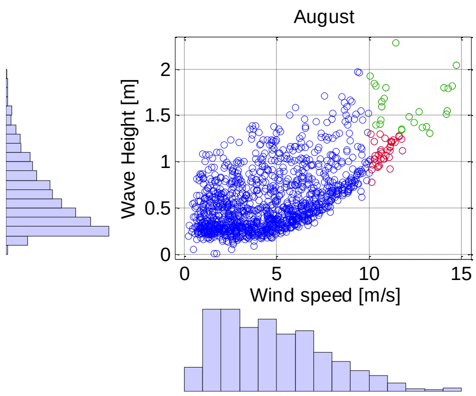
August
Wave Height [m]
Wind speed [m/s]

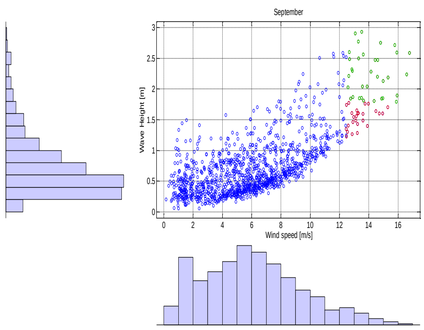
September
Wave Height [m]
Wind speed [m/s]

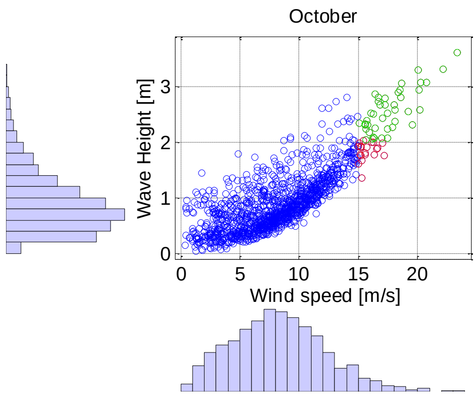
October
Wave Height [m]
Wind speed [m/s]

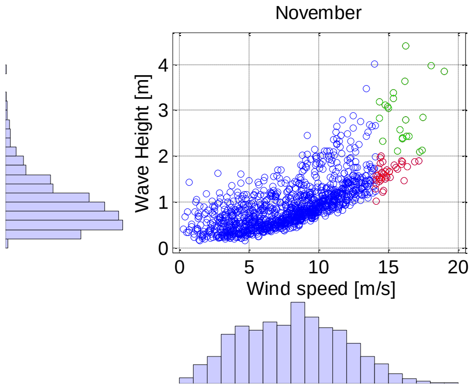
November
Wave Height [m]
Wind speed [m/s]
0
1
2
3
4
0
5
10
15
20

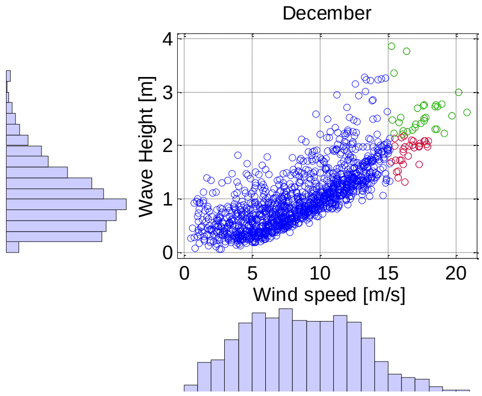
December
Wave Height [m]
Wind speed [m/s]
0
1
2
3
4
0
5
10
15
20

B.3 Exceedence probabilities for different percentiles (Van Oords weather data)

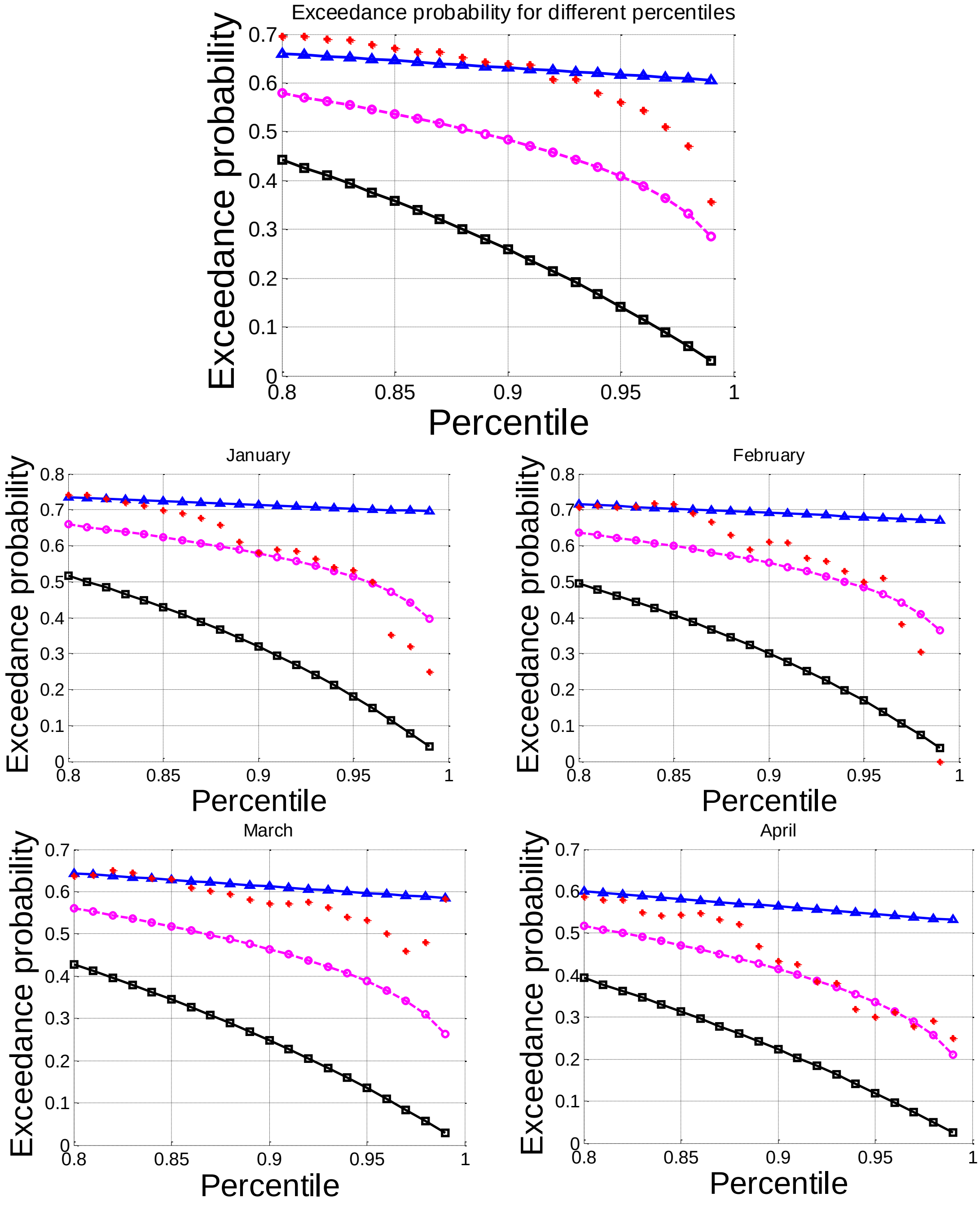

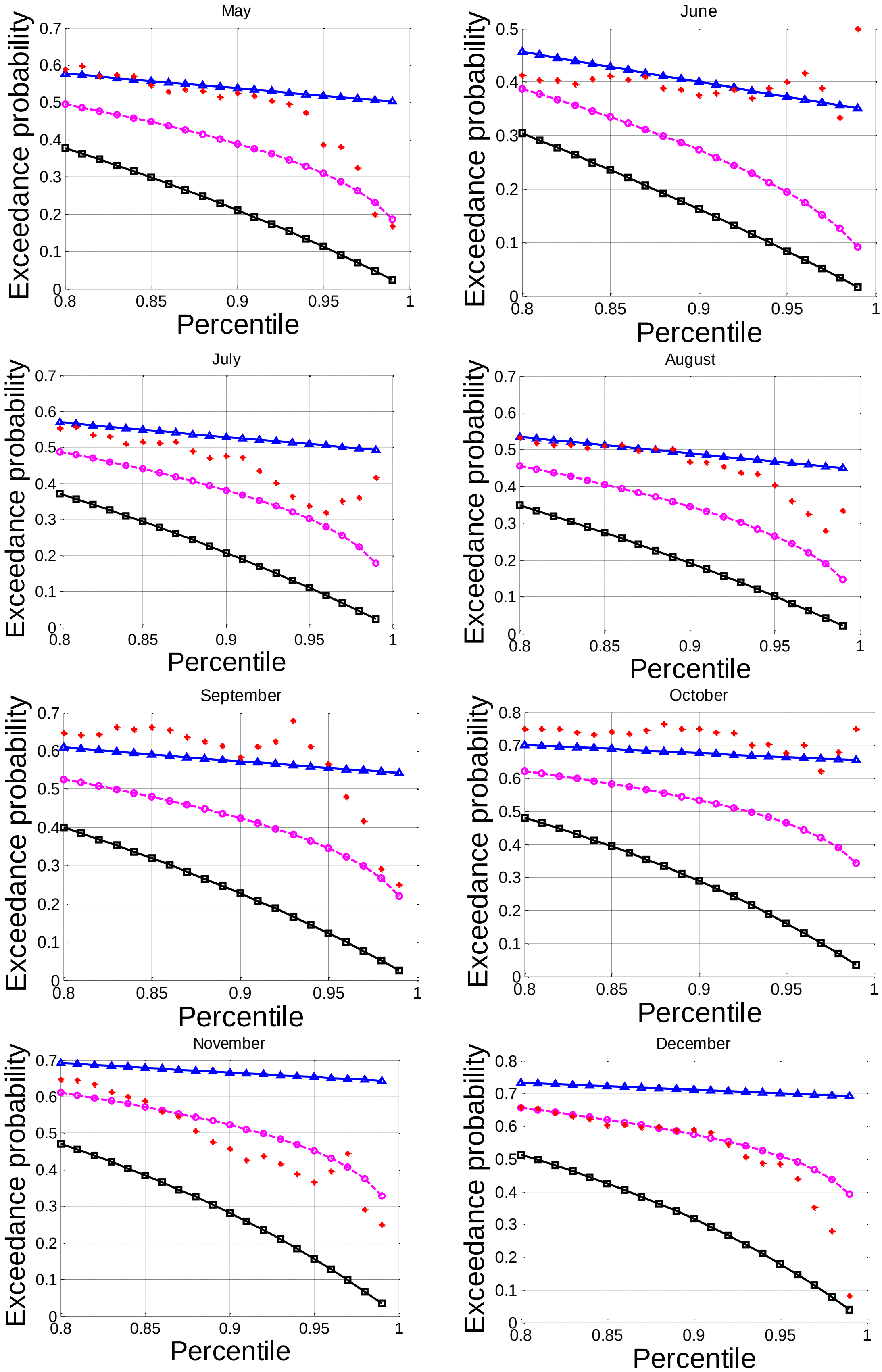
May
June
July
August
September
October
November
December
Exceedance probability
Percentile

B.4 Table of semi-correlations and square differences (Van Oord's weather data)

	ρ	ρ_{ne}	ρ_{sw}	G_N	G_{Gum}	G_{Cl}
Overall	0.6990	0.6782	0.1451	1.8123	1.0108	11.8385
January	0.7745	0.6897	0.3027	1.9535	1.3386	12.4617
February	0.7404	0.6650	0.0805	2.1142	1.4253	14.6171
March	0.6833	0.6237	0.1200	1.1496	0.5900	9.6137
April	0.6229	0.4520	0.1137	2.0580	1.4583	9.8580
May	0.5802	0.4991	-0.0278	2.3952	1.5528	10.6846
June	0.4337	0.3573	0.0548	2.4092	2.0362	5.1370
July	0.5674	0.4321	0.0177	1.9063	1.2905	9.3243
August	0.5347	0.4410	0.0018	1.6988	1.1798	7.4040
September	0.6469	0.6166	0.1306	1.8363	1.1126	8.8539
October	0.7683	0.7827	0.4084	1.4546	0.9653	9.1048
November	0.7316	0.5440	0.3274	1.2691	1.3622	8.8287
December	0.7644	0.5773	0.3065	1.4527	1.4814	11.0520

B.5 Scatter plots of 100 generated time series based on Van Oord's weather data

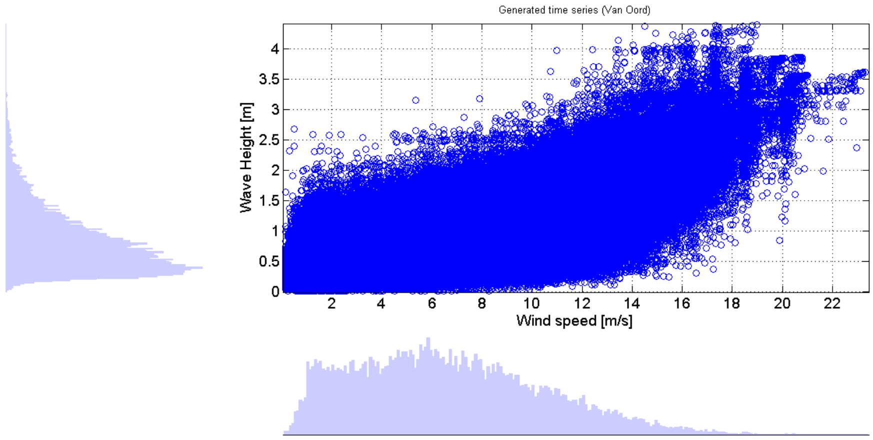

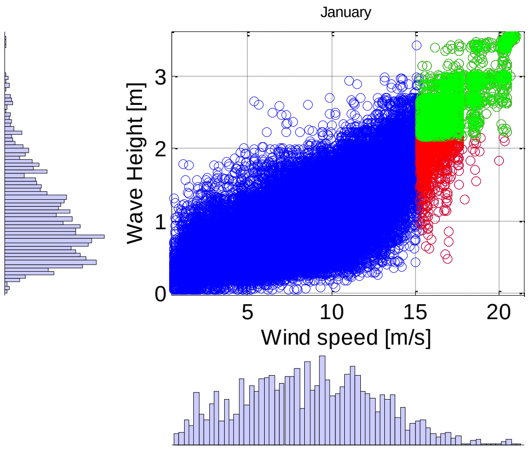

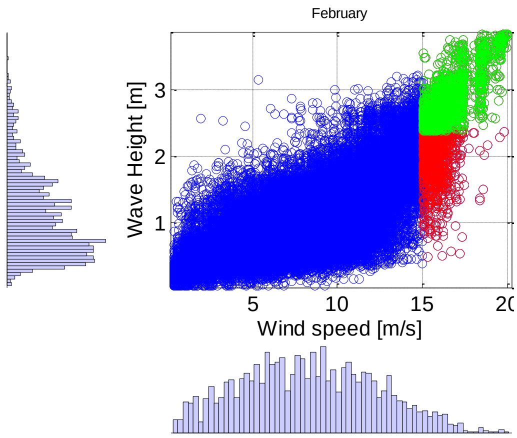

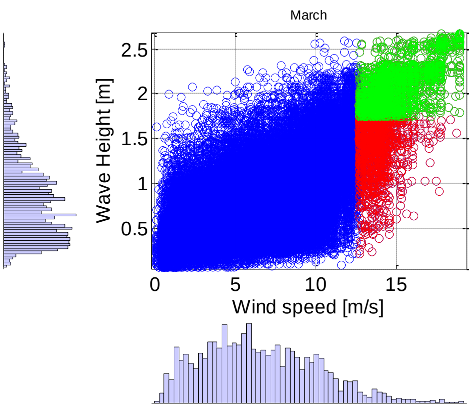

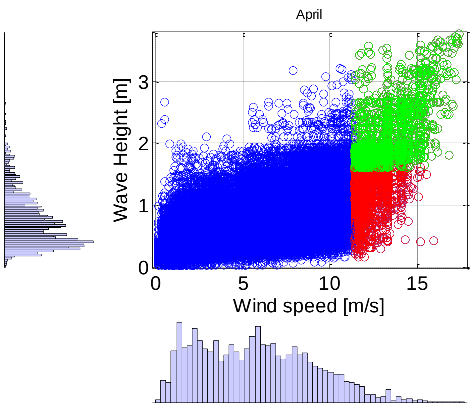

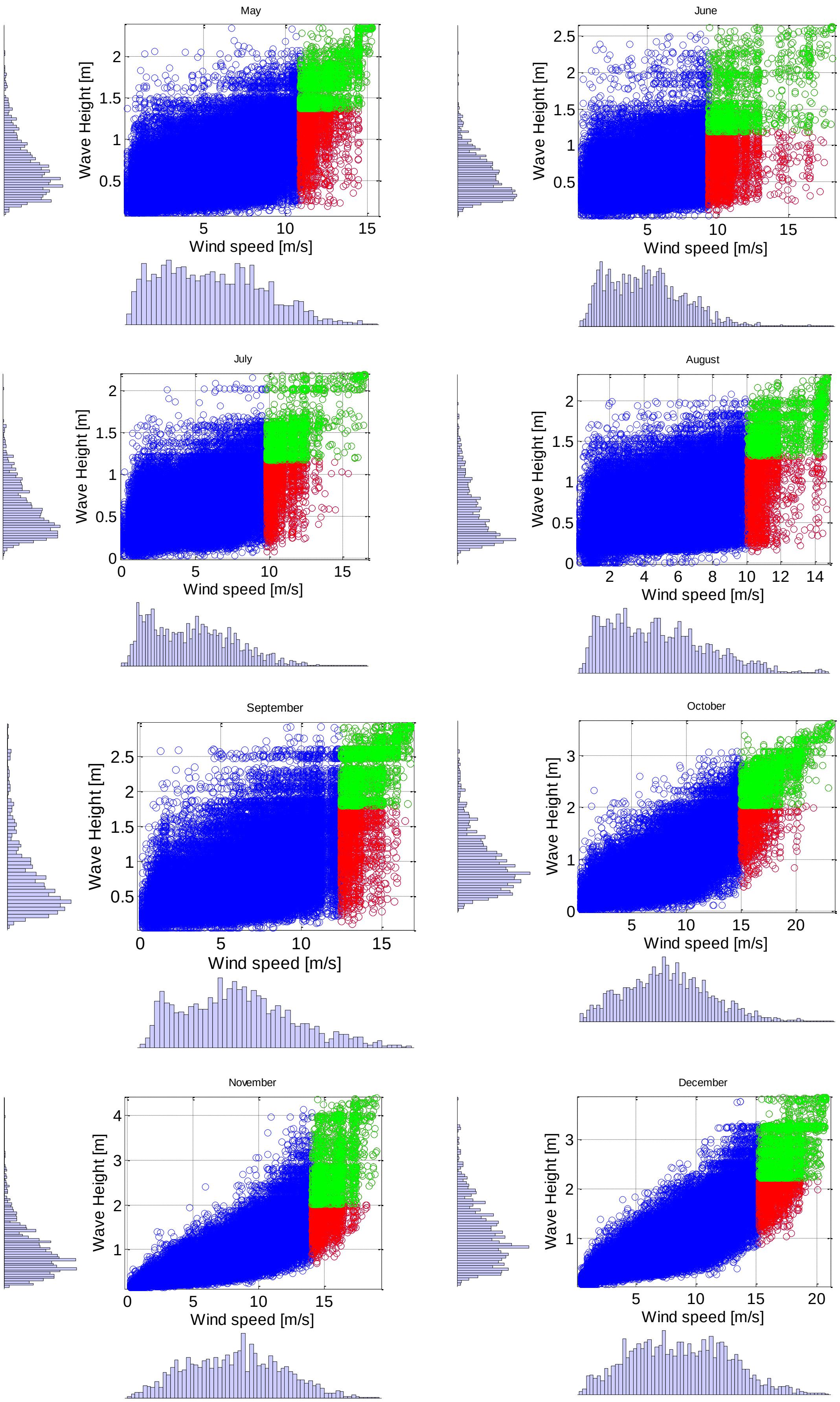
May
June
July
August
September
October
November
December
Wave Height [m]
Wind speed [m/s]

B.6 Exceedance probability for different percentiles (Generated time series based on Van Oord's weather data)

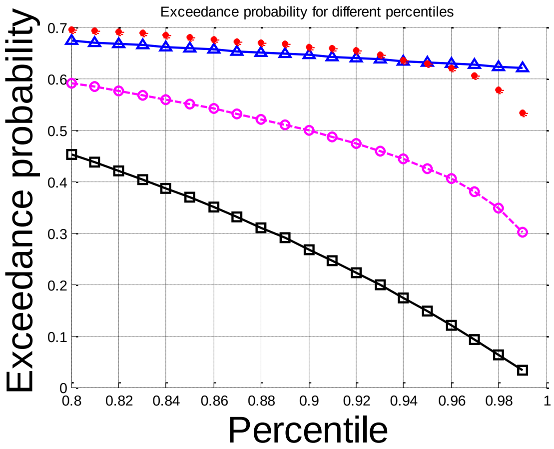

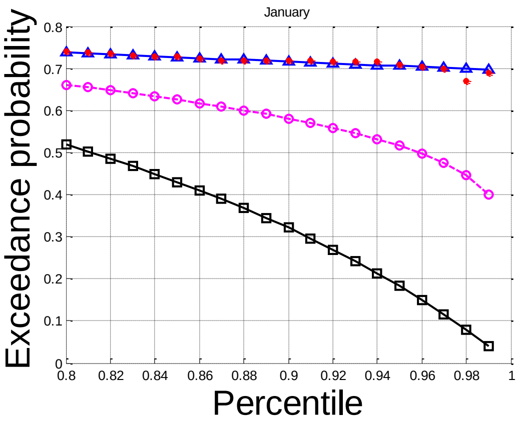

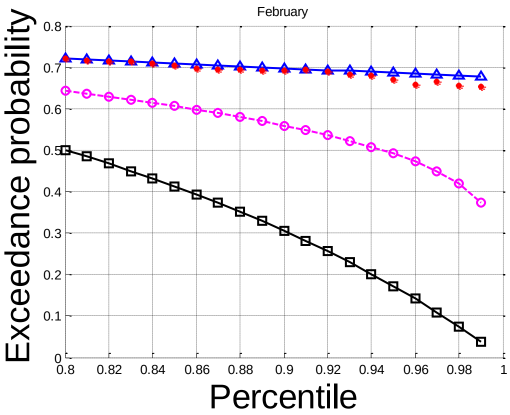

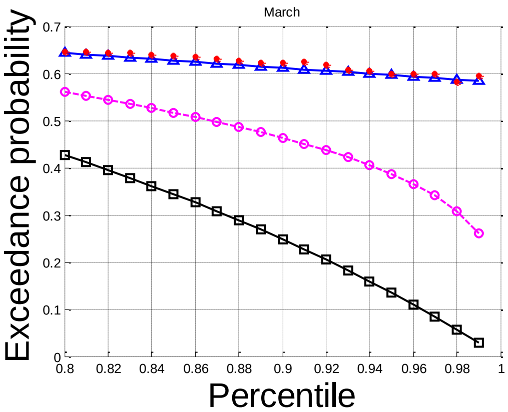

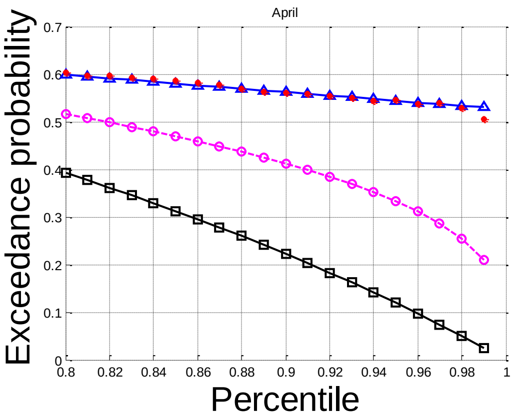

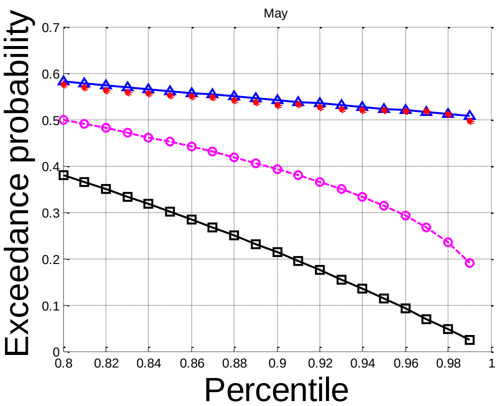

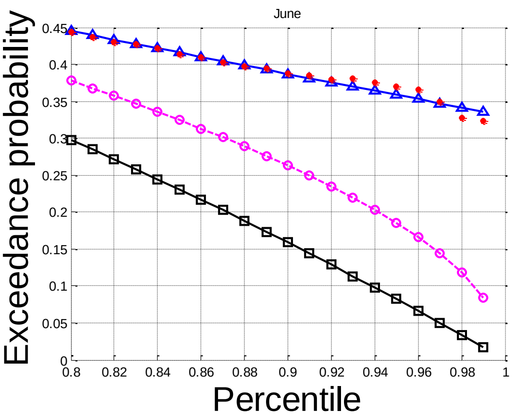

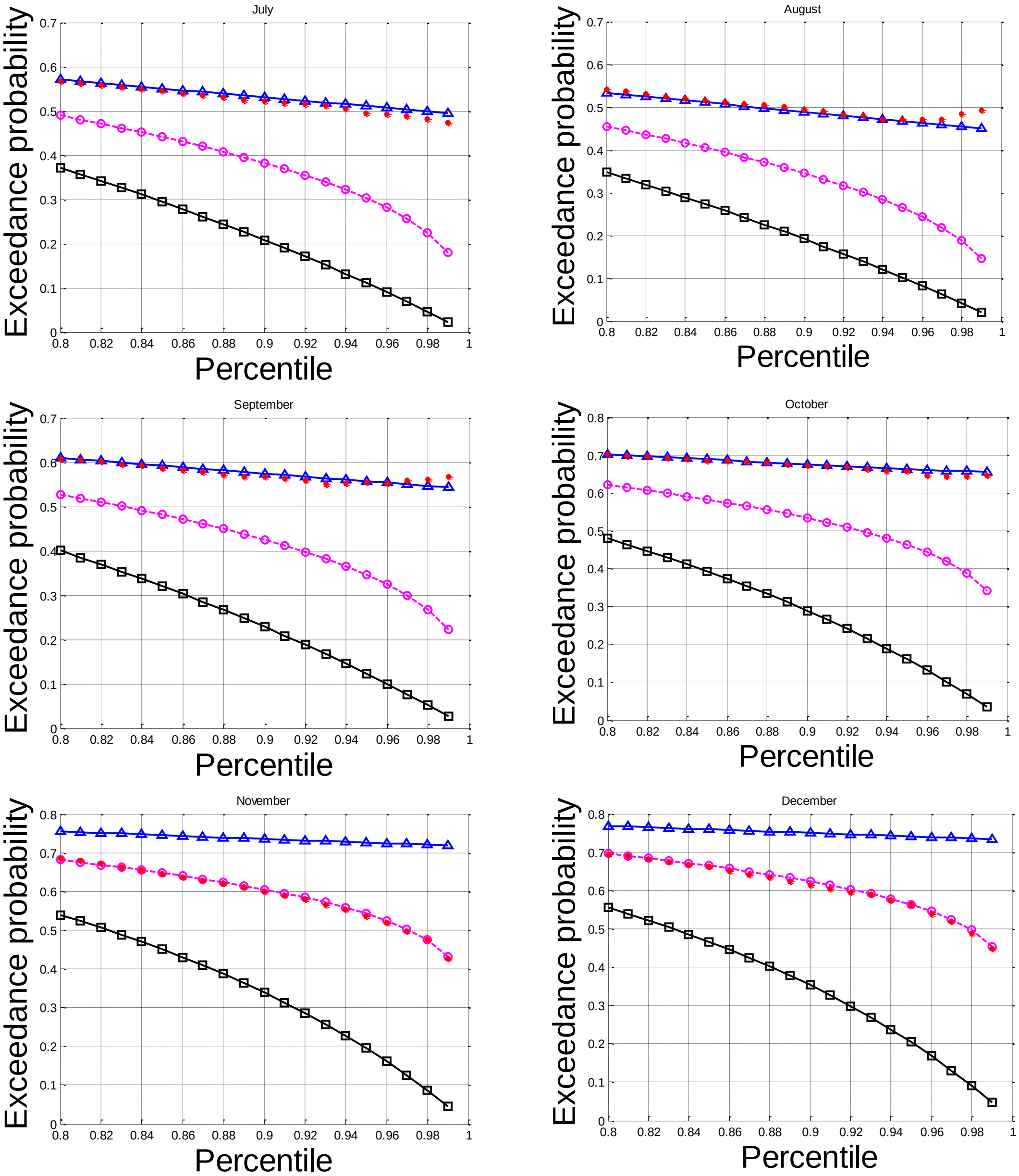
July
August
September
October
November
December
Exceedance probability
Percentile
0.8
0.82
0.84
0.86
0.88
0.9
0.92
0.94
0.96
0.98
1
0
0.1
0.2
0.3
0.4
0.5
0.6
0.7
0.8

B.7 Table of semi-correlations and square differences (Generated time series based on Van Oord's weather data)

	ρ	ρ_{ne}	ρ_{sw}	S_N	S_{Gum}	S_{Cl}
Overall	0.7290	0.7090	0.3402	0.5456	0.0424	8.1011
January	0.8157	0.7826	0.5154	0.2213	0.0013	6.3922
February	0.7960	0.7522	0.4886	0.2485	0.0018	6.5176
March	0.6962	0.6741	0.3501	0.3328	0.0027	6.3899
April	0.6357	0.6038	0.2848	0.3516	0.0050	5.7319
May	0.6102	0.5767	0.2695	0.2830	0.0042	5.1570
June	0.4040	0.4162	0.1316	0.2909	0.0036	2.8701
July	0.5918	0.5640	0.2564	0.3061	0.0050	5.2374
August	0.5406	0.5464	0.2113	0.3915	0.0048	4.7910
September	0.6482	0.6173	0.2889	0.3261	0.0032	5.9482
October	0.7718	0.7302	0.4442	0.2775	0.0020	6.6966
November	0.8380	0.6588	0.6567	0.0015	0.3734	3.3567
December	0.8526	0.6763	0.6807	0.0006	0.3741	3.1694